
**Università degli Studi di Catania**
**Scuola Superiore di Catania**

International PhD

in

Stem Cells
XXIII cycle

# High resolution molecular karyotyping and proteomic analysis in hematological malignancies

Alessandra Romano

Coordinator of PhD:

Prof. Daniele Filippo Condorelli

Tutor:

Prof. Francesco di Raimondo

Prof. Lance Liotta

Prof. Vincenza Barresi

A.A. 2007/2010

Stay hard, stay hungry, stay alive: dedicated to all people helped me to work on a dream

# Abstract

In this work we focused on two hematological malignancies to apply the translational meaning of functional genomics: myelodysplastic syndrome (MDS) and its potential evolution to frank acute myeloid leukaemia, and the broad set of monoclonal gammopathies up to multiple myeloma (MM). In both diseases the recent advances obtained thanks to the application of novel therapeutic agents have enlighten the need to target at the same time both neoplastic and surrounding microenvironment cells.

In MDS we applied the last generation of Affymetrix single nucleotide polymorphism (SNP)/copy number aberrations (CNA) platform to distinguish somatic and germline tumor-associated CNAs and loss of heterozigosity (LOHs) to identify possible recurring genomic abnormalities in high risk MDS evolving to AML. In particular in one patient, strictly followed in the clinical evolution from MDS to AML, we were able to define the unique features of the aberrant clone through a bioinformatic-based strategy.

For MM, we developed an *ex vivo* assay to identify signalling associated with differential treatments of fresh bone marrow aspirate samples, confirming the unique constellation of activation in the single patient, and the general trend of a differential behavior among neoplastic and surrounding cells.

Thanks to a global proteomic technique we identified compensatory pathways potentially responsible of chemoresistance in both MDS and MM sustained by the activation of autophagy and pro-survival signalling. In particular, we identified:

- Msi-2 as potential biomarker of stemness and aggressivity in MDS,

- PLC-y1Tyr783, SrcTyr416 and STAT-5Tyr694 as compensatory pathway responsible of side effects of treatment with azacitidine in MDS,
- NFkB status as potential mediator of chemoresistance to dexamethasone in MM,
- Akt/mTOR as biomarker of aggressiveness of plasmacells in MM;
- an abnormal compartmentalization of serotonin in MM peripheral blood and bone marrow, related to bone disease.

Taken together, our data provide potential insights into diagnosis, prognosis, and/or treatment strategies for MDS/AML and MM, through an integrative genomic and proteomic approach.

# Contents

**Foreword** **8**

**1 Background** **11**

1.1 Myelodysplastic syndromes as the premalignant form of AML . . 11

1.2 Multiple Myeloma . . . . . 15

1.2.1 *Targeting neoplastic plasmacells as paradigmatic approach* 18

1.2.2 *Multiple Myeloma bone disease* . . . . . 22

1.3 Serotonin metabolism . . . . . 23

**2 Methods** **29**

2.1 High-throughput genomic analysis: Affymetrix SNP 6.0 assay and CNV determination . . . . . 29

2.2 *Metaphase Cytogenetics* . . . . . 36

2.3 *c-Cbl mutational status screening* . . . . . 36

2.4 *Multiplexed ex vivo assay for the detection of proteomic profile in MM* . . . . . 37

2.5 The Reverse Phase Protein Microarray (RPMA) . . . . . 44

2.6 ELISA for detection of new markers in peripheral blood . . . . . 48

2.7 Statistics . . . . . 49

2.8 Ethics Statement . . . . . 50

**3 Results** **51**

3.1 Accumulation of genomic aberrations in MDS during progression to AML . . . . . 51

3.1.1 *Small copy number abnormalities (<1 Mb)* . . . . . 52
3.1.2 *Genes involved in progression to secondary AML in the region 11q14.1* . . . . . 60
3.2 Modulation of MDS proteome by new epigenetic drugs . . . . . 61
3.2.1 Proteomic profile as a means for combination therapy in MDS . . . . . 62
3.3 Signal pathway proteomic analysis of MM bone marrow microenvironment . . . . . 67
3.3.1 *Correlation between Protein Expression and Clinical Findings* . . . . . 67
3.3.2 *Baseline profile of plasmacells* . . . . . 69
3.4 Proteomic changes after ex vivo treatment of bone marrow as a whole . . . . . 73
3.5 Role of serotonin in MM . . . . . 80
3.6 Discussion of the results . . . . . 84

**4 Conclusion and Future Perspectives** **89**

**Bibliography** **93**

# *List of Abbreviations*

| | |
|---|---|
| **AML** | Acute Myeloid Leukemia |
| **BM** | Bone Marrow |
| **bp** | base pairs |
| **CNA** | Copy Number Aberrations |
| **CNV** | Copy Number Variations |
| **Dx** | Diagnosis |
| **HDAC** | Histone deacetylases |
| **HSC** | Hematopoietic Stem Cell |
| **MAPD** | Median Absolute Pairwise Difference |
| **MC** | Methaphase Cytogenetics |
| **MDS** | Myelodysplasia |
| **MGUS** | Monoclonal Gammopathy of Unknown Significance |
| **MM** | Multiple Myeloma |
| **NK-AML** | Normal Karyotype AML |
| **QC** | Quality Control |
| **R** | Remission |
| **RPMA** | Reverse Phase Micro Array |
| **SD** | Standard Deviation |
| **SERT** | Serotonin Transporter |
| **SNP** | Single Nucleotide Polymorphism |

# Foreword

Over the last three decades, more comprehensive sequencing of the genome, better and faster bioinformatics systems have played a role in developing *-omics* (proteomics, genomics, metabolomics, secretomics and so on) into a powerful suite of analytical tools. Faced with the avalanche of genomic sequences and data on messenger RNA expression, biological scientists have piles of information generated by the new array methods to synthesize into useful knowledge, opening the new era of *'functional genomics'*.

Although the genome provides information about the somatic genetic changes existing in the tissue and underpins pathology, it is the proteins that do the work of the cell and are functionally responsible for almost all disease processes. Particularly, cancer can be considered as a deranged cellular protein molecular network. Cell-signaling pathways contain a large and growing collection of drug targets, governing cellular survival, proliferation, invasion, and cell death, with a unique and differential profile in neoplastic and non neoplastic cells that can be followed as new class of biomarkers.

Currently, therapeutics is chosen based on population-based clinical trials using broad phenotypic analysis. Targeted approaches attempt to group patients based on larger histologic context (e.g. HER2 positivity in breast cancers) or mutational status of specific endpoints such as in the choice of second generation inhibitor of tyrosin kinase in chronic myelogenous leukaemia (CML). In view of the growing recognition of the individuality of diseases such as cancer, where each patient appears to possess a unique constellation of molecular derangements in their diseased cells and unique constitutional properties of their

non- diseased cells, a new opportunity exists to develop approaches and methods whereby each patient acts as his or her own *"clinical trial"*.

In the last 5 years new drugs (lenalidomide, Azacitidine, bortezomib) have been developed for hematological malignancies, able of modulating both neoplastic and microenvironment cells, and the impaired immunological context. For Multiple Myeloma (MM), Food and Drug Administration has approved lenalidomide and bortezomib based on the rapid translation of basic science to clinical medicine, and at least other 20 compounds are under investigation in phase 2-3 clinical trials. After CML and tyrosine kinase inhibitors, MM is a model disease for the development of novel therapeutic agents tested for their abilities to control at the same time both neoplastic and surrounding microenvironment cells.

In this dissertation we have chosen two paradigmatic models to apply the translational meaning of functional genomics: a myeloid disorder, represented by myelodysplasia (MDS) and its potential evolution to frank acute myeloid leukaemia (AML), and the lymphoproliferative set of monoclonal gammopathies (basically monoclonal gammopathy of unknown significance, MGUS up to evolution to multiple myeloma, MM). In fact, they are two excellent examples of incurable disease, with poor prognosis despite of the availability of new drugs, affecting progressively more and more subjects, being typical in the elder population.

For MDS/AML we privileged a genomic approach, showing that the new generation of SNP arrays can provide new insights in the pathogenesis, revealing areas of genomic instability, whose magnitude is responsible of progression, as we showed in the samples obtained from one MDS patient refractory to the new drugs lenalidomide and Azacitidine progressed to frank secondary AML. Treatment with an epigenetic drug, such as Vidaza, modifies protein expression in unpredictable pathways, suggesting the importance of integrating information at different level that can help to explain new compensatory pathways and reactions. On the other hand, primary AML with normal karyotype at conventional approach showed a pretty stable genome even when analyzed with the SNP

arrays, suggesting a different pathological mode, with key smaller alterations sustaining the selective advantage of the neoplastic clone.

For MGUS/MM we focused on the proteomic approach, being a large and contradictory literature on its genomics. We considered two kind of samples: core biopsy, with the bone and bone marrow in toto in order to have a baseline profile of active networks at neat, and cells obtained from the bone marrow aspirate (plasmacells vs microenvironment cells), studying the modulation of main pathways before and after treatment *ex vivo* with different classes of drugs. In chapter 1 we indicate the background and main aims that have led our work; in chapter 2 we provide details about the methods selected and clinical features of patients involved in our research. Results are reported and discussed in chapter 3. Data included in this dissertation have already been partially published in 3 different papers, have been included in 2 patents and three more manuscripts are in preparation.

# Chapter 1

# Background

## 1.1 Myelodysplastic syndromes as the premalignant form of AML

Myelodysplastic syndromes (MDS) are a group of heterogeneous clinical conditions characterized by a hyperproliferative bone marrow, reflective of ineffective hematopoiesis, and accompanied by one or more peripheral blood cytopenias (anemia, piastrinopenia, neutropenia). The resulting bone marrow failure leads to death from bleeding and infection in the majority, while the transformation to acute leukaemia occurs in up to 40% of patients [1]. Despite a normal or hypercellular marrow, most patients show peripheral blood cytopenias, consequence of an excessive programmed cell death or apoptosis of hematopoietic progenitors. Apoptosis in early disease may represent a pathophysiological mechanism whereby the hematopoietic system is able to abrogate defective and/or potentially harmful clones [2, 3]. Alternatively, an early *hit* in the multi step pathogenesis of MDS could give rise to a clone with a proliferative advantage. Increased apoptosis may thus represent a homeostatic process to control cell numbers. In turn, leukemic progression arises through the acquisition of genetic lesions that either block programmed cell death or promote proliferation over and above apoptosis [4]. The syndrome appears to represent a spectrum, where

the initial lesion in the genome, though clinically undetectable, subsequently evolves with the acquisition of additional lesions to a state of frank neoplasia [5]. The evolution of the disease proceeds in accordance with the multi-step theory of carcinogenesis and can thus serve as an important model in furthering our understanding of the processes involved in cancer transformation [6]. The most common chromosomal abnormalities in MDS are represented by a deletion of the long arm of chromosome 5 (del(5q)) or chromosome 7 (del(7q)), with a WHO-estimated frequency of 10 % and 50 % in therapy-related myelodisplastic syndromes [6]. Gondek [7] reported that SNP array karyotyping allows to detect 25-50% of clonal cells carrying abnormal karyotypes. Moreover, they demonstrated that new lesions were discovered by molecular cytogenetics and confirmed that these alterations are exclusively of somatic nature in patients with MDS, myelodysplastic/myeloproliferative disease (MDS/MPD), or MDS-derived acute myeloid leukaemia (MDS/AML). These lesions comprise copy number variations and loss of heterozigosity (LOH) in 6p21.2-pter, 11q13.5-qter, 4q23-qter and 7q11.23-qter. The recognition of epigenetic changes in DNA structure in MDS [8] has explained the success of two of three commercially available medications approved by the U.S. Food and Drug Administration to treat MDS [9]. Proper DNA methylation is critical in the regulation of proliferation genes, and the loss of DNA methylation control can lead to uncontrolled cell growth, and cytopenias. The recently approved DNA methyltransferase inhibitors take advantage of this mechanism by creating a more orderly DNA methylation profile in the hematopoietic stem cell nucleus, and thereby restore normal blood counts and retard the progression of MDS to acute leukaemia. However, the molecular basis for this outcome is unclear as the exact gene targets for the drugs have not been identified yet. Potential target genes are those of the p53 family, affecting cell differentiation and apoptosis, or the p21 and p18 genes affecting the behavior of stem cells. It is also unknown whether these drugs exert their effect by restoring gene expression and blast cell differentiation or by induction of apoptosis [10]. Moreover, the overall survival benefit observed with 5-azacitidine can be independent from the baseline methylation status

[10, 11]. Thus, the effects of these agents are not necessarily mediated by their hypomethylating features but might be exerted through non-hypomethylating pathways as well. However, there was no difference in freedom from RBC transfusions between patients receiving these treatments and patients treated with conventional care. This could be explained by limited data, since only two trials reported this outcome [10].

Despite recent advances in the comprehension of pathological mechanisms, progress has been slow with regard to treatment [9]. Five-year disease-free survival rates range from less than10% to 60% for specific risk groups [6]. Supportive care, with blood product support and hematopoietic growth factors (e.g. erythropoietin), remains the standard of treatment. In fact, the global clinical strategy takes into account the control of symptoms, improve quality of life, improve overall survival, and decrease/retard the progression to acute myelogenous leukaemia. The only treatment with a curative potential is allogeneic stem cell transplantation [12], particularly in younger patients (i.e. less than 45 years of age) or in more severely affected patients. However, in the majority of patients, this treatment is not applicable, mainly due to the age of the recipients and co-morbidity. Success of bone marrow transplantation has been found to correlate with severity of MDS as determined by the IPSS score, with patients having a more favorable IPSS score tending to have a more favorable outcome with transplantation. A concrete alternative is the chemotherapy with the novel agents: hypomethylating agents 5-Azacitidine (introduced in '60s but never approved by FDA for treatment of AML) and its deoxy-derivative decitabine, 10-fold more potent *in vitro* [9, 10]. However the real advantage for our patients is limited: Azacitidine, but not Decitabine [13], significantly prevents or delays transformation to AML and significantly prolongs AML-free survival globally in high risk- MDS [14]. The larger phase randomized phase III study (CALGB 9221) showed responses in patients with all MDS FAB subtypes. The overall response rates in patients treated with Azacitidine versus those given the best supportive care (BSC) were 60% versus 5% ($p<0.0001$), with a median response duration of 14 months. The median time to initial response was 64 days and

that to best response was 93 days. The median time to AML or death was 21 months in patients receiving Azacitidine, compared with 12 months in patients receiving BSC (p = 0.007; Fig.1.1). Transformation to AML as the first event occurred in 38% of those patients in the BSC group, as compared with 15% for those in the Azacitidine group. Overall, patients treated with Azacitidine survived longer than patients receiving supportive care (a median of 20 months versus 14 months, p = .01) [15].

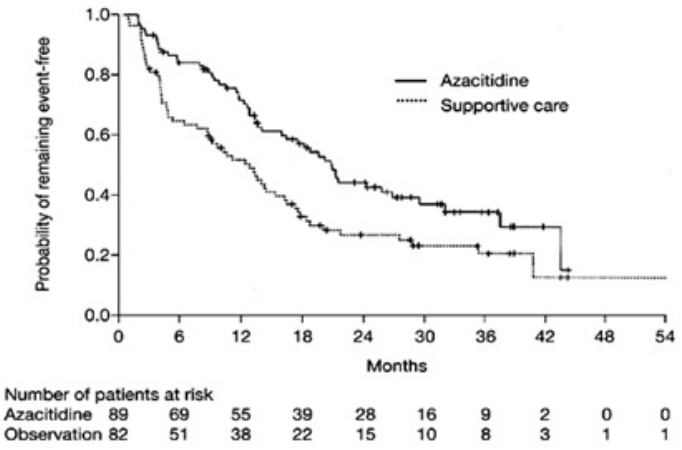


Fig. 1.1: Median time to transformation to acute myeloid leukaemia or death in patients with myelodysplastic syndrome treated with azacitidine or given best supportive care, as reported in [14]

.

Compared to conventional care, treatment with hypomethylating agents and specifically 5-azacitidine, prolongs overall survival and time to AML transformation or death, despite increased treatment-related mortality and lack of difference in early mortality [10, 16, 17, 15]. Azacitidine is listed as the preferred drug for high-risk MDS patients, and decitabine is listed as an alternative in the 2009 National Comprehensive Cancer Network guidelines, on the basis of survival data [18]. Nevertheless, there is still some uncertainty over some issues such as which drug to choose, which patients to treat, and how long to continue treatment.

## 1.2 Multiple Myeloma

Multiple myeloma (MM) is the second most prevalent hematological cancer, with over than 55,000 new cases diagnosed in USA each year [19]. MM and the monoclonal gammopathy of undetermined significance (MGUS) are characterized by proliferation of clonal B lymphocytes at various stages of maturation in the bone marrow (BM). Despite significant advances in therapy, MM is still an incurable disease: remissions are seldom sustained, the median survival ranges from 2-3 years for high risk MM to better than 5 years for low risk patients [20]. While this suggests the existence of different biologically defined subgroups, the knowledge about such biological differences is still limited.

Many experimental observations support the hypothesis that MM evolves through a multi-step transformation process: an inactive phase in which tumor cells are non-proliferating mature plasma cells, an active phase with a small percentage (<1%) of proliferating plasmablastic cells, and a fulminant phase with the frequent occurrence of extramedullary proliferation and an increase in plasmablastic cells [21].

The malignant plasma cells in MM are localized in the bone marrow (BM) in close association with stromal cells, and are rarely found in other locations. They are long-lived cells with a very low labeling index (LI= 1% to 2%) and a significantly lower rate of immunoglubulin secretion than the normal counterpart. It appears that the critical oncogenic events in MM cells either occur after or do not interfere with most of the normal differentiation process involved in generating a long-lived plasma cell [21]. Interaction of MM cells with bone marrow microenvironment cells has a pathogenetic role in the disease and confers tumor cell resistance to conventional therapies. Understanding molecular mechanisms triggered by tumor-microenvironment interactions plays a key role to envelop new treatment options and improve response quality [22].

The proliferation, differentiation, and function of lympho-hematopoietic cells are regulated by a complex network of lympho-hematopoietic growth factors and cell surface molecules which establish a fine-tuned communication between stroma cells and lympho-hematopoietic precursors in the BM. The cytokines

involved in MM pathogenesis are similar to those mediating the proliferation of normal early plasma cells (*plasmablastic cells*), and their differentiation to mature plasma cells (*plasmacytic cells*), such as IL-6 or IL-10.

**IL-6** has a well defined role in sustaining and progression MM primarily through Bcl-XL and the Ras-mitogen-activated protein kinase (MAPK) cascade [23, 24]. Using IL-6-dependent murine B9 hybridoma/ plasmacytoma cells it has been showed that [25]:

1. drug-mediated reversible G1 arrest triggered apoptosis despite the presence of IL-6;

2. short IL-6 pulse to G1-arrested cells was sufficient to induce S phase entry and prevent apoptosis;

3. phorbol ester and related derivatives promoted S phase entry and survival of IL-6-starved cells without up-regulating bcl-XL expression.

**IL-10** is also a growth factor for MM cells, because it enhances the proliferation of freshly explanted myeloma cells in short-term BM culture and supports the growth of myeloma cell lines [21]. IL-10 has inhibitory effects on the production of IL-6 by MM cells; therefore, its effects are probably not mediated by IL-6. More likely, IL-10 enhances the responsiveness of MM cells by regulating the expression of other cytokines and cytokine receptors [26]. Levels of IL 10 correlate with active disease, since patients in remission have a normalization of IL 10 levels in their bone marrow [27].

Tumor necrosis factor ($\alpha$ **TNF-**$\alpha$) is the most potent inducer of NFkB activation and IL-6 secretion from bone marrow microenvironment cells produced by neoplastic plasmacells, although it is not involved in mediating growth or drug resistance [28, 29]. However, circulating TNF-$\alpha$ levels are higher in MM patients with overt bone disease [29].

The **NFkB** family of transcription factors is composed by an array of homo- and heterodimers (containing p50, p52, c-Rel, p65/RelA, and RelB), held in the cytoplasm of most normal cells as an inactive latent form by specific inhibitor proteins (IkB). Part of NFkB's importance in regulating cellular responses is

that it belongs to the category of *rapid-acting* primary transcription factors, i.e., transcription factors that are present in cells in an inactive state and do not require new protein synthesis to be activated (other members of this family include transcription factors such as c-Jun, STATs, and nuclear hormone receptors). This allows NFkB to act as a *first responder* to harmful cellular stimuli. Stimulation of a wide variety of cell-surface receptors, such as RANK, TNFR, leads directly to NFkB activation and fairly rapid changes in gene expression [30, 31, 32]. Two major pathways, the classical and the alternative one, summarised in fig. 1.2, lead to the activation of NFkB: in both cases the activation can be effectively blocked by proteasome inhibitors, which interrupt NFkB translocation from the cytoplasm to the nucleus by inhibiting degradation of IkB proteins. This mechanism has been demonstrated in different malignancies, where NFkB is aberrantly activated and contributes to the drug resistance [33].

However, Romano et al. [33] and Hideshima et al. [34, 35] recently demonstrated that blocking of IkB degradation is not the only mechanism responsible for proteasome inhibitor-induced apoptosis and for the proven clinical activity of Bortezomib. Using human MM cell lines and primary tumor specimens, Hideshima showed that Bortezomib actually activates 2 upstream NFkBactivating kinases (RIP2 and IKK), promotes down-regulation of NFkB's inhibitor (IkB), and increases NFkB DNA binding in vitro. Another structurally unrelated proteasome inhibitor (lactacystin) induces the same effects, strongly suggesting that NFkB activation is an *on-target* effect of the drug. If NFkB inhibition is not involved in bortezomib's cytotoxic effects,the cell death results from protein build-up and aggregation, as is the case in neurodegenerative diseases. In this model, the high levels of immunoglobulin production and ER-Golgi protein transport would sensitize MM cells to proteotoxic stress, providing an attractive explanation for bortezomib's clinical activity and a potential means of identifying bortezomib-based combination approaches that will display even greater antitumor effects.

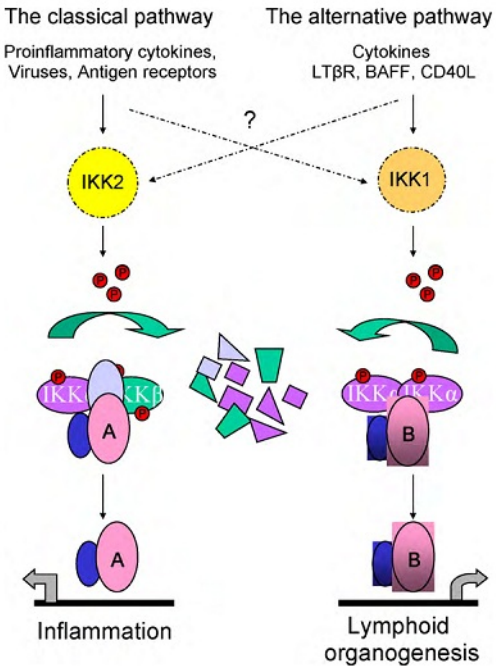


Fig. 1.2: Crosstalk between canonical and non-canonical signalling pathways is of current research interest. The so-called classical/canonical NFkB pathway is triggered by many inflammatory stimuli to induce IKK2-containing IKK complexes that specifically phosphorylate the three canonical IkB proteins, thereby marking them for ubiquitination and proteasome-mediated proteolysis. Cytoplasmic RelA (A) as well as cRel-containing dimers are thereby released to translocate to the nucleus and activate genesmainly involved in inflammatory processes. The alternative/non-canonical pathway is mediated by IKK1, is strictly dependent on IKK homodimers and is activated by lymphotoxin receptor (LTR), B cell-activating factor belonging to the TNF family (BAFF), and CD40 ligand (CD40L). This pathway induces the release of RelB (B)- containing dimers to the nucleuswhere NFkB plays a central role in the expression of genes involved in development and maintenance of secondary lymphoid organs. Adapted from [33].

### 1.2.1 *Targeting neoplastic plasmacells as paradigmatic approach*

Most of the commonly used anti-cancer drugs included in MM chemotherapy protocols non-specifically target fundamental cellular processes of DNA metabolism and cell division, like alkylants, complicating efforts to elucidate specific molecular determinants of differential treatment response. The emerg-

ing use of *'rationally targeted'* agents, which disrupt specific oncogenic signaling processes, has provided an opportunity to elucidate the molecular basis for differential clinical sensitivity and, possibly, to implement strategies that match individual patients with cancer to specific drug therapies to which they are more likely to respond. In the last five years, novel therapeutic agents, such as bortezomib and lenalidomide, have showed exciting activity in vitro and in vivo, moving so rapidly from the bench to the bedside to be already included in pivotal phase III trials up to being the backbone of MM clinical management [22, 28, 36]. Nowadays, the major challenge facing clinicians is to determine which combination of drugs will prove to be the most effective and result in a cure, even if a personalized approach is probably needed.

**Steroids** Glucocorticoids (GCs) are involved in physiological regulation of a variety of processes, including immune responses, metabolism, cell growth, and development. Their therapeutic value is enormous, in a wide range of autoimmune/inflammatory diseases, and GCs have been widely used since the late 1940s for treating autoimmune disorders, allergy, allograft rejection, and euplastic diseases. Their therapeutic activity reflects the physiological effects of endogenous steroids, although with greater potency and efficacy. Among these effects, GC-mediated inhibition of cell proliferation and modulation of apoptosis, which is either induced or inhibited-have considerable biological and clinical significance. Indeed, modulation of apoptosis and proliferation has been implicated in GC regulation of immune development and provides grounds for the inclusion of GCs in treatment regimens of lymphoid malignancies [37]. In autoimmune/inflammatory diseases, inhibition of apoptosis may result in failure of GC therapy or even in disease worsening. Resistance to GC therapy, often because of resistance to GC-induced apoptosis, is a major clinical problem in hematopoietic malignancies and inflammatory/autoimmune diseases [38, 39, 40]. GCs induce their effects mainly through transcriptional regulation of glucocorticoid-receptor (GR) target genes: the activated GR complex upregulates the expression of anti-inflammatory proteins in the nucleus (a process

known as *transactivation*), such as annexin-1, MAPK, phosphatase 1, IkB,IL-10 and represses the expression of pro-inflammatory proteins in the cytosol by preventing the translocation of other transcription factors from the cytosol into the nucleus (*transrepression*). In addition, GR mediates GC effects indirectly through protein-protein interactions with other transcription factors, cofactors, regulators, and signaling proteins, such as members of STAT family, NFkB, activator protein-1 (AP-1), 14-3-3, and Raf-1 protein. Moreover, nongenomic GR-dependent effects are known to contribute to the modulation of signal transduction pathways. As an example, GC-activated apoptosis of murine thymocytes requires both genomic and nongenomic signals. Dexamethasone (DEX) treatment of thymocytes first causes release of the dimeric complex GR-associated Src kinase (Src)/phosphatidylinositol-specific phospholipase C (PI-PLC) from the multimeric complex, including GR and HSP-90, and it then results in PI-PLC phosphorylation and activation, acidic sphingomyelinase (aSMase) activation, and ceramide production, which, in turn, regulates both gene transcription and caspase-8 activation [41]. GCs are an integral component of many regimens of MM chemotherapy. However, after an initial response, most patients acquire resistance [42]. This phenomena have been attributed to point mutations in the GR gene, to the expression of HBD (hormon binding domain)-deficient isoforms and to decreased GR expression [43, 44]. For this reason steroids are used in a pulsed way(for example only 4 days/month or week to avoid the continue exposure and the receptors downregulation). However, a unique theory able of explaining steroid refractariety has not been achieved.

**Lenalidomide** IMiDs (Immuno Modulatory Drugs) CC-5013 (Revlimid TM, Lenalidomide) and CC-4047 (ActimidTM, Pomalidomide) are a series of synthetic compounds derived using structural modifications of glutamic acid derivative (Thalidomide) with anti-angiogenic properties and potent anti-inflammatory effects owing to its anti-TNF-$\alpha$ activity [36, 28]. Research into the mechanism of action of Thalidomide revealed an immunological and immunomodulatory basis for the effect, notably inhibition of denovo IgM antibody synthesis, by

possibly affecting the macrophages, B-cells, helper or suppressor lymphocytes, decreasing TNF-$\alpha$ synthesis and modulating the T cell subsets by increasing the T-helper population after therapy [45, 46]. Lenalidomide has been shown to inhibit production of pro inflammatory cytokines TNF-$\alpha$, IL-1, IL-6, IL-12 and elevate the production of anti-inflammatory cytokine IL-10 from human peripheral blood mononuclear cells (PBMCs). The downregulation of TNF-$\alpha$ secretion is particularly striking and is up to 50,000 times more when compared to thalidomide [47]. Although the precise mechanism of TNF-$\alpha$ down regulation by lenalidomide is not known, it is likely related to a transcriptional effect, similarly to that observed with thalidomide, able of increasing the degradation of TNF-$\alpha$ mRNA. Effects on apoptosis in MM cells is secondary to increased potentiation of TNF-elated Apoptosis inducing ligand (TRAIL), inhibition of apoptosis protein-2, increased sensitivity to Fas mediated cell death, and up regulation of caspase-8 activation, down regulation of caspase-8 inhibitors (FLIP, cIAP2), down regulation of NFkB activity and inhibition of pro survival effects of IGF-1. The synergic effect of old and new drugs can be explained by their different abilities to trigger apoptosis in neoplastic plasmacells involving different targets: IMiDs predominantly trigger caspase-8 apoptotic signaling, while dexamethasone uses caspase-9-mediated cell killing (as summarised in fig.1.3).

**Bortezomib** The dipeptide boronic acid Bortezomib (formerly, PS-341; marketed as Velcade by Millennium Pharmaceuticals) is the first-in-class proteasome inhibitor of 26S proteasome activity. Bortezomib acts directly on MM cells to induce apoptosis of MM cells resistant to known conventional therapies, overcomes the protective effects of IL-6, and adds to the anti-MM effects of dexamethasone (fig.1.3) by affecting cytokine circuits, cell adhesion and angiogenesis in BM microenvironment [28]. However, there are several experimental evidences that Bortezomib may also act to switch mechanisms different from the simple inhibition of NFkB and it is not clear if there is a correlation between the NFkB status and the response to Bortezomib [33, 35].

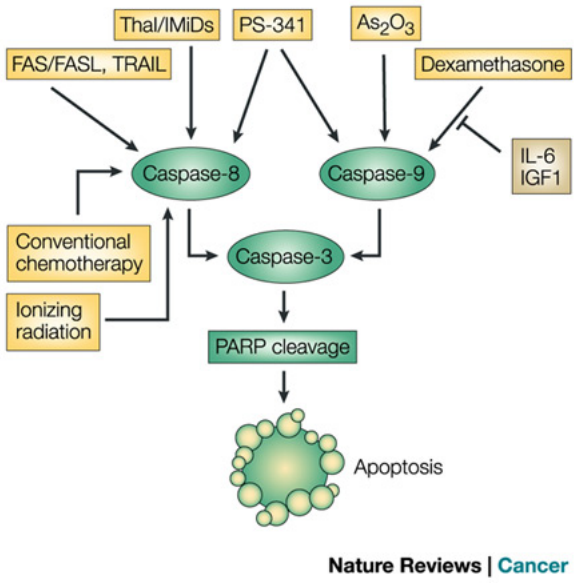


Fig. 1.3: Ionizing radiation, conventional chemotherapy, FAS/FASL, TRAIL and thalidomide/IMiDs trigger caspase-8 activation, whereas As2O3 and dexamethasone trigger caspase-9 activation. Bortezomib induces both the caspase-8 and caspase-9 apoptotic pathways. Interleukin-6 (IL-6) and insulin-like growth-factor 1 (IGF1) activate the phosphatidylinositol 3-kinase (PI3K)/AKT cascade, which inhibits caspase-9/caspase-3 apoptotic signalling. IMiDs, immunomodulatory derivatives; PARP, poly-(ADP-ribose) polymerase; TRAIL, tumour necrosis factor TNF-related apoptosis-inducing ligand. Adapted from [47].

### 1.2.2 *Multiple Myeloma bone disease*

Bone disease is a mjor cause of morbidity in MM and results in many of the debilitating features of the disease, with high impact on the overall quality of life of our patients. In some series, more than 50% presented vertebre fractures and up to 30% with non vertebral fractures, 60% generalized osteopenia, of which 5% without associated lytic lesions [48, 49].

The integrity of the skeleton, including its initial morphogenesis and the bone remodeling that occurs throughout life, requires the coordinated regulation and activity of bone-forming cells (osteoblasts) and bone-resorbing cells (osteoclasts). Disregulated activities between the 2 cell types can result in severe skeletal abnormalities, characterized by either decreased or increased bone mass. The number of active osteoclasts is determined by the net result of dif-

ferentiation and fusion of osteoclast precursors and by the loss of osteoclasts through apoptosis. An increase in active osteoclast pool size, with increased bone resorption and decreased bone mass, occurs in many osteopathic disorders, including postmenopausal osteoporosis, Paget's disease, lytic bone metastases and MM related bone disease.

In effects, MM-related bone disease is consequent to an uncoupled osteoblast inactivation and osteoclast activation adjacent to tumor foci within bone. Histologic studies of bone biopsies show that increased osteoclast activity occurs adjacent to MM cells, including aberrancies in genome and acquired mutations, as consequence of either contact or secretion of growth factors [50]. There is a vicious cycle in which the bone resorptive process releases growth factors that increase MM tumor burden that in turn results in increased bone destruction. In addition, adhesive interaction between MM cells and cells of the bone marrow microenvironment result in production of factors, which also increase angiogenesis and make the cells more chemotherapy resistant [51].

## 1.3 Serotonin metabolism

The monoamine serotonin [5-hydroxytryptamine (5- HT)] is found in the central nervous system, gastrointestinal tract, and blood with broad physiological functions.

As a neurotransmitter it is involved in cognition, feeding behavior, mood, anxiety, aggression and pain, sexual activity, sleep, and other body rhythms; playing as hormone serotonin regulates vascular tone and intestinal activity. These actions are mediated through interaction with membrane-bound receptors, which are categorized into 7 families (5HT1-7) with at least 21 subtypes [52, 53]. Overall, serotonin receptors are coupled to G-proteins with the exception of 5HT3, which is an ionotropic receptor [53], for example 5-HT may increase IL-6 production by stimulating 5-HT2BR [54].

Non-receptor-mediated serotonin mechanisms of action have been described as well. For example, in neuronal cells oxidative metabolism of the monoamines

has been implicated in apoptosis [55]. In immune cells, a serotonin-associated induction of apoptosis depends on the uptake of serotonin (via 5-HT transporters) independent of intracellular oxidative transformation [56] and can be modulated by selective serotonin reuptake inhibitors [57].

Serotonin is the product of a multistep metabolic pathway showed in fig. 1.4).

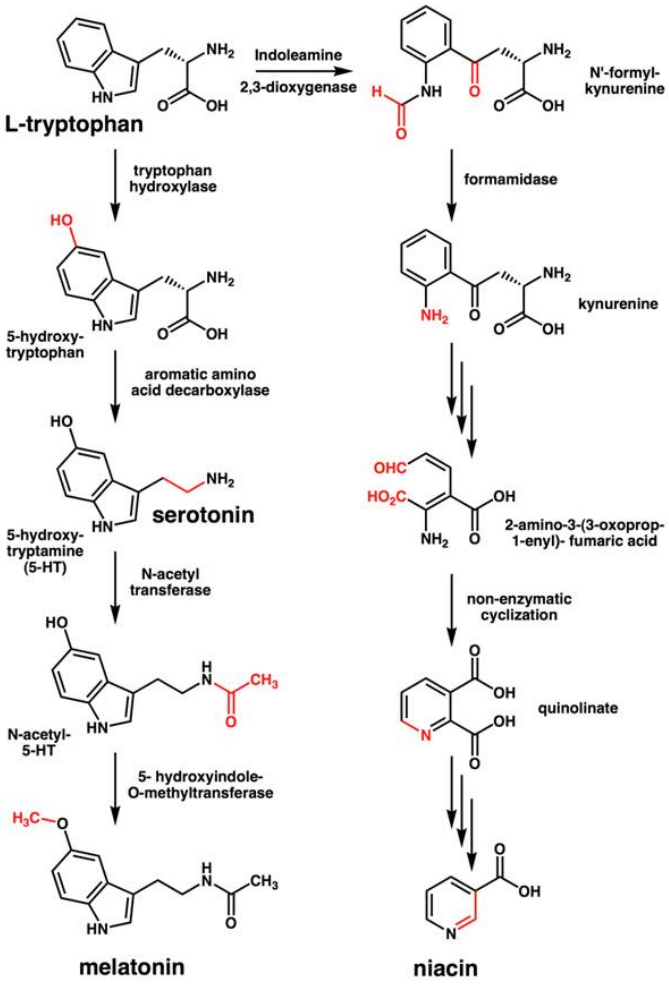


Fig. 1.4: The metabolic pathway of serotonin synthesis. Explanation in the text and reviewed in [58]

.

Serotonin is synthesized from the amino acid L-tryptophan, an essential amminoacid that can cross membrane thanks to non specific transporter LAT-1,

by two enzymes: amino acid decarboxylase (DDC) and tryptophan hydroxylase (TPH) [58]. Although decarboxylase activity is ubiquitous in peripheral tissues, the reaction catalysed by TPH is the rate-limiting step. TPH has been shown to exist in two forms: the brain-specific isoform TPH2 [59] and the peripheral one TPH1. Serotonin released into the blood is actively taken up by platelets and stored in their solid granules; there is active uptake of serotonin by lymphocytes via serotonin transporters [60], aberrantly expressed universally in B-cell neoplasms [61]. Plasma serotonin is cleared by the liver and lung endothelial cells, where serotonin is stored in vesicles until released or converted (by deamination) into 5-hydroxyindoleacetaldehyde through the action of mitochondrial monoaminooxidase (MAO). In turn, 5-hydroxyindoleacetaldehyde may be oxidized to 5-hydroxyindole acetic acid, by aldehyde dehydrogenase, or reduced to 5-hydroxytryptophol, by alcohol dehydrogenase.

Extracellular levels of 5-HT are determined by the 5-HT transporter (5-HTT or SERT, coded by the gene SCL6A4), which is involved in the uptake and clearance of extracellular 5-HT. Serotonin itself does not cross the blood-brain barrier, differently from its precursors tryptophan 5-hydroxytryptophan (5-HTP) that can and do cross the blood-brain barrier. Platelets serve as the major reservoir of serotonin in the bloodstream and the treatment with Selective Serotonin Uptake Inhibitors (SSRIs) dramatically reduces platelet serotonin concentrations [62]. When activated, platelets release serotonin into the bloodstream where it acts as a powerful vasoconstrictor. Thus, 2 serotonin systems exist: one known as brain-derived serotonin system (BDSS), active at level of central nervous system and one peripheral, mainly under the control of platelet-derived serotonin (PDSS), both under control of tryptophan availability and TPH1 activity.

Under physiological conditions, TPH1 expression is limited to a few specialized tissues: raphe neurons, pinealocytes, mast cells, mononuclear leukocytes, beta-cells of the islets of Langerhans, and intestinal and pancreatic enterochromaffin cells [63]. However several solid cancer cell types (breast, lung, cholangiocarcinoma)show an aberrant expression of TPH1 [64]. Similarly, LAT-1 is

overexpressed in cancer cells [65], and more in general serotonin system seems to be involved in cancer progression and metastasis. Role for serotonin in carcinogenesis [64] has been reported in skin [66], breast [65], lung [67], prostate [68], and colon cancer [69]. In a fascinating working model, tumour progression could be substained acquire genetic or epigenetic alterations in 5-HT signaling which then make them resistant to suppressive 5-HT actions and favor tumor-promoting actions (e.g., dynamic cell junctions and cell shedding), as well as acquisition of new receptors and functions (e.g., stimulated proliferation and epithelial-mesenchymal transition), in a similar way proposed for the TGF-$\beta$, as shown in Fig.1.5.

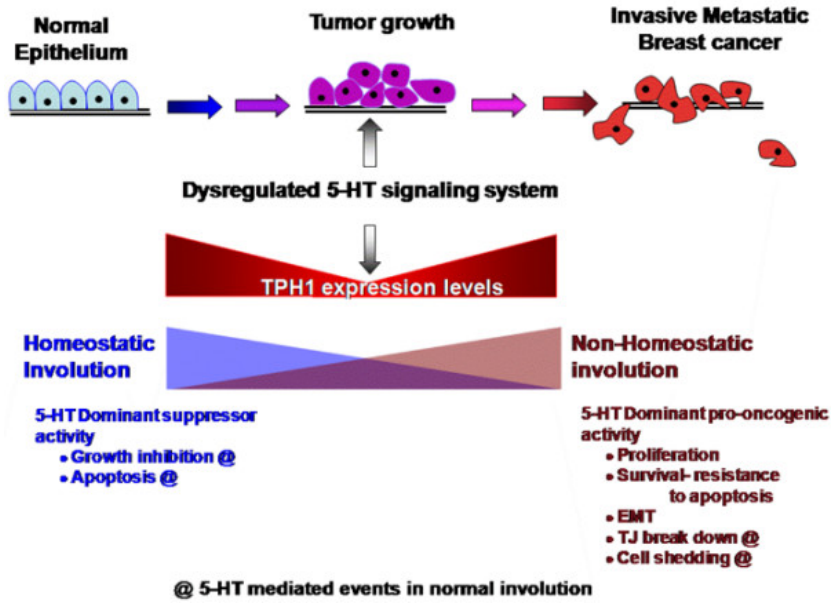


Fig. 1.5: Double behavior of Serotonin in promoting cancer, from [65]

In cancer progression, the amminoacid metabolism changes. In several solid cancers [70], the tumour metabolism is supported by the recruitment and enhanced expression of neutral amino acid transporters, included LAT-1 and 4F2hc, following the induction of aberrant growth factors receptors present on the membrane [71] and regulated by mTOR activation status. For example, in vascular smooth muscle the induction of LAT1 by PDGF was dependent on mTOR activity and de novo RNA and protein synthesis [72]. In a murine T-cell

line, growth factor withdrawal led to the endocytosis of CD98 and other nutrient transporters; however, the growth factor requirement was circumvented by expression of a constitutively active Akt isoform, whose maintenance of cell surface 4F2hc was rapamycin-sensitive, implicating mTOR role [73]. Another group, using microarray analysis to study lymphoma cells, confirmed that rapamycin treatment selectively downregulates LAT1 and 4F2hc[74].

With respect to the mechanism of bone loss from sympathetic activity, activated adrenergic receptors on osteoblasts suppress critical transcription factors necessary for bone formation but also enhance osteoclastogenesis, principally by up-regulating the osteoclast differentiation factor RANKL. This is not a diversion of osteoblasts to osteoclasts, but rather a dynamic process of coupling that involves two cell types originating from distinct progenitor cells.

The brainstem-derived serotonin (BDS) favors bone mass accrual following its binding to Htr2c receptors on ventromedial hypothalamic neurons. Leptin inhibits these functions and increases energy expenditure because it reduces serotonin synthesis and firing of serotonergic neurons. This pathway is counterbalanced by noradrenalin at level of neurological synapses of the bone, as showed in figure 1.6 and reviewed in [75, 76].

Immunoglobulins have been shown to induce platelet release a) when participating in immune reactions as antigen-antibody complexes or b) by nonimmune mechanisms such as coating of glass or polymethylmethacrylate beads. More interestingly, aggregated immunoglobulins of all the IgG subclasses, isolated from healthy controls or myeloma patients, induce platelet release in the absence of antigen or particulate matter, in a dose dependent manner [78].

The concentration of serum tryptophan, quinolinic acid, and serotonin was increased in the plasma, while that of tyrosine, dopamine, and noradrenaline was decreased in multiple myeloma [79].

No evidences have been reported until now about serotonin involvement in MM. Our group demonstered fort the first time increased levels of serotonin in bone.

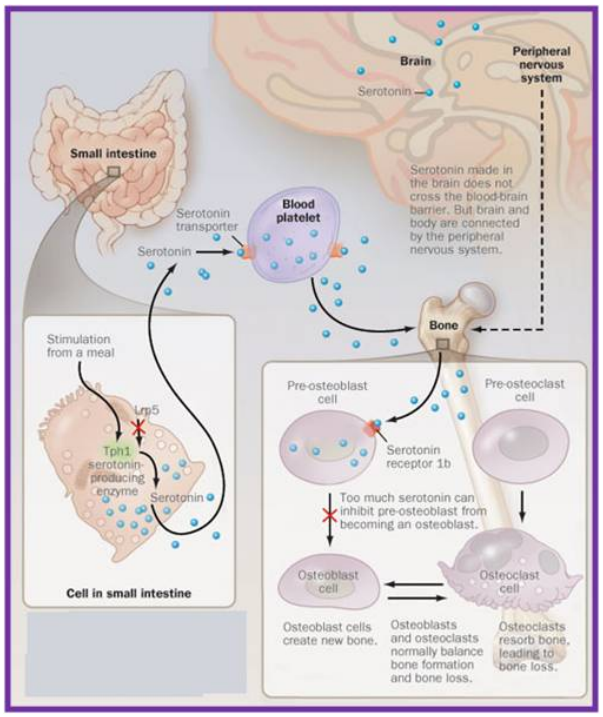


Fig. 1.6: Serotonin regulates bone accrual. Adapted from [77].

# Chapter 2

# Methods

## 2.1 High-throughput genomic analysis: Affymetrix SNP 6.0 assay and CNV determination

Today, in addition to high resolution chromosome banding and advanced chromosomal imaging technologies, chromosome aberrations in cancer cells can be analyzed with an increasing number of large-scale, comprehensive genomic and molecular technologies such as fluorescence in situ hybridization (FISH), spectral karyotyping (SKY), comparative genomic hybridization (CGH), and other high-throughput methods. Among them, array-based karyotyping can be done with several different platforms, both laboratory-developed and commercial [80].

The arrays themselves can be *genome-wide*(probes distributed over the entire genome) or *targeted* (probes for genomic regions known to be involved in a specific disease) or a combination of both. Arrays used for karyotyping may use non-polymorphic probes, polymorphic probes (i.e., SNP-containing), or a combination of both. Non-polymorphic probes can provide only copy number information, while SNP arrays can provide both copy number and loss-of-heterozygosity (LOH) status in one assay. The probe types used for non-polymorphic arrays include cDNA, BAC clones (e.g., BlueGnome), and oligonucleotides (e.g., Agilent, Santa Clara, CA, USA or Nimblegen, Madison, WI, USA).

Commercially available oligonucleotide SNP arrays can be solid phase (Affymetrix, Santa Clara, CA, USA) or bead-based (Illumina, SanDiego, CA, USA). Despite the diversity of platforms, ultimately they all use genomic DNA from disrupted cells to recreate a high resolution karyotype in silico. The main applications of these technologies are the detection of copy number changes and evaluation LOH, Autozygous Segments, and Uniparental Disomy.

***Detection of copy number changes***

Copy number variations *(CNVs)* are segments of DNA physiologically present in the normal population at a variable copy number in comparison with a reference genome [81, 82, 83]. This broad definition for CNVs makes no reference to the clinical impact of a given genomic imbalance and can be confusing for clinical genetists who have traditionally understood chromosomal '*variants*' as being alterations that are not clinically significant. Indeed, CNVs can have dramatic phenotypic consequences as a result of altering gene dosage, disrupting coding sequences, or perturbing long-range gene regulation. For this reason, they are themselves potential predisposition factors in disease. Recent advances in genome-wide analysis of submicroscopic DNA segments (CNVs) may allow the identification of novel molecular tumor-associated abnormalities in the normal cytogenetics group (so-called *somatic CNVs*). Therefore, the term CNV is now used to describe copy number differences in studies of both disease and normal controls as well as imbalances that cause well-known microdeletion and microduplication syndromes [81, 84]. To minimize confusion, it may be justified to use qualifiers for the term 'CNV' when discussing functional or clinical significance. The terms 'pathogenic CNV', 'benign CNV' or 'CNV of unknown clinical significance' may be useful for this purpose. In this report we have chosen to call *pathogenic CNV* as *somatic CNV*, because they are present in pathologic tissue (e.g. exclusively at diagnosis) and not at remission, since we cannot establish the real pathogenicity of our findings, while the others as *germline CNV*, probably related to susceptibility, detectable either at diagnosis as at remission.

Human beings are diploid, so a normal copy number is always two for the

non-sex chromosomes:

- *Gains and deletions.* In tumour cells may represent the inactivation of a tumour suppressor gene, and may have diagnostic, prognostic, or therapeutic implications. A deletion is the loss of genetic material, either heterozygous (if copy number of 1) or homozygous (when copy number is 0, nullisomy). On the opposite, a copy number gain represents the gain of genetic material. If the gain is of just one additional copy of a segment of DNA, it may be called a duplication. If there is one extra copy of an entire chromosome, it may be called a trisomy;

- *Amplifications.* Technically, an amplification is a type of copy number gain in which there is a copy number 10. In the context of cancer biology, amplifications are often seen in oncogenes. This could indicate a worse prognosis, help categorize the tumor, or indicate drug eligibility. An example of drug eligibility is Her2Neu amplification and Herceptin [85].

***Evaluation of Loss of Heterozygosity (LOH), Autozygous Segments, and Uniparental Disomy***

Autozygous segments and uniparental disomy (UPD) are diploid/'copy neutral' genetic findings and therefore are only detectable by SNP-based arrays. Both autozygous segments and UPD show loss of heterozygosity (LOH) with a copy number of two by SNP array karyotyping.

- *Autozygous segment.* An autozygous segment is bi-parental and seen only in the germline. They are extended runs of homozygous markers in the genome, and they occur when an identical haplotype block is inherited from both parents. They are also called *'identical by descent'* (IBD) segments, and they can be used for homozygosity mapping.

- *Uniparental Disomy (UPD).* UPD occurs when both copies of a gene or genomic region are inherited from the same parent. This is uniparental, in contrast to autozygous segments which are bi-parental. When present in the germline, they can be harmless or associated with disease, such as

Prader-Willi or Angelman syndromes. Also in contrast to autozygosity, UPD can develop in tumor cells, and this is referred to as acquired UPD or copy neutral LOH in the literature. Acquired UPD is quite common in both hematologic and solid tumors, and is reported to constitute 20 to 80% of the LOH seen in human tumors. Acquired UPD can serve as the second *hit* in the *Knudson Two Hit Hypothesis of Tumorigenesis*, and thus can be the biological equivalent of a deletion.

#### *The Affymetrix SNP 6.0 array*

In this work we present data obtained with the commercially available SNP 6.0 array, released by Affymetrix, based on oligonucleotide probes homologous to areas located throughout human genome. DNA probes are designed to distinguish various genotypes, and their distribution is dictated by the location of the SNPs [86, 87]. Areas known to contain more SNPs can be better covered, whereas, as expected, the resolution within *SNP deserts* is poor.

The chip contains more than 1.8 million markers of genetic variation. Approximately 482,000 SNPs are derived from the previous-generation Mapping 500K and SNP 5.0 Arrays. The remaining 424,000 SNPs include tag SNP markers derived from the International HapMap Project, SNPs on chromosomes X and Y, mitochondrial SNPs, SNPs in recombination hotspots and new SNPs added to the dbSNP database after completion of the Mapping 500K Array. The array also contains 202,000 probes targeting 5,677 known regions of copy number variation from the Toronto Database of Genomic Variants. These regions resolve into 3,182 distinct, non-overlapping segments, each interrogated with an average of 61 probes. In addition to the interrogation of these regions of known copy number polymorphism, more than 744,000 probes were chosen, evenly spaced along the genome, to enable the detection of novel CNV. The median inter-marker distance taken over all 1.8 million SNP and copy number markers combined is less than 700 bases (680 bp).

The protocol (schemed in figure 2.1) suggested by the manufacturer has been designed to improve the signal-to-noise ratio: DNA was first digested

with restriction enzymes, then ligated to adapters and amplified. During the PCR amplification only the smaller restriction fragments (up to about 1.2 kbp, 200-1100bp size range) were amplified, reducing the complexity (but also the representation) of DNA.

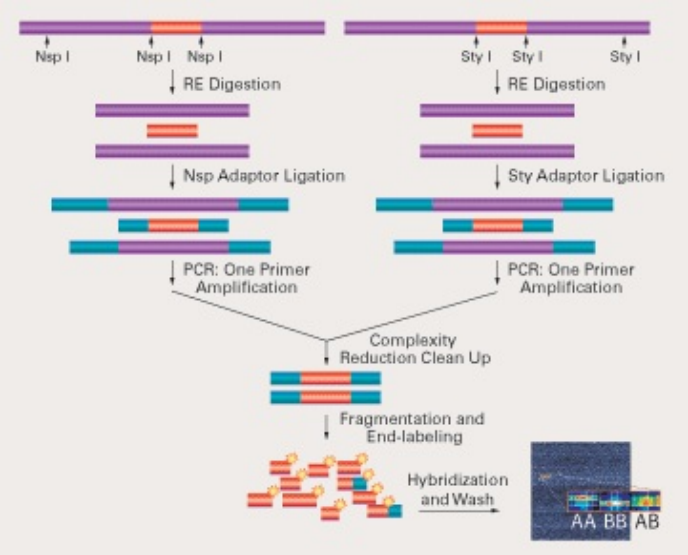


Fig. 2.1: ***Genotyping Mapping Assay Overview***: probes are chosen from restriction digestion fragments selected in order to reduce target complexity before labeling and hybridization.

The main stages are:

1. *DNA extraction*: Genomic DNA was extracted using the DNA Blood Mini kit (Qiagen, Valencia, CA, USA) from mononuclear cells isolated from bone marrow aspirate samples by Ficoll gradient centrifugation. DNA quantity and quality were assessed using the NanoDrop 1000 Spectrophotometer (Thermo Scientific,) and for selected cases by agarose gel electrophoresis. The high quality DNA is a critical step, since PCR inhibitors, including high concentrations of heme (from blood) or chelating agents (i.e., EDTA) or salts, used to precipitate DNA during extraction, can interfere with the restriction enzymes of following steps;

2. *Digestion*: two aliquots of each DNA sample (5.00 uL at concentration of 50 ng/uL, totally 500 ng) were digested by two restriction enzymes, Nsp I

and Sty I, capable of recognising specific sequences (5' RCATG Y 3' and 5'C/CWWGG 3' respectively) to obtain fragments in the 200 to 1,100 bp size range, compatible with the distribution of SNPs on the array in the human genome. With this approach, it is possible to obtain a set of fragments which guarantee a large coverage of the whole genome (70-80%), except telomers and centromers, characterised by a low SNPs rate;

3. *Ligation*: all fragments resulting from restriction enzyme digestion, regardless of size, were ligated to two annealed oligonucleotides (which act as adaptators), capable of recognizing the cohesive 4 bp overhangs derived from Nsp l or Sty l restriction site. The key enzyme is the T4-DNA ligase, typical of bacteria infected by T4 phagus, which uses ATP as cofactor and can ligate only sharp extremities. This step is needed for the next PCR, so that a generic primer could recognize the adaptor sequence to amplify adaptor-ligated DNA fragments;

4. *PCR*: it was performed to select and amplify fragments, using a single primer with the TITANIUMTM DNA Amplification Kit (Clontech Laboratories, Inc. Montain View, CA). The reaction conditions have been optimized to preferentially amplify fragments in the 200 to 1,100 bp size range, which guarantee from 30% to 50% genome coverage. The fragments size range was confirmed by an agarose gel running;

5. *Purification*: PCR products were purified with Agencourt AMPure Magnetic Beads (Agencourt Bioscience Corporation, Beverly, MA) and the amplicons were quantified using a NanoDrop-1000 spectrophotometer.

6. *Labelling*: fragmented PCR amplicons were end-labelled with a specific proprietary biotin-labeled reagent by a Terminal Deoxynucleotidyl Transferase for 4 hours and finally hybridized at $50^0$C overnight (16-18 hours)in a GeneChip Hybridization Oven 640 (Affymetrix, Inc.);

7. *Washing*: chips were washed for several minutes in decreasing salt buffers, stained and dried in a GeneChip Fluidics Station 450 (Affymetrix, Inc.).

Arrays were scanned with a GeneChip Scanner 3000 7G (Affymetrix, Inc.) and a raw file was generated for each of them. Data coming from scansion were analysed using Affymetrix Genotyping Console(GTC) version 3.0.1, which implements the novel genotype calling algorithm *Birdseed*, which performs a multiple-chip analysis to estimate signal intensity for each allele of each SNP, fitting probe-specific effects to increase precision. Anyway, the reduced complexity of the hybridization brings with it the possibility of amplification bias of different regions of the genome and detection of changes reflecting differences in restriction digestion patterns between individuals rather than in true copy number.

The following algorithms were used: 1) SNP 6.0 Birdseed v2 algorithm for genotyping; 2) BRLMM-P-Plus algorithm and Hidden Markov Model with regional GC correction for copy number analysis; 3) the LOH algorithm. As a quality control of the genotyping and copy number results Contrast QC value and Median Absolute Pairwise Difference (MAPD) were calculated as implemented in the GTC 3.0.1 software. The log2ratio between signal for each marker in each sample and the corresponding median value in a reference group (270 HapMap individuals) provided an estimate of copy number. The log2ratio has been smoothed using a Gaussian kernel to lower noise to improve per marker Signal to Noise ratio at the expense of blurring boundaries where copy number state changed. For each marker, the smooth was constructed using a weighted mean of the log2ratios of surrounding markers with weights proportional to the Gaussian transform of their genomic distance from that marker. The Gaussian transform had standard deviation equal to 50000. The *allele difference value* was evaluated as the difference of allele A signal and allele B signal each standardized with respect to their median values in the reference HapMap population. A script in Python was implemented in order to calculate the percentage of overlap between the segments revealed at diagnosis and those at remission and to identify tumor-associated somatic CNA.

## 2.2 *Metaphase Cytogenetics*

Cytogenetic analysis was performed on metaphase cells obtained from unstimulated 24 hours culture of patients bone marrow. Cells were treated with colcemid for 1 hour, with hypotonic for thirty minutes and than fixed in methanol and acetic acid. Metaphase preparations were G-banded using standard trypsin method. The Karyotypic results were described according to the International System for Human Cytogenetic Nomenclature (ISCN 1995-2005). FISH was performed using a whole chromosome paint 8 (WCP) probe (Cambio, U.K.) and a two color, two fusion traslocation probe t(15;17) (Cancer Genetic, Inc., Rutherford, NJ). Co-denaturation was performed for 5 min at $72^0$C. Hybridization was done overnight. Slides were post hybridisation washed according to the manufacturers instruction and counterstained with 4,6-doamidino-2-phenylindole (DAPI). The preparations were observed with a BX51 Olympus microscope equipped with Olympus filters (Texas Red, FITC, DAPI and Triple-band), a CCD 1300 QDS camera and Applied Spectral Imaging (ASI) BandView5.5 Karyotyping and FISH Software.

## 2.3 *c-Cbl mutational status screening*

Direct genomic DNA sequencing was performed as previously described in [88]. Exons 7, 8, and 9 from genomic DNA were amplified using the following primer sets:

- 7F, 5-ACACCACGTTGCCCTTTTAG-3;
- 7R, 5-GTCAATGGGTTCCAATGAAT-3;
- 8F,5-GGACCCAGACTAGATGCTTTCT-3;
- 8R, 5-8GAAAATACATTTCCTAGAGATCAAAAA-3;
- 9F,5-CTGGCTTTTGGGGTTAGGTT-3;
- 9R, 5-TCGTTAAGTGTTTTACGGCTTT-3.

PCR reaction conditions were as follows: 94°C for 4 min, 30 cycles of 94°C for 30 s, 48.5°C for 30 s, and 72°C for 30 s; 1 cycle at 72°C for 5 min. PCR products were sequenced by standard dideoxy chain termination procedure with the Abi Prism 377 automatic sequencer in both directions.

## 2.4 *Multiplexed ex vivo assay for the detection of proteomic profile in MM*

A workflow using protein kinase signal pathway mapping technology was developed [89] for the *ex vivo*, short-term drug treatment of fresh, living human multiple myeloma (MM) bone marrow aspirate tumor cells, compared to non MM bone marrow cells for the same patient.

Bone marrow aspirates were immediately subdivided and treated *ex vivo* with a panel of molecular inhibitors that target a wide range of cellular pathways (e.g. protein degradation, cell proliferation/survival, insulin response, protein translation). In set A (including GMU samples, collected at Virginia Cancer Specialists, Fairfax, VA) we explored changes occurred after exposure to tyrosine kinase inhibitors with a well-defined target on the cancerous cell (e.g. the c-kit inhibitor Imatinib or the multikinase inhibitor Sorafenib), while in set B ((including CT samples, collected at Division of Hematology, Ospedale Ferrarotto, Catania) was evaluated the predictive ability of the assay, treating the cells with drugs routinely used in clinical practice (dexamethasone, lenalidomide, bortezomib). Clinical characteristics of enrolled patients are summarised in table 2.1 (for set A) and 2.2 (for set B).

Specifically, IOOuL bone marrow aspirate was mixed with 200uL RPMI-1640 serum free media (ATCC) either alone or in combination with specific kinase inhibitors, drugs, or ligands. The inhibitors listed in Table 2.3 were evaluated.

Drugs were dissolved in dimthyl sulfoxide (DMSO) to prepare stock solutions. The final concentration of DMSO was kept at 0.1% for all the assays.

Table 2.1: Clinical characteristics of patients included in set A

| Patient | Sex | Age | | Isotype | Stage ISS | Status disease | Last treatment |
|---|---|---|---|---|---|---|---|
| 09-180-B | M | 55 | MGUS | IgG$\kappa$ | n.a. | | |
| 10-081-A | M | 65 | MGUS | IgG$\kappa$ | n.a. | | |
| 08-305-A | M | 51 | MM | IgG$\kappa$ | 1 | naïve | |
| 08-312-A | M | 75 | MM | $\lambda$ | 3 | naïve | |
| 09-030-A | M | 81 | WD | IgM | 2 | naïve | |
| 09-033-A | F | 83 | MM | IgG$\kappa$ | 1 | naïve | |
| 09-180-A | M | 78 | MM | IgG$\kappa$ | 2 | naïve | |
| 09-219-A | F | 62 | MM | IgG$\kappa$ | 3 | naïve | |
| 09-226-A | M | 61 | MM | IgG$\kappa$ | 3 | naïve | |
| 09-226-B | M | 44 | MM | IgG$\lambda$ | 3 | naïve | |
| 09-232-A | M | 63 | MM | IgG$\kappa$ | 2 | naïve | |
| 10-146-A | M | 62 | MM | IgA$\kappa$ | 3 | naïve | |
| 10-125-A | M | 73 | MM | $\kappa$ | 1 | naïve | |
| 10-025-A | M | 60 | sMM | IgG | 1 | naïve | |
| 08-259-A | M | 57 | MM | IgG | 1 | relapse | Rd, EBMT |
| 08-292-A | M | 58 | MM | IgA$\kappa$ | 1 | relapse | Rd, EBMT |
| 08-302-A | M | 62 | MM | IgG$\kappa$ | 1 | relapse | Rd, EBMT |
| 08-302-B | M | 44 | MM | IgG$\kappa$ | 2 | relapse | Dexamethasone |
| 08-310-A | M | 59 | MM | IgG | 3 | relapse | TD |
| 08-322-A | M | 55 | MM | IgA$\kappa$ | 3 | relapse | BMT |
| 08-336-A | F | 59 | MM | IgA | 3 | relapse | Rd |
| 08-339-A | M | 61 | MM | IgG$\lambda$ | 2 | relapse | Rd |
| 09-008-A | F | 68 | MM | IgG | 2 | relapse | Rd |
| 09-261-A | M | 46 | MM | IgG | 1 | relapse | BMT |
| 10-138-A | F | 72 | MM | $\lambda$ | 1 | relapse | Bortezomib, Lenalidomide, BMT |
| 10-146-B | M | 71 | MM | IgA$\kappa$ | 1 | relapse | VMP |
| 09-266-A | F | 64 | MM | IgG$\kappa$ | | follow up | BMT |
| 10-013-A | F | 65 | MM | IgG$\lambda$ | | follow up | VTD |
| 10-007-A | M | 62 | MM | IgG | | follow up | Thalidomide, Dexamethasone |
| 10-074-A | F | 71 | MM | IgG$\lambda$ | | follow up | Lenalidomide, Dexamethasone |
| 10-075-A | M | 61 | MM | $\lambda$ | | follow up | Lenalidomide, Dexamethasone |
| 10-055-A | M | 64 | MM | IgG$\kappa$ | | follow up | BDR |
| 10-050-B | F | 63 | MM | $\lambda$ | | follow up | Support only |
| 10-050-A | M | 57 | MM | IgG | | follow up | Bortezomib, Lenalidomide, Thalidomide |

Table 2.2: Clinical characteristics of patients included in set B

| Patient | Sex | Age | | Isotype | Stage ISS | Status disease | Last treatment |
|---|---|---|---|---|---|---|---|
| MM-CT-17 | F | 49 | MGUS | IgA$\kappa$ | | naïve | |
| MM-CT-20 | M | 52 | MM | IgG$\kappa$ | 1 | naïve | |
| MM-CT-21 | F | 58 | MM | IgG$\kappa$ | 3 | naïve | |
| MM-CT-05 | F | 49 | MM | $\lambda$ | 2 | naïve | |
| MM-CT-06 | M | 48 | MM | IgA$\kappa$ | 2 | naïve | |
| MM-CT-07 | F | 47 | MM | IgA$\kappa$ | 1 | naïve | |
| MM-CT-09 | M | 59 | MM | IgG$\kappa$ | 3 | naïve | |
| MM-CT-13 | M | 67 | MM | IgA$\kappa$ | 1 | naïve | |
| MM-CT-16 | M | 67 | MM | IgA$\kappa$ | 1 | naïve | |
| MM-CT-18 | M | 78 | MM | IgG$\kappa$ | 2 | relapse | Bortezomib, Dexamethasone |
| MM-CT-23 | M | 76 | MM | $\lambda$ | 3 | relapse | Bortezomib, Thalidomide, Dexamethasone |
| MM-CT-24 | M | 76 | MM | IgG$\kappa$ | 3 | relapse | Bortezomib, Thalidomide, Dexamethasone |
| MM-CT-14 | M | 38 | MM | IgA$\lambda$ | 1 | relapse | Bortezomib, Dexamethasone |
| MM-CT-02 | M | 62 | MM | IgG$\kappa$ | 3 | refractory | Lenalidomide, Dexamethasone, Dasatinib |
| MM-CT-15 | M | 52 | MM | IgA | n.a. | follow up | Lenalidomide, Dexamethasone |
| MM-CT-10 | F | 57 | MM | IgA$\kappa$ | n.a. | follow up | Lenalidomide, Dexamethasone |
| MM-CT-11 | F | 78 | MM | IgA$\kappa$ | n.a. | follow up | Melphalan, Bortezomib, Prednisone |
| MM-CT-12 | F | 53 | MM | IgG$\kappa$ | n.a. | follow up | Lenalidomide, Dexamethasone |
| MM-CT-08 | F | 46 | MM | $\kappa$ | n.a. | follow up | Lenalidomide, Dexamethasone |
| MM-CT-01 | M | 56 | MM | IgA$\kappa$ | n.a. | follow up | Lenalidomide, Dexamethasone, EBMT |
| MM-CT-03 | M | 54 | MM | IgG$\kappa$ | n.a. | follow up | Lenalidomide, Dexamethasone |
| MM-CT-04 | F | 62 | MM | IgG$\kappa$ | n.a. | follow up | Lenalidomide, Dexamethasone |
| MM-CT-22 | F | 78 | MM | $\kappa$ | n.a. | follow up | Lenalidomide, Dexamethasone |
| MM-CT-19 | M | 47 | MM | IgG | n.a. | follow up | Lenalidomide, Dexamethasone |

Table 2.3: Drugs used for ex vivo assay

| Drug | Stock Solution | Drug | Stock Solution |
|---|---|---|---|
| **Bortezomib** | 10mM | **Dasatinib** | 1.6 mM |
| **Lenalidomide** | 30mM | **Erlotinib** | 1.6 mM |
| **Thalidomide** | 100 mM | **Imatinib** | 1.6 mM |
| **Pomalidomide** | 100 mM | **Dexamethasone** | 85uM |
| **Imatinib** | 10mM | **IGFR inhibitor** | 4.6mM |
| **Dasatinib** | 100mM | **Rapamycin** | 170uM |
| **Nilotinib** | 100mM | **Bcl-2 inhibitor** | 4mM |
| **Sunitinib** | 1.6mM | **Sorafinib** | 1.6mM |
| **IL-6 ligand** | 75ng/mL | **IGF-1 ligand** | 10 ng/mL |

All treatments were performed in duplicate. One aliquot was incubated with RPMI- 1640 media only as an untreated control. The treated and untreated bone marrow aspirates were incubated overnight (about 18 hrs) with constant rotation in a 37°C incubator at ambient humidity and oxygen saturation. The overview of sample processing for both GMU and CT set is reported respectively in fig.2.2 and 2.3.

To properly elucidate deranged or hyperactive protein signaling networks within a patient's tumor, protein signatures in tissue specimens have been stabilized prior to cell sorting or separation, since RBC hemolysis, cell separation or centrifugation can perturb the signaling and confound the analysis. In one embodiment, a combination of precipitating fixative, PEG and enzyme inhibitors was used to stabilize protein signatures, to prevent the fluctuations in the cellular analytes of interest, according to [90, 91]. This solution effectively stabilizes labile signal pathway phosphoproteins accordingly to [90], preserves cell surface markers for flow cytometry analysis (see fig.2.4) and the cellular morphology for cytological diagnosis (see fig.2.5).

MM $CD138^+$ cells were separated from the non-$CD138^+$ bone marrow mi-

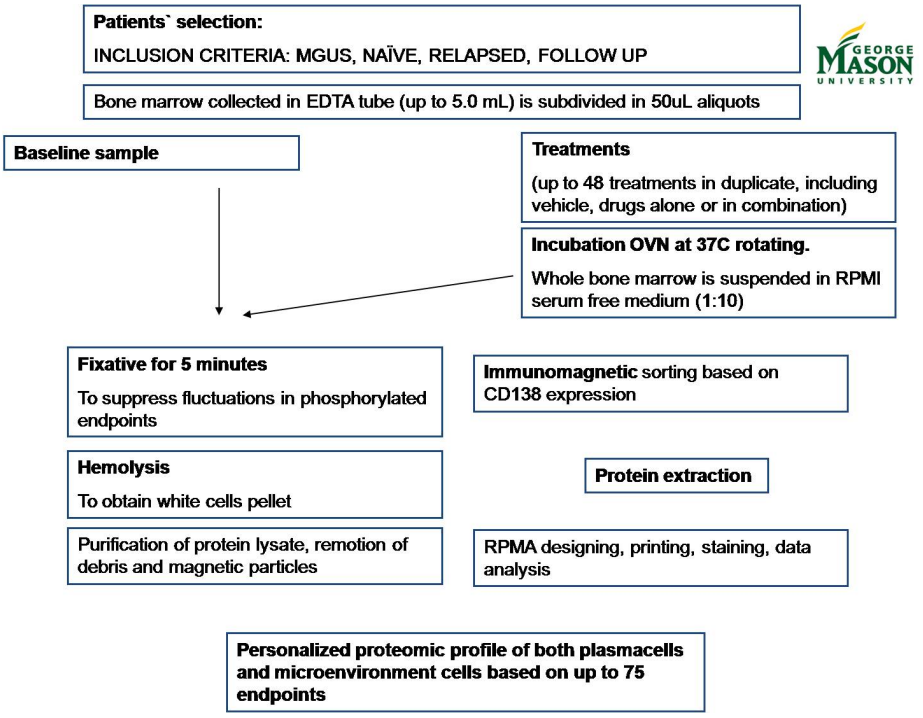


Fig. 2.2: Workflow of processing for samples of set A

croenvironment cells via immunomagnetic sorting. Briefly, cells were incubated with magnetic beads (Stem Cell Technologies) coated with antibodies against CD138 and positioned directly on top of a 48 well microtiter plate containing aligned neodymium magnets. Afterwards, the cell solution was transferred in a column placed in a strong magnetic field. In this step, cells attached to the beads (the plasmacells) remained on the column, while the bone marrow microenvironment elements (not expressing the CD138 marker) flow through. An example of worksheet used during the experiments is reported in fig.2.6.

Reverse phase protein arrays (see below, and reviewed in [92, 93, 94] were used to quantitatively map 60 to 75 signal pathway endpoints (as reviewed in [95]) in $CD138^{+}$ and $CD138^{-}$ cell populations at the same time. The impact of each treatment was measured on the selected endpoint compared to the vehicle control. Comparisons were made for the relative sensitivity between the myeloma cells and the non-myeloma cells for each endpoint and treatment. Induction of cell death was inferred by activation of a series of apoptosis pathway

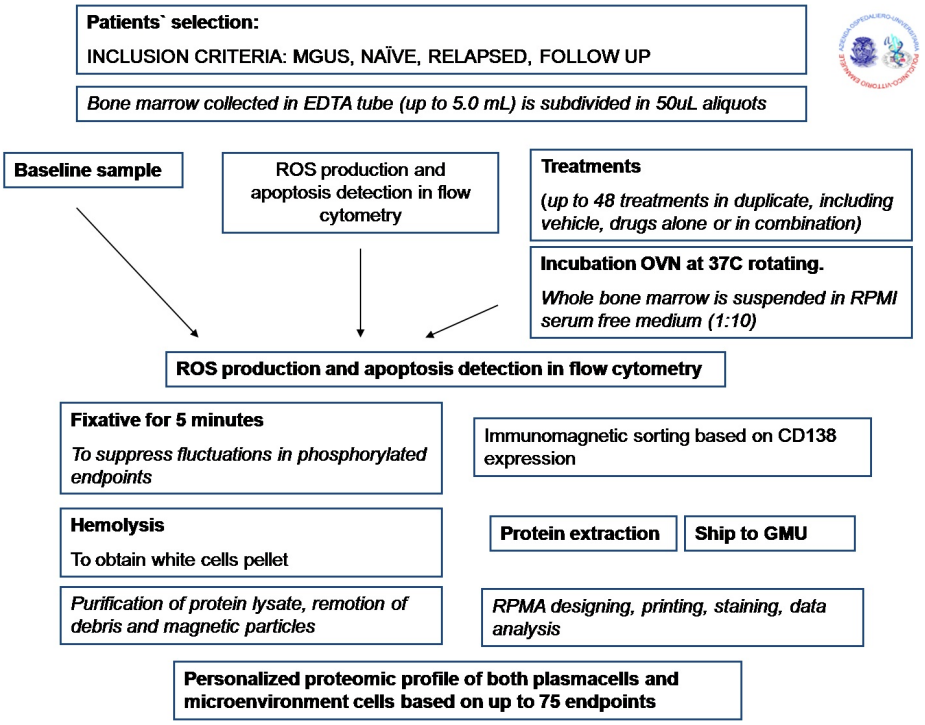


Fig. 2.3: Workflow of processing for samples of set B

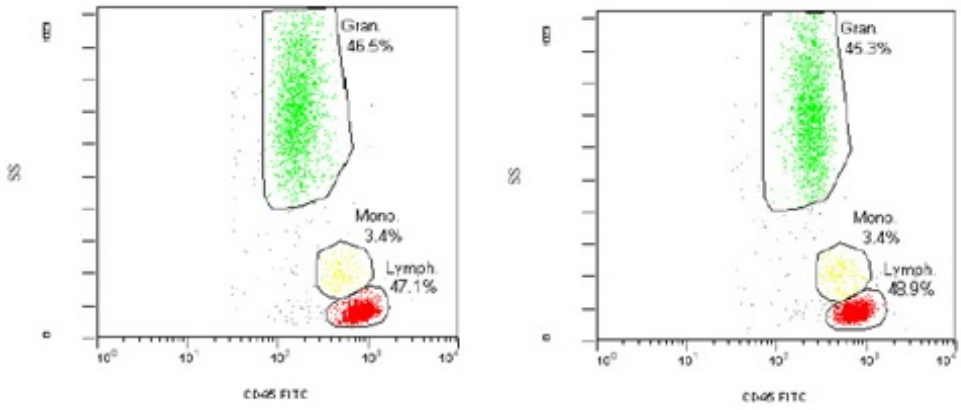


Fig. 2.4: CD45 vs Side Scatter in peripheral blood unfixed (left panel) or treated with GMU fixative for 15 minutes

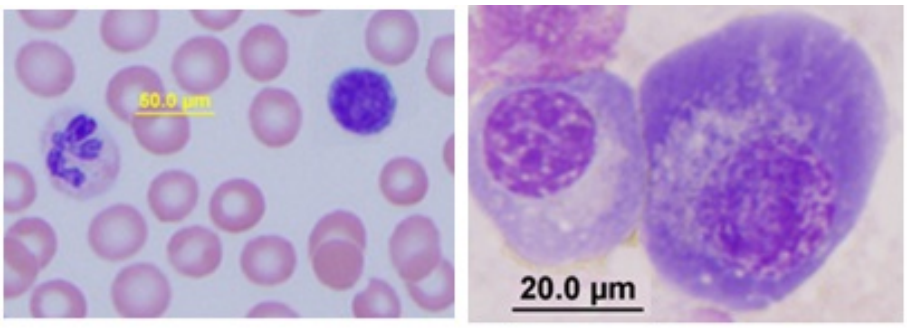


Fig. 2.5: Peripheral blood smear after treatment with GMU fixative for 15 minutes (left panel) and Plasma cells' morphology in the cytospin after treatment with GMU fixative for 15 minutes.)

| Tube | Treatment/Inhibitor | Working Stock Concentration | Amount of inhibitor to add to 100.0 µL aspirate | Volume of RMPI | Notes |
|---|---|---|---|---|---|
| A1 | Untreated Time zero (time fixed ) | Add fixative immediately post collection. Incubate 15 min. Spin 2.5min 3400rpm. Remove fixative. Wash 1x in PBS. Remove PBS, perform RBC lysis. Resuspend in 250uL RoboSep Medium. | | | |
| A2 | Untreated Time zero (time fixed ) | | | | |
| A3 | Untreated Time zero (time fixed ) | | | | |
| A4 | Untreated Time zero (time fixed ) | | | | |
| A5 | Untreated +RPMI | | | 150uL | Incubate 37°C |
| A6 | Untreated +RPMI | | | 150uL | Incubate 37°C |
| A7 | DMSO Control | undiluted | 0.75 µl | 150uL | Incubate 37°C |
| A8 | DMSO Control | undiluted | 0.75 µl | 150uL | Incubate 37°C |
| B1 | DMSO Control | undiluted | 1.5 µl | 150uL | Incubate 37°C |
| B2 | DMSO Control | undiluted | 1.5 µl | 150uL | Incubate 37°C |
| B3 | Dasatinib (10uM) | 1.6mM | 1.5ul | 150uL | Incubate 37°C |
| B4 | Dasatinib (10uM) | 1.6mM | 1.5ul | 150uL | Incubate 37°C |
| B5 | Dasatinib +Chloroquine | 1.6mM+1.9mM | 1.5uL+ 6.6uL | 150uL | Incubate 37°C |
| B6 | Dasatinib +Chloroquine | 1.6mM+1.9mM | 1.5uL+ 6.6uL | 150uL | Incubate 37°C |
| B7 | | | | 150uL | Incubate 37°C |
| B8 | | | | 150uL | Incubate 37°C |
| C1 | Imatinib (10uM) | 1.70mM | 1.5 µl | 150uL | Incubate 37°C |
| C2 | Imatinib (10uM) | 1.70mM | 1.5 µl | 150uL | Incubate 37°C |
| C3 | Nilotinib (10uM) | 3.30mM | 0.75 µl | 150uL | Incubate 37°C |
| C4 | Nilotinib (10uM) | 3.30mM | 0.75 µl | 150uL | Incubate 37°C |
| C5 | Bortezomib (100nM) | 33.0uM | 0.75 µl | 150uL | Incubate 37°C |
| C6 | Bortezomib (100nM) | 33.0uM | 0.75 µl | 150uL | Incubate 37°C |
| C7 | Bortezomib + Chloroquine | 33.0uM+1.9mM | 0.75ul+6.6uL | 150uL | Incubate 37°C |
| C8 | Bortezomib + Chloroquine | 33.0uM+1.9mM | 0.75ul+6.6uL | 150uL | Incubate 37°C |
| D7 | Dexamethasone (500nM) | 84uM | 1.5 µl | 150uL | Incubate 37°C |
| D8 | Dexamethasone (500nM) | 84uM | 1.5 µl | 150uL | Incubate 37°C |
| E1 | Lenalidomide | | | 150uL | Incubate 37°C |
| E2 | Lenalidomide | | | 150uL | Incubate 37°C |
| E3 | 0.9% Saline vehicle control | 0.9% | 0.75 µl | 150uL | Incubate 37°C |
| E4 | 0.9% Saline vehicle control | 0.9% | 0.75 µl | 150uL | Incubate 37°C |
| E3 | | | | 150uL | Incubate 37°C |
| E4 | | | | 150uL | Incubate 37°C |

Fig. 2.6: Worksheet for the treatment ex-vivo of set A

endpoints.

First 15 samples of set A were used to optimize the method, the efficiency of magnetic separation and the stability of phospo-endpoints after collection. Clinical characteristics of resting 15 patients are reported in table 3A. We had 2 main subgroups: nave patients (6/15, 40%) vs relapse/refractory (9/15, 60%).

## 2.5 The Reverse Phase Protein Microarray (RPMA)

RPMA is a micro-cell lysate dot-blot that allows measurement of protein expression levels in a large number of biological samples, simultaneously, in a quantitative manner when high-quality antibodies are available.

The name *'reverse phase'* is derived from the fact that this type of protein microarray immobilizes the protein to be analyzed. In contrast to the antibody array, where antibody probe is immobilized, in RPMA the protein lysate are denaturated prior to immobilization and thus does not do not require labeling of cellular protein lysates, thus constituting a sensitive high throughput platform for marker screening, pathophysiology investigation and therapeutic monitoring.

Technically, minuscule amounts of cellular lysates are immobilized on individual spots on a microarray that is then incubated with a single specific antibody to detect expression of the target protein across many samples, using either a primary or a secondary labeled antibody by chemiluminescent, fluorescent or colorimetric assays. The array is then imaged and the obtained data is quantified.

**Protein extraction** Sorted cells (for MM project) or PBMNCs isolated from the bone marrow (MDS project) were lysed into 10 uL of lysis buffer containing a 1:1 mixture of 2x Tris-Glycine SDS sample buffer (Invitrogen Life Technologies) and Tissue Protein Extraction Reagent (Pierce) plus 1.0% beta-mercaptoethanol for 5 min at $100^0$C, saved at $-80^0$C. Once collected all samples (set B) were packaged and sent to GMU laboratories for additional processing.

**Printing** This step consists in the analyte immobilization on a nitrocellulose coated glass slide (array). A solution of 10% TCEP in T-PER/ 2X SDS Tris-glycine SDS buffer was used to solubilize the cells and denature the cellular proteins.

Immediately prior to arraying, lysates were denatured by heating for 5 minutes at $100^0$C, diluted in protein extraction buffer in accord to Test Print findings and loaded into a 384-well plate. Serial two-fold dilutions were printed in duplicate on glass backed nitrocellulose array slides (FAST Slides, Whatman or Schott) using an Aushon 2470 arrayer equipped with 350um pins(Aushon Biosystems, Billerica, MA). Each spot was printed with approximately 30.0 nL of lysate/spot in a dilution curve representing undiluted and 1:4 dilutions. Positive control samples included A431 control and A431+EGF lysates (BD Pharmingen) at 1.0 mg/mL.

Once printed, the slides were either stored with desiccant (Drierite, W.A. Hammond, Xenia, OH) at $-20^0$C or immediately processed for immunostaining. For each array, 3 or 4 slides were washed and baked at $80^0$C for ssDNA detection (see below).

**Staining** For estimation of total protein amounts, selected arrays were stained with Sypro Ruby Protein Blot Stain (Molecular Probes) according to the manufacturer's instructions and visualized on a Fluorchem imaging system (Alpha Innotech).

Lysate arrays were treated with Reblot antibody stripping solution (Chemicon) for 15 min at room temperature, washed 2 x 5 min in PBS, and then incubated for at least 1 hour in blocking solution (1g I-block (Tropix), 0.1% Tween-20 in 500 mL PBS) at room temperature with constant rocking. Blocked arrays were stained with antibodies on an automated slide stainer (Autostainer CSA kit, Dako, Carpinteria, CA). using the Catalyzed Signal Amplification System kit according to the manufacturer's recommendation (CSA; Dako Cytomation). Briefly, endogenous biotin was blocked for 10 min using the biotin blocking kit, followed by application of protein block for 5 min; primary antibodies were di-

luted in antibody diluent and incubated on slides for 30 min and biotinylated secondary antibodies were incubated for 15 min. Signal amplification involved incubation with a streptavidin-biotin-peroxidase complex provided in the CSA kit for 15 min, and amplification reagent, (biotinyl-tyramide/hydrogen peroxide, streptavidin-peroxidase) for 15 min each. Development was completed using diaminobenzadine/hydrogen peroxide as the chromogen/substrate. Slides were allowed to air dry following development.

Each array was probed with a single polyclonal or monoclonal primary antibody (e.g. see 2.4). The negative control slide was incubated with antibody diluent. Secondary antibody was goat anti-rabbit IgG H+L (1 :7500 for Whatman slides, 1:500 for Schott slides) (Vector Labs, Burlingame, CA) or rabbit anti-mouse IgG (1:10) (Dako).

Each array was scanned using an UMAX flatbed scanner at 600 dpi (Adobe Photoshop software), spot intensity analyzed, data normalized to total protein and ssDNA/spot, and a standardized, single data value was generated for each sample on the array (Image Quant v5.2, GE Healthcare, Piscataway, NJ). For samples treated ex vivo changes in proteomic profile was indicated as relative percentage of the correspondant vehicle (DMSO or saline solution for samples treated with the only bortezomib).

**Calibration and quality control arrays** Since RPMA uses the whole-cell or tissue lysate, it can provide access to post translationally modified proteins that are not accessible with other high-throughput techniques. However, since RPMA does not account for antibody specificity and performance, the signal from a single spot could be due to cross-reactivity. Thus, the antibodies used in RPMA must be validated for specificity and performance against cell lysates by Western blot.

GMU antibodies library contains more than one hundred fifty phosphoprotein antibodies validated by Western blotting using a heterogenous tissue sample and a series of cell lines as the input. Validation requires a single band at the expected molecular weight (the green circle in fig.2.7 in left panel), or multiple

bands with 80% of signal in a band at the correct molecular weight (the blue circle in fig.2.7 in left panel), or multiple bands if known cleavage products or degradation of the protein are known and the bands are at the corresponding molecular weights of the degraded proteins (less than parent protein, see fig.2.7.

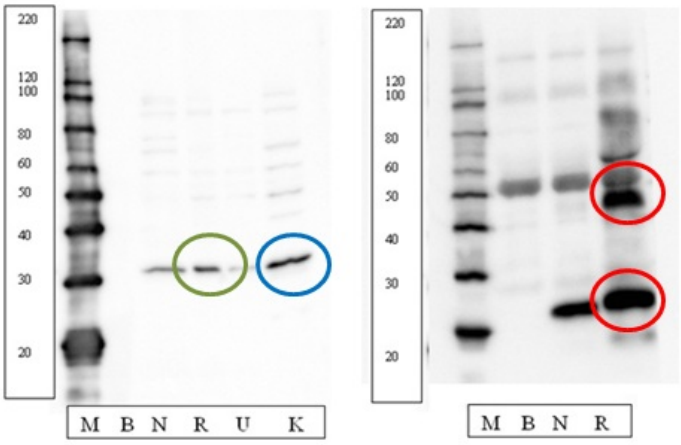


Fig. 2.7: Example of a validated antibody (panel left) and not validated (panel right, the antibody recognizes different epitopes at different molecular weight).

The optimal dilution for each antibody has been determined in an array format that included either positive and negative controls. Positive controls are cultured human myeloma cell lines (U266, RPMI-8224, NCIH929) expressing the cognate phospho-antigen. Acceptable calibration has a sensitivity level equal to 10 cellular equivalents for the antigen of interest and/or a sensitivity of at least 5000 molecules 2 SD above background. Background and negative control were determined by developing the array signal in the absence of a primary antigen. All values have been normalized to both total protein and single strand DNA.

We reported in tab 2.4 a selection of validated antibodies used for this study and their optimal dilution for RPMAs.

Table 2.4: Selection of antibodies used on arrays and their dilutions

| Antibody | Catalog number | Dilution on arrays |
|---|---|---|
| Serotonin | INVITROGEN 18077 | 1:20 |
| AMPK Ser108 | CS 4181 | 1:50 |
| Prot 20S | ABCAM 3325 | 1:1000 |
| PRAS40 Tyr246 | BioSource 44100 | 1:2000 |
| Survivin | CS2808 | 1:100 |
| Beta Actin | CS 4967 | 1:500 |
| BCL-2 Ser70 | CS 2827 | 1:100 |
| FADD Ser194 | CS 2781 | 1:200 |
| CC3 Asp175 | CS 9661 | 1:50 |
| CC6 Asp162 | CS 9761 | 1:50 |
| CC7 Asp198 | CS 9491 | 1:100 |
| CC9 Asp330 | CS 9501 | 1:50 |
| Caspase 8 | Upstate 06-775 | 1:1000 |
| Cl PARP Asp214 | CS 9541 | 1:100 |
| mTOR Ser2448 | CS 2971 | 1:200 |
| IRS-1 Ser612 | CS 2386 | 1:100 |
| GSK3a/b Ser21/9 | CS 9331 | 1:100 |
| B-RAF Ser445 | CS 2696 | 1:50 |
| C-RAF Ser338 | CS 9427 | 1:500 |
| ERK Thr202/Tyr204 | CS 9101 | 1:2000 |
| Mek1/2 Ser217/221 | CS 9121 | 1:500 |
| NFKB p65 Ser536 | CS 3031 | 1:50 |
| SHC Tyr317 | UPSTATE 07-206 | 1:200 |
| Src Tyr416 | CS 2101 | 1:250 |
| STAT3 Ser727 | CS 9134 | 1:100 |
| Atg5 | CS 2630 | 1:500 |
| Beclin1 | CS 3738 | 1:100 |
| LC3B | CS 2775 | 1:100 |

## 2.6 ELISA for detection of new markers in peripheral blood

Peripheral blood was collected by venipuncture into plastic tubes containing EDTA. For sera collection, blood was centrifuged by 2 hours at 1600 x g for 10 minutes at room temperature and surnatant saved at $-80^0$C for maximum 2 months. For platelets isolation, we collected the white buffy coat layer with a plastic pipette and transferring to a fresh plastic tube noting the volume

collected. After counting platelets in a hemocytometer, we washed them with twice the original volume using physiological saline and centrifugation at 2000 x g for 10 minutes, and then we resuspended the platelet pellet back to the original volume using distilled water. Pellets were saved at $-80^0$C for maximum 2 months.

Enzyme-linked immunosorbent assay (ELISA) is an enzyme immunoassay to detect the presence of an antibody or an antigen in a sample. Briefly, an unknown amount of antigen is affixed to a surface, and then a specific antibody is applied over the surface so that it can bind to the antigen. The antibody is linked to an enzyme, and in the final step a substance is added that the enzyme can convert to some detectable signal, most commonly a colour change in a chemical substrate. Performing an ELISA involves at least one antibody with specificity for a particular antigen. The sample with an unknown amount of antigen is immobilized on a solid support (usually a polystyrene microtiter plate). After the antigen is immobilized the detection antibody is added, forming a complex with the antigen. The detection antibody can be covalently linked to an enzyme, or can itself be detected by a secondary antibody which is linked to an enzyme through bioconjugation. Between each step the plate is washed with a mild detergent solution to remove any proteins or antibodies that are not specifically bound. After the final wash step the plate is developed by adding an enzymatic substrate to produce a visible signal, which indicates the quantity of antigen in the sample.

## 2.7 Statistics

Two tailed p-value was estimated using Mann-Whitney test for data obtained from RPMA and t-test for data coming from ELISA. Pearson‘s chi-squared test was used for clinical variables and to evaluate the strenght of the association between cytokine levels and serotonin. All calculations were performed using GraphPad Prism version 5.00 for Windows, GraphPad Software, San Diego California USA, www.graphpad.com. Heatmaps were generated using JMP 5.1.2

to highlight the relationships between clustering and protein expression levels.

## 2.8 Ethics Statement

All the studies included in this work (Molecular characterization of a single MDS patient, Proteomic profile of 17 MDS patients, Ex-vivo assay on 37 (set A) and 24 (set B) MM patients, Serotonin detection in peripheral blood in 20 MM patients and healthy voulenteers) were approved by the Ethical Committee Board of the Clinical Division of Hematology, Ospedale Ferrarotto, Catania, Italy and the IRB of Virginia Cancer Specialist in Fairfax, VA, USA. Patients provided written informed consent in accord to Declaration of Helsinki.

# Chapter 3

# Results

As a whole, the goal of our work was to characterize and to track changes in intracellular pathway profiles in cell subpopulations and their potential clinical applications, such as the selection of beneficial targeted agents. As detailed in the Chapter 1, we focused on two hematological malignancies: MDS (up to transformation in frank AML) and MM.

## 3.1 Accumulation of genomic aberrations in MDS during progression to AML

We evaluated the quality and the extension of genomic aberrations in an unique patient affected of MDS, followed in his clinical evolution up to frank secondary AML. Main stages considered were:

1. at baseline before starting treatment with Azacitidine, four months after diagnosis (TP1);
2. complete remission (TP2);
3. early relapse after treatment with Azacitidine (TP3);
4. late relapse after treatment with Lenalidomide (TP4).

At TP1 (fig. 3.1) an aberrant karyotype was observed: 45, XY, -7, del(20)(q11) by conventional cytogenetics, without additional abnormalities at SNP array, except for a better definition of the boundaries of the 19 Mb interstitial deletion on chromosome 20 (q11.22-q13.13; see table 3.1 for start and end positions).

At clinical remission (TP2), induced by chemotherapy with 4 cycles of Azacitidine, the sample (fig. 3.2) was essentially normal with a few of CNA, while at early relapse (TP3) the patient presented the same abnormalities of TP1 plus a duplication at 8(q24.21-qter), resulting in partial 17 Mb trisomy 8 (fig. 3.3). The dup(8)(q24.21-qter) was further converted into a partial tetrasomy during the progression of the disease (relapse samples) by the addition of a supplementary copy of the whole chromosome 8 (Fig. 3.4 and 3.6). At TP4, conventional cytogenetics pointed out the trisomy 8 sideline as unique clone (100%). SNP/CNV array analysis (fig. 3.5 and 3.6) confirmed trisomy 8, additionally detecting a dup(8)(q24.21-qter) resulting in a partial tetrasomy.

MDS and secondary AML often exhibit the gain of the whole chromosome 8, suggesting that likely the overexpression of several genes, located in different portions of the chromosome, cooperate in the progression. Rucker [96] found a restricted amplified segment (approximately 10.2 Mb) which is located on (8)(q24.13q24.22) between 122.9 Mb and 133.1 Mb. TRIB1 and MYC genes belong to this region, even though their amplification was not confirmed at level of gene expression. Indeed, the MYC gene is a well-known oncogene involved as an amplification target in AML [97], while TRIB1 overexpression is observed only in MDS carrying MYC-containing double minutes [98]. However, in our patient the region containing TRIB1 and MYC was not included in the translocated segment and did showed a normal diploid copy number. It is likely that other genes, downstream to MYC, are involved in gene dysregulation associated to amplification of 8q24 as recently suggested [99].

### 3.1.1 *Small copy number abnormalities (<1 Mb)*

The high resolution of the SNP 6.0 array allows detection of gains and losses of segments smaller than 1 Mb (with a lower size limit of 10 kb). Segments

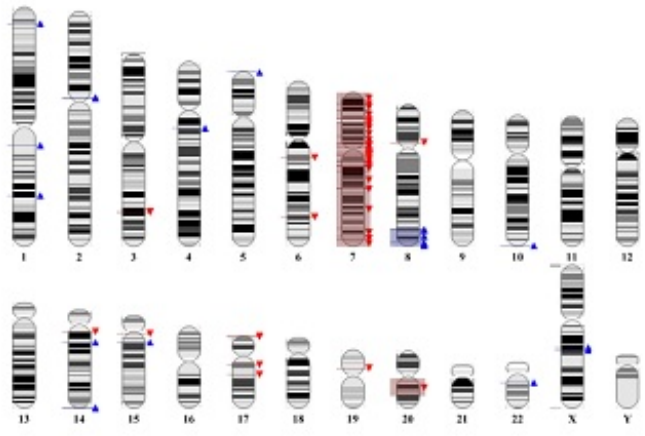

Fig. 3.1: Overview of CNVs at TP1. Gains and losses are represented on chromosome ideograms by blue and red triangles respectively (karyoview by Affymetrix Genotyping Console 3.0.1). Size threshold for detection of gain and loss segments was set to 50 kb.

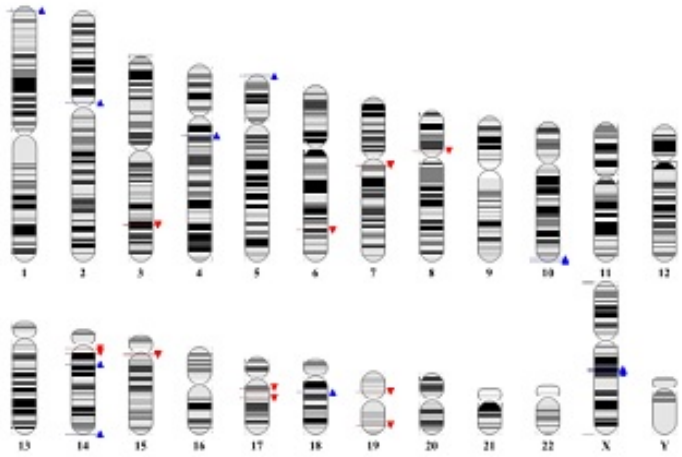

Fig. 3.2: Overview of CNVs at TP2. Gains and losses are represented on chromosome ideograms by blue and red triangles respectively (karyoview by Affymetrix Genotyping Console 3.0.1). Size threshold for detection of gain and loss segments was set to 50 kb.

present in the remission phase (TP2) were considered as germline CNVs and an algorithm was implemented to subtract those segments from leukemic samples (TP1 and TP4) in order to identify only somatic changes. Once the copy number changes have been established in the enriched blast population at TP1, the $\log_2$

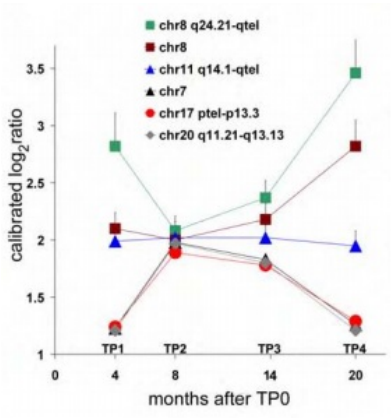


Fig. 3.3: Graph showing calibrated $\log_2$ ratios of revealed genomic lesions at all Timepoints (TP). The averages of calibrated $\log_2$ ratios for genomic markers located in the specific abnormal chromosomal segments at different phases of the disease. All segments that, at Timepoint 1(TP1), showed values of 1.2 (-7 and -20q) or 2.7 (partial trisomy 8q), returned to the normal diploid value of 2 at Timepoint 2 (TP2). At Timepoint 4 (TP4), became predominantly trisomy 8, tetrasomy chr8 q24.21-qtel, deletions of chr20 q11.21-q13.13 and chr11 q14.1-qtel that show values of 2.82, 3.46, 1.21 and 1.26 respectively. The $\log_2$ ratio for chr11 q14.1-qtel, a CN-LOH alteration, is approximately 2 at each Timepoint.

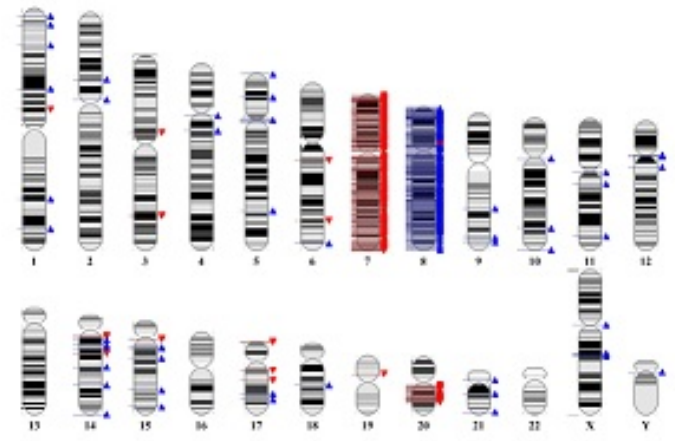

Fig. 3.4: Overview of CNVs at TP4. Gains and losses are represented on chromosome ideograms by blue and red triangles respectively (karyoview by Affymetrix Genotyping Console 3.0.1). Size threshold for detection of gain and loss segments was set to 50 kb.

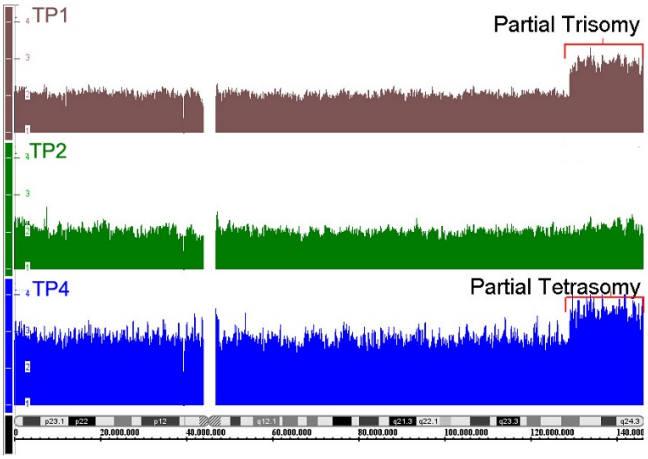


Fig. 3.5: View of whole chromosome 8. The smoothed $\log_2$ ratios, an estimate of copy number,is calibrated to Copy Number and anti-logged. In Y-axis is reported the Copy Number State values: 2 = disomy, 3 = trisomy, 4 = tetrasomy. In X-axis the position (bp) along the chromosome according to hg 18 build. An horizontal ideogram of chromosome 8 is reported at the bottom of the figure. Sample at Timepoint 1 is brown (TP1, top plot), Timepoint 2 is green (TP2, middle plot), Timepoint 4 in blue (TP4, bottom plot)

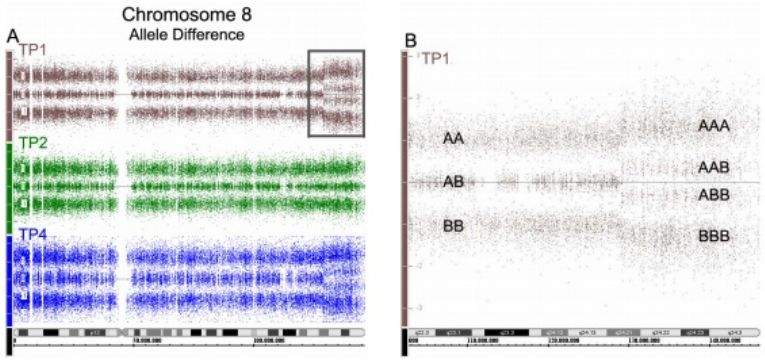


Fig. 3.6: A) View of whole chromosome 8 at Timepoint1 (TP1), Timepoint 2 (TP2) and Timepoint 4 (TP4). B) Zoomed view of (8q)(q24.1q24.3): the rectangle in A shows the magnified zone. Allele Difference is the signal intensity of allele A minus the signal intensity of allele B. In the diploid status each SNP marker can have three possible genotypes (AA, AB, BB) and allele difference values fluctuate around three values (-1, 0, 1). In case of trisomy four genotypes are possible (AAA, AAB, ABB, BBB) around four value (- 1.5, -0.5, +0.5, +1.5). Brown dots represent sample at TP1 (top plot in A, enlarged trace in B), green dots represent TP2 (middle plot in A), blue dots represent TP4 (bottom plot in A)

ratio was calibrated to copy number (GTC software v.3.01, see material and methods) to obtain an estimate of the percentage of cells bearing a specific copy number abnormality in the later samples. All segments that, at TP1, showed values of 1.2 (-7 and -20q) or 2.7 (partial trisomy 8q), returned to the normal diploid value of 2 at TP2 (fig. 3.3, where SNP findings are plotted with changes clinically detectable). Therefore, we were able to reveal a multi-clone karyotype constituted by 25% of the previous complex karyotype with additional trisomy 8 [46, XY, -7, +8, add(17)(p13), del(20)(q11)], 15% of an isolated del(20)(q11) clone and 60% of normal cells.

The small (size <1 Mb) somatic copy number abnormalities found both at TP1 and TP4 are reported in table 3.1. 5 out of 6 CNA were contained in the Database of Genomic Variants, suggesting that genomic regions responsible for interindividual variability are also involved in tumor-associated genomic changes. The majority of these submicroscopic somatic CNA are probably *passenger mutations* reflecting the basal genomic instability of MDS and secondary AMLs.

| Chr | Band | Abnormality type | Start (bp) | End (bp) | Size (kb) | Genes |
|---|---|---|---|---|---|---|
| 1 | p36.13 | Gain | 16902000 | 17121000 | 219 | MSTP9 - KIAA0445 |
| 1 | q31.3 | Gain | 195005000 | 195080000 | 75 | CFHR3 - CFHR1 |
| 3 | q21.3 | Loss | 131258000 | 131274000 | 16 | none |
| 5 | q33.1 | Gain | 149212000 | 149256000 | 44 | PDE6A |
| 14 | q11.2 | Loss | 21924000 | 21939000 | 15 | TCRA |

Table 3.1: Somatic tumor-associated copy number abnormalities <1 Mb revealed at SNP 6.0 array

As shown in the Venn diagram in fig. 3.7 and in the virtual karyotype of more involved chromosomes in fig. 3.8, the number of somatic gains and losses present at TP4 is higher than that observed at TP1, thus confirming the accumulation of chromosomal abnormalities during the progression.

The LOH algorithm implemented in GTC software looked for runs of homozygous SNP calls, taking into account the overall heterozygousity rate and the error rate in calling. In addition, a new parameter, called *allele difference* (difference of allele A signal and allele B signal, each standardized with respect

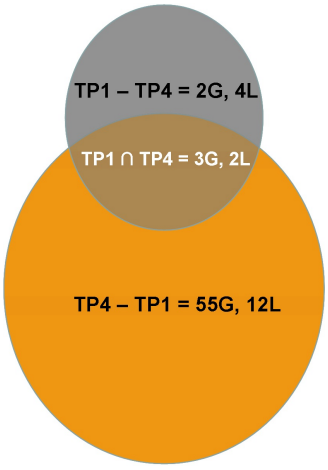


Fig. 3.7: Venn diagram summarizing the number of somatic alterations, gain (G) and losses (L), revealed at TP1 and TP4. An accumulation of somatic changes have been revealed during a progression of disease (G3; L2). Details of somatic tumor-associated chromosomal abnormalities revealed at TP1 and TP4 are reported in Table 3.1. G2 and L4 represent the somatic alterations that have been revealed at TP1.

to their median values in the reference population) was integrated for the visualization of CN-LOH region. In the relapse (TP4) sample a large region of CN-LOH was identified on the long arm of chromosome 11 extending from band q14.1 to qter (TP4, Fig. 3.9; see table 3.1 for start and end positions).

As shown in fig. 3.9, where the *allele difference* values are plotted for consecutive SNP markers along the chromosome 11, at TP2 a normal three-band pattern, corresponding to the three genotypes (AA, AB, BB), could be observed along the entire extension of chromosome (fig. 3.9, middle plot). In the late relapse sample (TP4) such normal three-bands pattern at the chromosome 11 is replaced by a two-bands pattern, lacking the heterozygous genotype AB, from band q14.1 to the telomere (fig. 3.9, bottom plot). Such region of extended homozygousity in the presence of a normal diploid copy number (see fig.3.3 for $\log_2$ ratio values in chromosome 11 q14.1-qter at different stages of disease) is the typical hallmark of CN-LOH regions and shows that the vast majority (>90%) of the cells in the late relapse sample (TP4) are carrying the 11q CN-LOH. Interestingly, in the sample at TP1 an anomalous four-bands pattern can be observed in the same segment of 11q (fig.3.9, top plot). The four-bands pattern

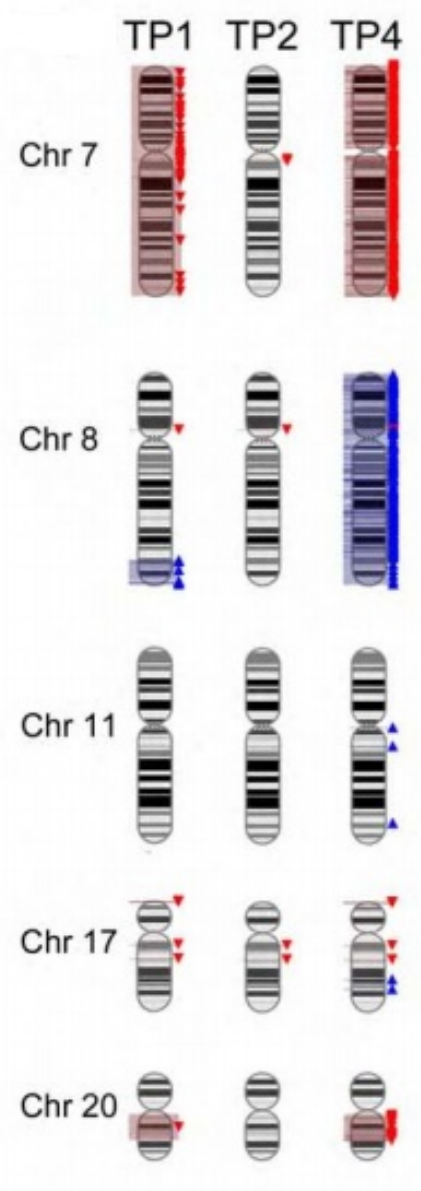


Fig. 3.8: Overview of copy number changes at TP1, TP2 and TP4. Gains and losses are represented on chromosome ideograms by blue and red triangles respectively (karyoview by Affymetrix Genotyping Console)

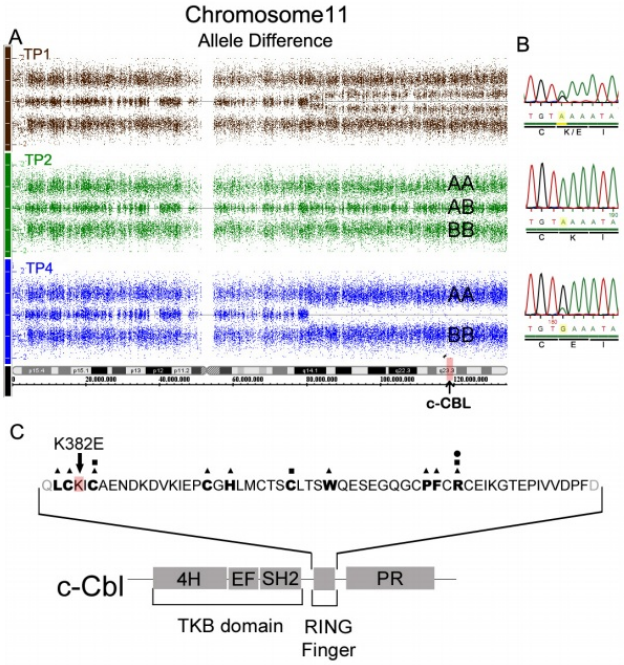


Fig. 3.9: 11q CN-LOH and K382E cCBL mutation in reported MDS/AML case. A) View of whole chromosome 11 at Timepoint 1 (TP1), Timepoint 2 (TP2) and Timepoint 4 (TP4). Allele Difference is the signal intensity of allele A minus the signal intensity of allele B. In the diploid status each SNP marker can have three possible genotypes (AA, AB, BB) and allele difference values fluctuate around three values (-1, 0, 1). In case of CN-LOH two genotypes are possible (AA, BB) around two values (-1, +1). Brown dots represent sample at TP1, green dots represent TP2, blue dots represent sample TP4. B) Sequence analysis of DNA from the bone marrow cells obtained to TP1, TP2 and TP4 reveals a missense mutation A $G$ at position 1282 of the cCBL transcript (NM-005188) leading to different codon (AAA GAA). The mutation was found to be present in a subpopulation of the cells at the diagnosis (TP1), was not detectable in the remission phase and fully present at the TP 4 of the same individual. C) Schematic representation showing the major domains of c-Cbl protein : the tyrosine kinase binding (TKB), RING finger domain and proline-rich (PR) region. The aminoacidic sequence of RING finger domain is reported. Residue affected by missense mutation and found in this study is indicated by red box and marked with *K382E*.

is the typical hallmark of a trisomy which produces 4 genotypes (see for example fig. 3.5) for trisomy 8, but the presence of a normal diploid copy number in 11q does not support this conclusion.

Alternatively, it is possible that the presence of the CN-LOH in a subclone

represents only a fraction of the examined cells. Indeed, mathematical simulation of the results, obtained with a 50% mixture of CN-LOH bearing and not bearing cells, produced a similar four-bands pattern with a concomitant normal diploid copy number. Since the other chromosomal abnormalities detected at TP1 (loss whole chromosome 7, loss 20q11.22-q13.13, gain 8q24, loss 17p13.3) are present in the majority of the cells of the sample, as shown by their $\log_2$ ratio values (see graph in fig. 3.3), we conclude that the CN-LOH 11q likely occurred on the background of -7, del(20q), add(17p). Cells bearing the CN-LOH 11q took place during the progression to AML. To our knowledge this is the first report providing a semiquantitative estimate of the fraction of leukemic cells carrying the 11q CN-LOH and showing an expansion of this clone during the AML progression.

Formally the CN-LOH of 11q might represent only a *passenger mutation*, caused by the chromosomal instability typical of MDS, and devoid of the pathogenetic properties of a *driver mutation*. However, the concomitant recurrency of abnormalities already detected in other myeloid malignancies as well as the appearance of an additional copy of the entire chromosome 8, in the predominant clone at TP4, support the hypothesis that such aberrations confer growth advantage to the clonal cells and as a consequence they are positively selected. Therefore the 11q CN-LOH should be considered a late event during the progression up to AML secondary to MDS.

### 3.1.2 *Genes involved in progression to secondary AML in the region 11q14.1*

On the basis of recent literature [88, 100, 101] we selected the c-CBL oncogene in order to identify the CN-LOH 11q mutations involved in the pathogenesis of this MDS case. cCBL is an E3 ubiquitin ligase involved in the ubiquitylation and degradation of active protein tyrosine kinase receptors, mutated in more than 50% of MDS patients bearing 11q CN-LOH [88]. Mutant forms of c-Cbl serving as *dominant negatives* reportedly have transforming activity, presumably as a consequence of either decreased turnover or increased activity of

tyrosine kinases, which are known as negative regulators of receptor tyrosine kinases signalling.

We sequenced exons 7-9 of c-CBL at TP1, TP2 and TP4 and one missense heterozygous mutation was detected on exon 8 at position 1282 of cCBL transcript (NM_005188). The codon AAA changes in GAA, determining a single aminoacidic substitution at position 382: lysine (K) changes in glutamic acid (E)(fig.3.9B). Half of the revealed mutation reflects the heterogeneity in tumor samples constituted by a mixture of tumor and non tumor cells and it gives a correct interpretation of allele difference signals obtained by SNP analysis for chromosome 11q (fig.3.9A, top plot). The mutation disappeared at TP2 but resulted predominant at TP4 (fig.3.9B): allele difference at TP4 for chromosome 11q showed only two bands typical of CN-LOH pattern (fig.3.9, bottom plot) thus confirming the sample was predominantly costituted by a clone bearing a mutation present in homozygous. This K382E mutation, never been identified before(Fig.3.9C), was localized within the RING finger domain and seemed essential to the E3 ubiquitin ligase activity. In agreement with recently published data [100, 101] the RING mutations can negatively modulate tyrosine kinase signalling by inhibition of its ubiquitinating activities, enhancing the cell proliferation or inhibiting the apoptosis.

## 3.2 Modulation of MDS proteome by new epigenetic drugs

We analyzed 17 patients affected by high risk MDS, diagnosed at our Division of Hematology from January 2009 to February 2010. For 5 patients a bone marrow sample was available after 4 cycles of therapy with Azacitdine, matched to the sample collected before the therapy start.

We compared the pool of patients at the diagnosis (n=17) to a pool of patients (n=9, matched only in 5 cases) treated for 4 months with Azacitidine. Since samples have been collected in the past for a biobank purpose, they were stored unsorted, and therefore we studied the profile on the whole bone marrow.

Main findings are reported in fig.3.10, where the values of intensity (mean of 3 independent observations) of endpoints are plotted, normalized on the values of total protein.

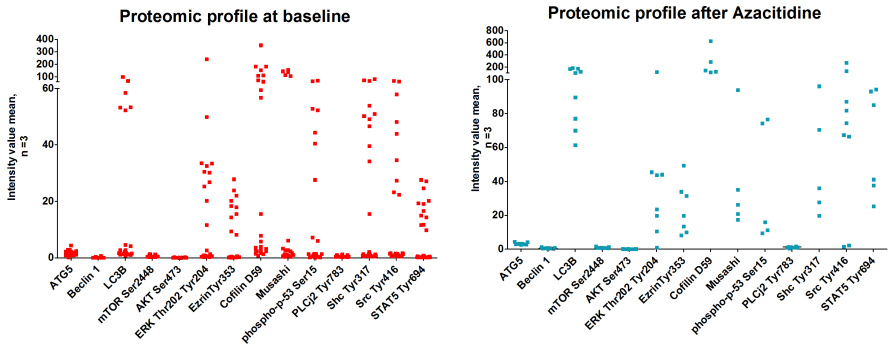


Fig. 3.10: Mean of intensity pixel value: 3 independent observations in the pool of 17 patients at diagnosis (red squares, in left panel) and in the pool of 9 after 4 cycles of treatment with Azacitidine (blue squares, in right panel)

Each patient exhibited a unique proteomic profile, as we show in fig.3.11 where we report the number of fold changes for each patient (data coming from 5 patients with matched samples at diagnosis and after 4 cycles of therapy, mean of 3 independent observations).

We found an activation of autophagy pathway, independent from the status disease and quality of achieved response after therapy (fig.3.12). The main proteins involved are ATG5, Beclin1 and LC3B. We hypothesized that autophagy is a means to resist to apoptosis in MDS progenitors in advanced disease. However, additional in vitro experiments are required in order to identify a synergic role of inducers or inhibitors of autophagy with current drugs to confirm and apply this fascinating observation.

### 3.2.1 Proteomic profile as a means for combination therapy in MDS

After 4 cycles of Azacitidine patients were considered responders in accord to IWG criteria. We identified two potential new biomarkers as possible tools

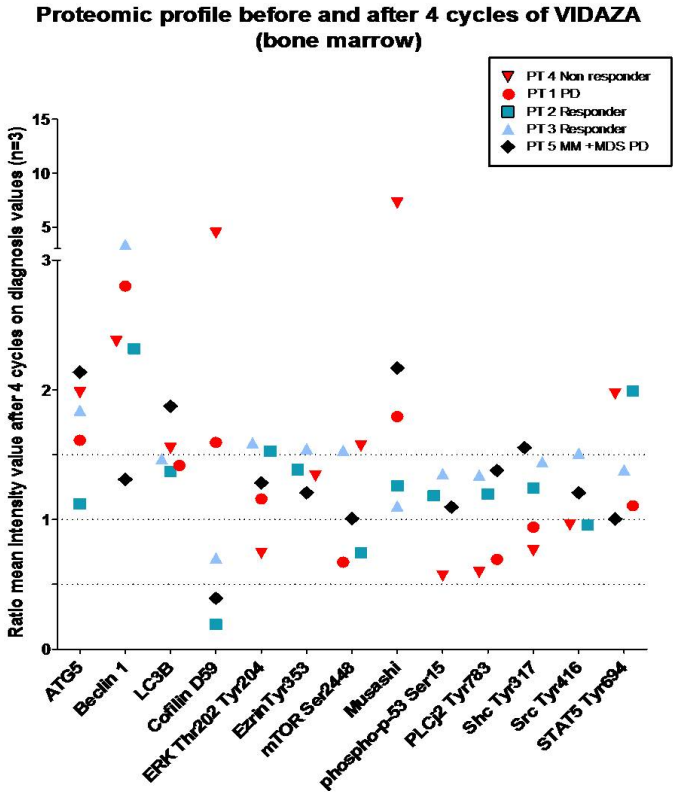


Fig. 3.11: Ratio between mean intensity at diagnosis vs post-treatment in not responder patients (pts #1,#4) are indicated in red, responder (pts #2,#3) in blue and pt5 in brown, affected of MM and MDS, never treated for MM and progressed to AML under Azacitidine, is plotted for each endpoint. All resistant patients but pt#5 exhibited a decrease in activation in pathway PLC-y1Tyr783, SrcTyr416 and STAT-5Tyr694, and a concomitant increase of Musashi (Msi-2).Activation of autophagy pathway seems to be independent from status disease and the quality of achieved response.

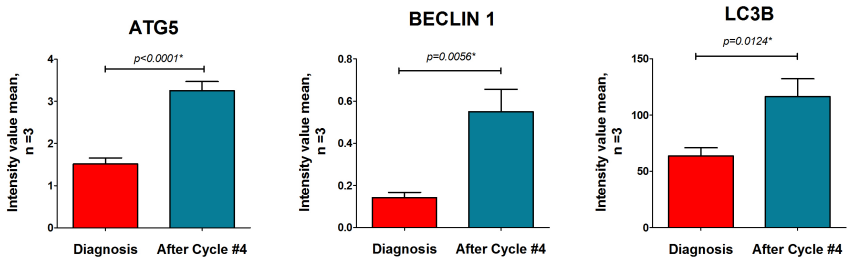


Fig. 3.12: The three main markers of induced autophagy have a differential expression in the pool of diagnosis vs the pool of post-treatment, independently from the quality of achieved response. **t test with Welch's correction for unpaired data*

predictive of response to therapy and progression to disease: Msi-2 and upstream signalling of STAT5.

Musashi-Msi 2 encodes a protein containing two conserved tandem RNA recognition motifs. Recently, Msi2, but not Msi1, has been identified as a novel functional marker of primitive hematopoietic stem cells (HSCs) and regulator of their self-renewal process based on the following functional data:

1. Musashi-Msi2 is required for the maintenance of HSCs [102];
2. Musashi-Msi2 overexpression enhances stem cell activity, inducing an increased expression of a number of known stem cell agonists and indicators of Notch and Sonic Hedgehog signaling, such as the Notch effector Hes1 [103];
3. Msi2 binds the 3'UTR of the Notch inhibitor Numb, mediating its translational repression, thereby enhancing Notch signaling. Notch dysregulation in the early stem/progenitor cell compartment of MDS patients is well established, although the molecular mechanism behind this phenomenon is unclear. Thus, we are working on a model of disease in which Msi2/Notch balance is required to maintain stemness, and can be controlled by Azacitidine, through downregulation of Musashi-Msi2 [104].

The stemness factor Musashi shows a significative reduction after therapy with Azacitidine; on the other hand, refractory patients who progressed to

AML under treatment with Azacitidine (n=3) showed an increase of Msi-2 level (fig.3.13). We observed lower levels of Musashi at diagnosis in refractory patients, but lacking statistical significance.

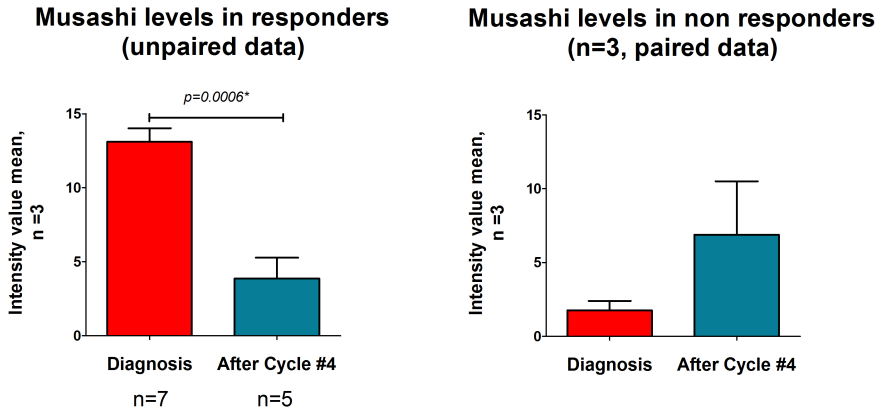


Fig. 3.13: Patients who achieved a response after 4 cycles of treatment with Azacitidine showed a concomitant decrease of levels of protein Musashi in the bone marrow cells. Data (left panel) are referred to a pool of samples collected at diagnosis vs samples collected after therapy, belonging to not matched patients. On the right panel we plotted the trend of Musashi expression in the three refractory patients of the cohort

Additionally, the compensatory pathway of PLC-$\gamma$1Tyr783, SrcTyr416 and STAT-5Tyr694 is induced after the treatment with Azacitidine, independently of the quality of achieved response (fig. 3.14).

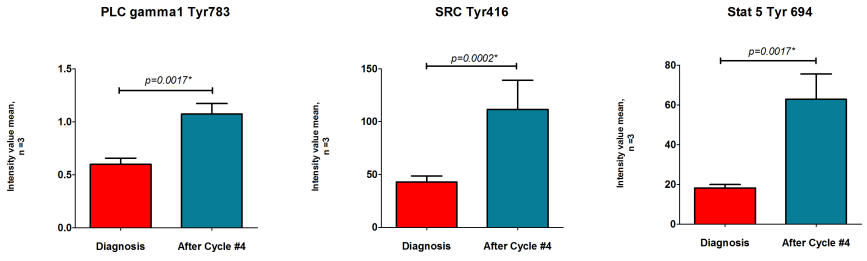


Fig. 3.14: PLC-$\gamma$1Tyr783, SrcTyr416 and STAT-5Tyr694 activation status in MDS before and after treatment with Azacitidine (Vidaza)

PLC-$\gamma$1Tyr783, SrcTyr416 and STAT-5Tyr694 are the downstream targets

of EPO/IL3 pathway [105], notably imbalanced in MDS. Indeed, the neoplastic clone is refractory to EPO, especially in advanced clinical stages and high risk MDS. Our observation suggests that the ability of Azacitidine to restore EPO sensitivity can be mediated by its indirect control of PLC-$\gamma$1Tyr783, Src-Tyr416 and STAT-5Tyr694. Moreover, STAT5 is a well-known factor involved also in the transcriptional regulation of hystones H3/H4. The reduced methylation status induced by Azacitidine can change the levels of acetylation status of histones, thus providing a rational for the development of a combinatorial approach based on Azacitidine + HDAC inhibitors, acting upstream [104] and EPO.

Finally, the observation that Azacitidine does not affect proliferative pathways (see fig.3.15), identified as new potential target in AML, suggests the need to combine Azacitidine to anti-proliferative agents, such as Rapamycin or RAD001, in order to target proliferation of neoplastic cells.

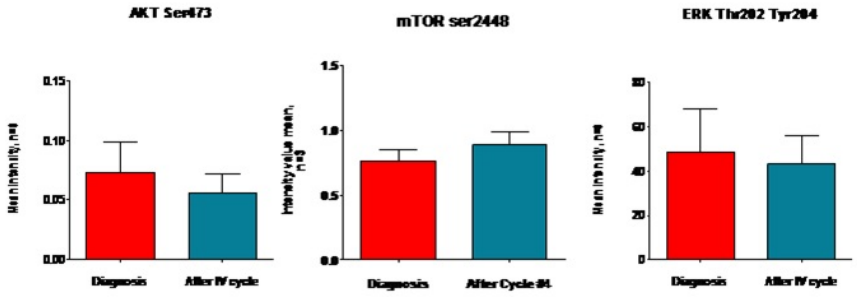


Fig. 3.15: No appreciable differences (p=ns, *t test for unpaired data*) can be detected before and after treatment in AKTS473, mTORSer2447, ERKThr202Tyr204 pathway, independently from the quality of achieved response.

## 3.3 Signal pathway proteomic analysis of MM bone marrow microenvironment

Individual classes of pathways were affected differentially between the two cell populations ($CD138^+$ plasmacells and $CD138^-$ bone marrow cells) in each patient, reflecting a unique constellation of kinase-driven signaling events. This observation concurs with recent gene and SNP microarray findings in MM and indicates that although some haematological malignancies, like CML, are underpinned by a common pathway defect (e.g., c-kit family signaling activation), other ones are controlled by a multiplex of protein circuitry derangements.

### 3.3.1 *Correlation between Protein Expression and Clinical Findings*

We searched first for correlation between protein expression/activation at baseline, before any treatment, either *ex vivo* or *in vivo*, and patients clinical characteristics, for set# 2 (CT patients). The independent set # 1 (GMU patients) was used to optimize the final protocol for the assay, to generate hypothesis, based on individualized drug-response circuitries, to combine new drugs even if not specifically indicated for MM, the library of drugs available at GMU being larger.

In particular we considered the followings: age (18-65 years vs. >65 years), sex, stage in accord to ISS (International Staging System), chromosomal aberrations detected in conventional cytogenetics (normal karyotype, del(13q), t(4;14), del(17p)), presence of bone disease, status disease (naïve vs. relapsed/refractory vs. follow up (defined as patients with documented complete remission from at least 9 months) through Wilcoxon tests or two-sample Welch t-tests as detailed in Chapter 2. No correlation was found between protein expression/activation and age, sex, stage (data not shown), but we observed differentially activated/expressed proteins based on status disease and presence of bone disease. Interestingly, based on levels of 5 endpoints in $CD138^+$ cells related to proliferation in response to autocrine/paracrine molecules (Il-6, Il-10, TNF-$\alpha$, Erk Thr202-Tyr204, Akt

Ser473) we distinguished three groups related to chromosomal aberrations (see fig. 3.16). All cases with normal karyotype at conventional cytogenetics clustered all together, while cases with partial losses of chromosomes 13 and/or 17 revealed a not unique behavior, suggesting the superiority of protein activation status on genomic instability markers. Patients belonging to the third cluster, indicated in green in fig. 3.16, presented a more aggressive/active disease (three cases of shifting from MGUS to MM plus one patient relapsed and then became refractory to conventional chemotherapy).

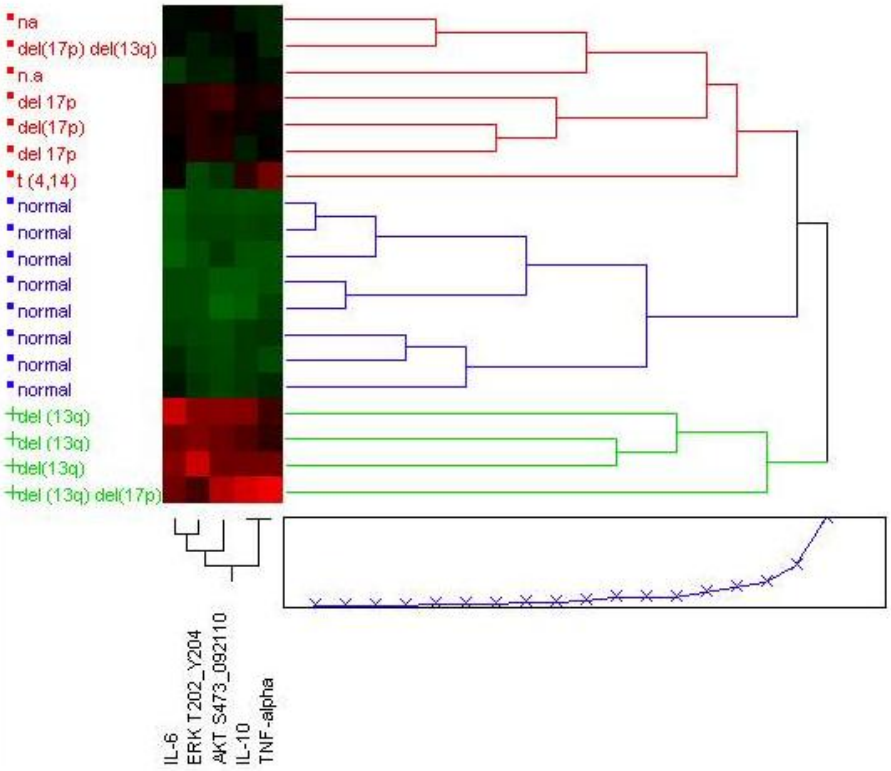


Fig. 3.16: Heatmap with hierarchical clustering, generating used proteins differentially expressed/phosphorylated in the patients with or without chromosomal aberrations detected at conventional cytogenetics. N.A. indicates not conclusive findings at conventional cytogenetics for poor replication rate of plasmacells.

### 3.3.2 *Baseline profile of plasmacells*

The PI3K/Akt pathway has been evaluated in MM, functionally distinguishable thanks to the phosphorylation of Akt1 in two key amino-acid residues: serine 473 and threonine 308. In GMU set # 1, we distinguished plasmacells in two clusters on the basis of AkT status and upstream and downstream endpoints (respectively B-Raf Ser445, SEK/MEKK4, mTOR Ser2448 and NFkBp65 Ser536, p53 Ser15,fig. 3.17). These clusters were related to the levels of induced autophagy, evaluated on the basis of the expression of ATG5, LC3B, p62/SQSM1. We confirmed it in the set#2 (fig.3.18), where a trend of a larger activation status in symptomatic patients (naïve and relapsed) compared to those who achieved complete remission (in follow up after autologous transplantation) was evident.

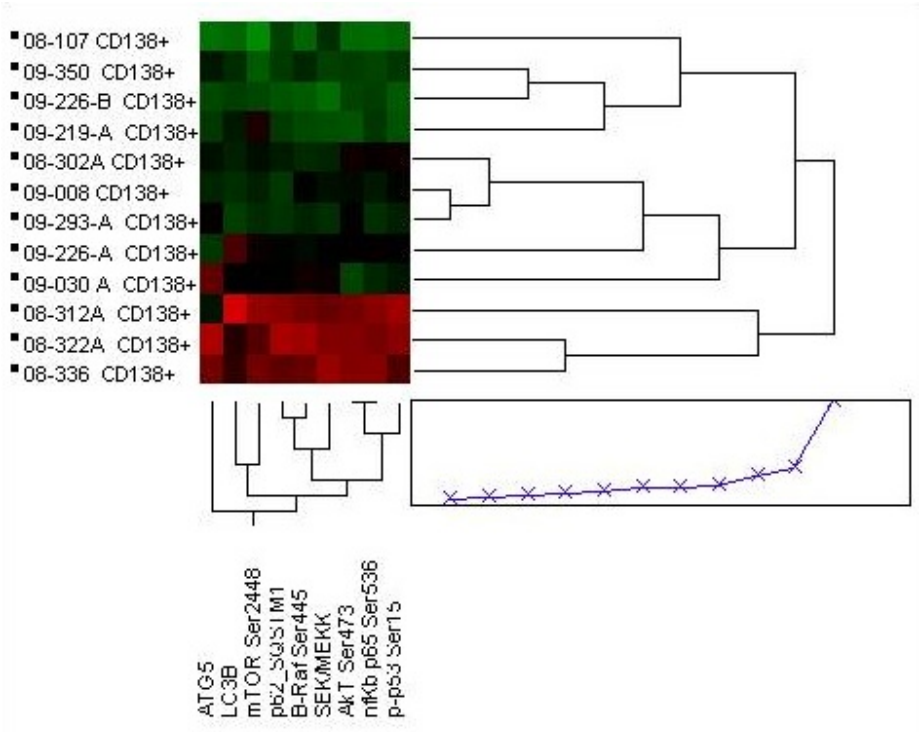


Fig. 3.17: Heatmap with hierarchical clustering, generating used proteins described in the text. Clinical details are reported in 2.1

Akt was shown to be frequently activated (at least 50% of cases) in primary

MM specimens [106, 107]. Functionally, the PI3K/Akt pathway is implicated in cell cycle and apoptosis regulation in MM cells [108].

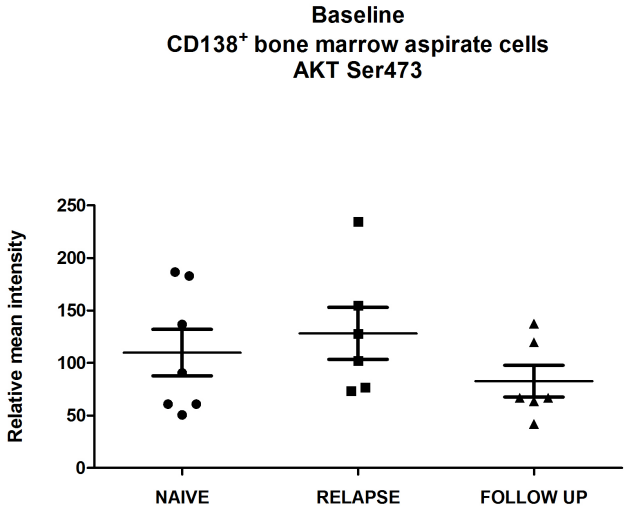


Fig. 3.18: Levels of activated Akt phosphorylated in Serine 473 related to the disease status in CT set # 2.

Again, patients with more aggressive clinical presentation (for refractary disease, time to progression, bone disease) presented an overactivation of PI3K/AkT/mTOR: we confirmed this trend in CT set, as showed by the behaviour of other endpoints (fig. 3.19). We looked specifically at these endpoints since they can be targetted all together by Lenalidomide-based regimens (as clearly demonstered for AktSer473 and Caspase 8, respectively down- and up-regulated by Lenalidomide).

Thus, both independent sets confirmed the evidence that the PI3K/Akt pathway contributes to clinical behavior of MM, as suggested in [109] using cell-line and xenograft models, where restoration of a functional PTEN/PI3K/Akt axis in PTEN-null cell lines leads to apoptosis in dexamethasone-resistant cell lines.

Crosstalk between surface glycoproteins and extracellular receptors can lead to increased activity of the PI3K/Akt pathway in myeloma using different ways:

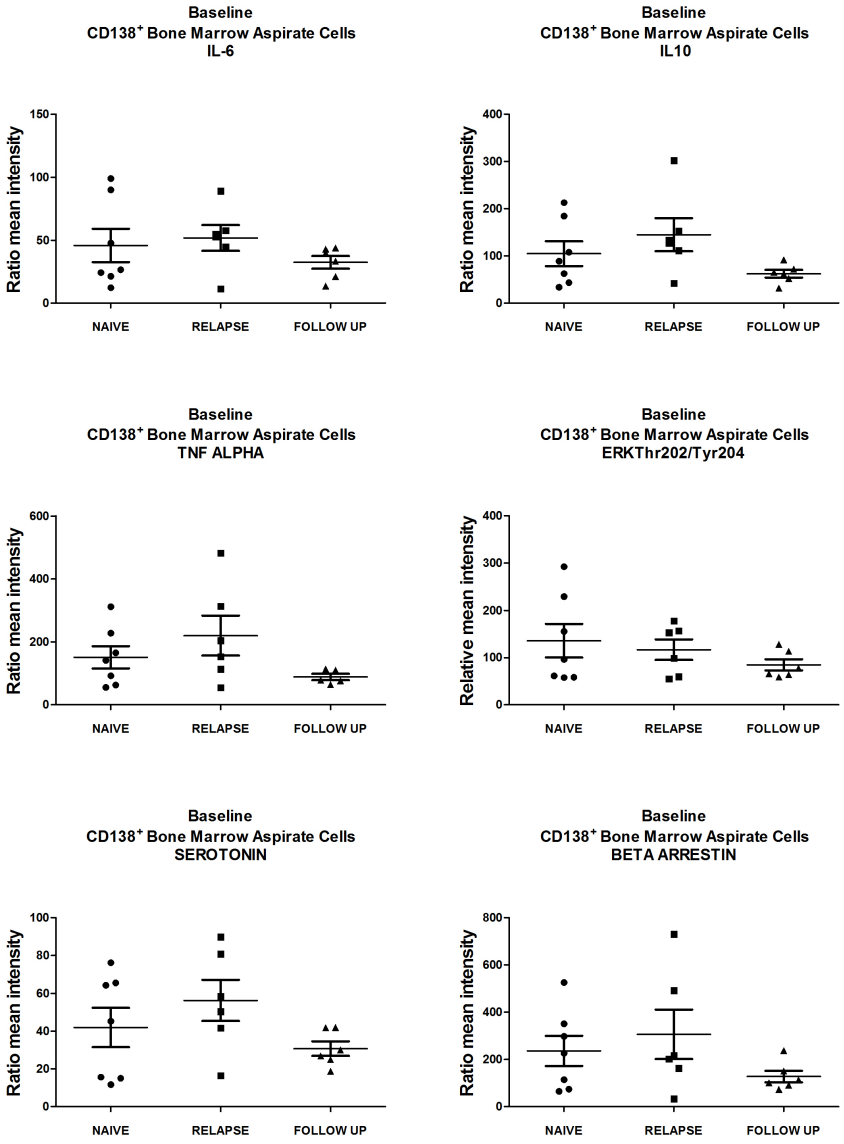


Fig. 3.19: Proteins related to autocrine and paracrine crosstalking in MM microenvironment, measured by RPMA in MM plasmacells.

- Plasma cell migration is stimulated by CD40-induced activation of PI3K[110];
- The growth of $CD45^-$ myeloma cells is dependent on stimulation of the IGFR1, with subsequent phosphorylation of Akt;
- Blocking the PI3K pathway with the selective inhibitor wortmannin (a fungal derivative that irreversibly binds to the p110 subunit) causes a 70-85% reduction in $CD45^-$ myeloma cell growth compared to 20% for $CD45^+$ cells, demonstrating the reliance on this pathway for proliferation [111];
- IL-6 activates the pathway through two independent means: a ras-dependent but p85-independent pathway, and a STAT-3-containing complex pathway that is p85-dependent [112]. The Akt phosphorylation induce by IL-6 is abrogated by the PI3K inhibitor LY294002;
- The effects of IL-6 on the PI3K/Akt pathway appear to be in concert with extracellular IGF-1 signaling and independent of ERK activation [113].

Recently, several targets of PI3K/AkT pathway have been identified which contribute to its promotion of cell survival. Among these, BAD, caspase 9, the forkhead family, and the NFkB trascription factor [113]. AkT can promote the activation of NFkB by phosphorylation of IkB kinase (IKK), which in turn, augments the trascriptional activity of p65, with the final promotion of antiapoptotic gene expression and inhibition of p53 activity.

Thus, we were wondering how this proliferative pathway could be modulated by different drugs and if this signature of activity/aggressiveness could be followed during the treatment being able to predict response to the global therapy. We investigated the ability of old and new drugs to modulate Akt/mTOR pathway.

## 3.4 Proteomic changes after ex vivo treatment of bone marrow as a whole

For each monotherapy or combination therapy evaluated, we were able to analyze up to 50 different protein endpoints relevant to the drug targets. Individual classes of pathways were affected differentially between the two cell populations in each patient.

Let us consider as example the response to Dexamethasone, as reported in figure 3.20 respectively indicating the activation profile in patients affected by MGUS (A), MM at diagnosis (B), relapsed MM (C), MM in complete remission after treatment with Bortezomib-based regimen (D), as examples of a continuum of alterations and aggressiveness of disease.

Symptomatic patients with active disease responded differently to dexamethasone, on the basis of their ability to modulate the signalling downstream to MAP-kinase in plasmacells. Dexamethasone can induce Akt activation, needed to control off-trascrptional cascade, as NFkB, and it is able to explain resistance after long exposure. Fig. 3.20 A provides *ex-vivo* treatment response profiles to Dexamethsone 500nM for a male multiple myeloma patient at dignosis: the AKT activation is more evident on the microenvironment cells, while is downregulated in plasmacells, similarly to patients reported in fig. 3.20 B, in complete remission after thalidomide/dexamethasone based regimen.

Despite these theorical circuitries, targetting AkT is not enough for MM control, since poor results obtained by clinical trials with drugs directed selectively against AkT such as perifosine.

Thus we explored two possible strategies: targetting downstream, studying different ways to modulate the final PI3K/AkT downstream, involving mTOR complex, or evaluating the contribute of Akt to possible escape pathways using drugs directed against the microenvironment such as Lenalidomide and Bortezomib. In this latter case, we used the signature PI3K/AkT/mTOR as predictive marker of possibility to develop resistance under treatment.

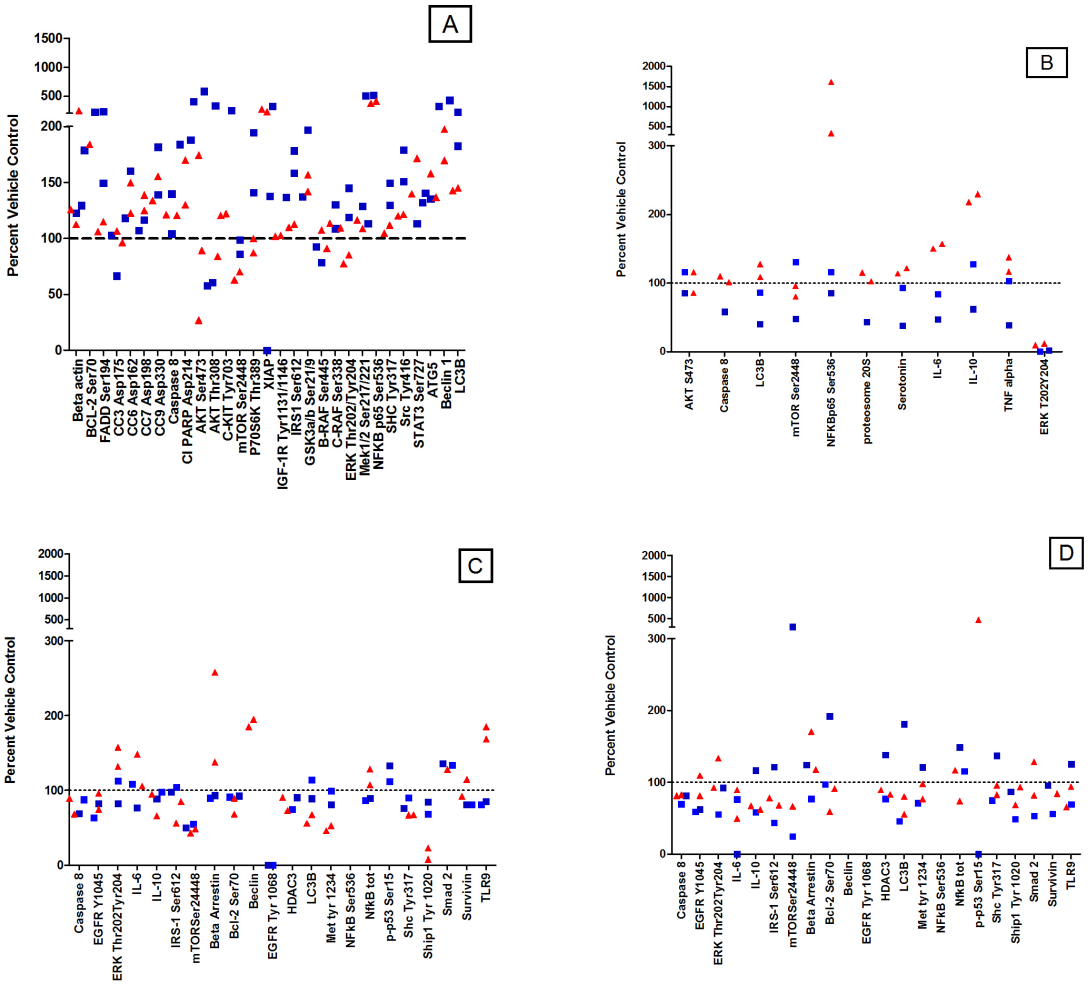


Fig. 3.20: Variable response to treatment ex vivo with 500nM Dexamethasone. Values on the y-axis represent treatment as a percentage of vehicle control. CD138+ cells: triangles; bone marrow cells (BMC): squares. Explanation in the text.

**Strategies to modulate mTOR status in MM** Rapamycin was used at 500nM and tested as unique agent in 3 patients from GMU set. Independently from status disease, we noticed an enhanced basal AKT activity evaluated in terms of AKT phosphorylation on Serine 473 and Threonine 308 (see Fig. 3.21 as example), thus confirming findings from [114] showing PI3K activity in multiple myeloma cells and prolonged activation of AKT induced by exogenous IGF-I. CCI-779, used in a xenograft model, also resulted in multiple myeloma cell AKT activation in vivo: thus, authors [114] concluded that mTOR inhibitors activate PI3-K/AKT in multiple myeloma cells; activation depends on basal IGF-R signaling and enhances IRS-1/IGF-I receptor interactions secondary to inhibited IRS-1 serine phosphorylation. In other cell types, Ser312 phosphorylation of IRS-1 is an integral piece of a feedback inhibition pathway that down-regulates signaling. Following IGF-I/insulin-induced stimulation of the PI3K/AKT/mTOR pathway, an mTOR-dependent serine phosphorylation of IRS-1 uncouples it from its IGF-I/insulin receptors thus inhibiting its tyrosine phosphorylation and further capacity to signal downstream. However we were not able to confirm the downregulation of IRS-1 serine phosphorylation ex-vivo, likely since the authors simulated it adding IGF1 to medium culture.

Although acting similarly by blocking IRS-1 degradation, proteasome inhibitors do not activate AKT 3.22. We did not test the combination of Bortezomib and Rapamycin since in cotreatment experiments [114], rapamycin inhibited myeloma cell apoptosis induced by Bortezomib. These results provide a caveat for future use of mTOR inhibitors in myeloma patients if they are to be combined with apoptosis-inducing agents. In effect, phase 2 trials with mTOR inhibitors in MM have had poor results and combination with Rapamycin has been tested only in conditioning regimens for transplantation (e.g., modified BEAM, poster communication at ASH 2009).

Blockade of IGF-I receptor function prevented rapamycin's activation of AKT 3.23, likely preventing serine phosphorylation of IRS-1, enhancing IRS-1 association with IGF-I receptors, and preventing IRS-1 degradation. Similarly, agents able to interact with both lips of mTOR pathway such as RAD-001 can

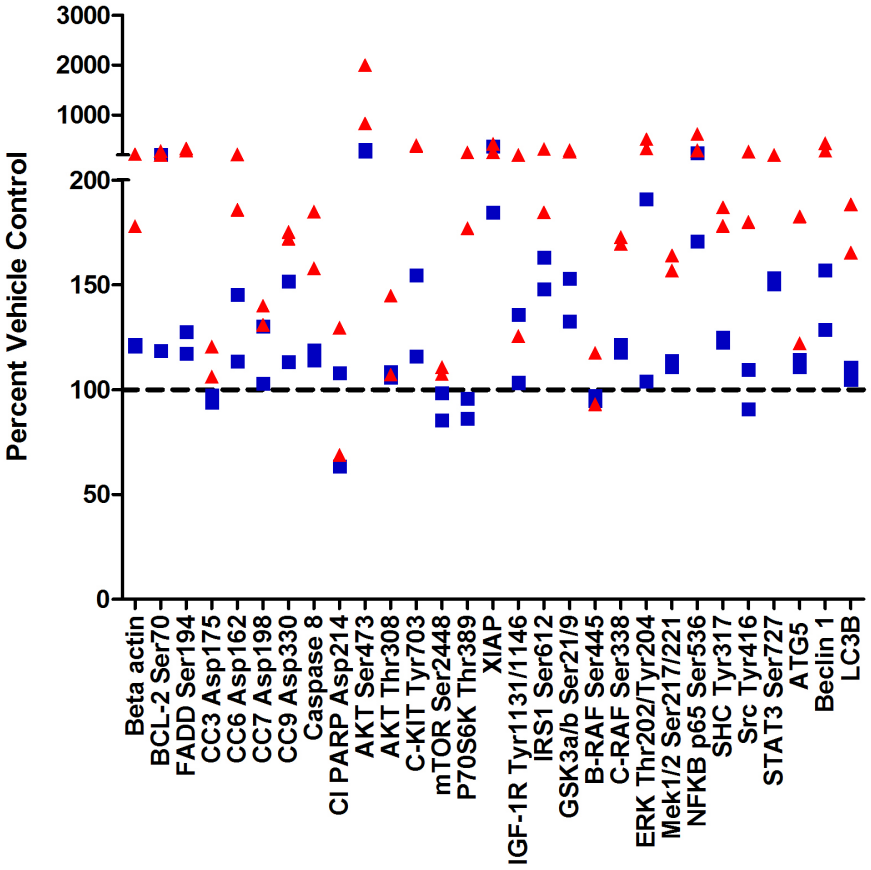


Fig. 3.21: Ex-vivo treatment with 500nM Rapamycin response profile for a female, treatment naıve, multiple myeloma patient: despite of mTOR inhibition, a compensatory pathway is activated, since the increased levels of phosphorylated residues in serine 312 for IRS-1 and AkT in Serine 473 and Threonin 308. Values on the y-axis represent treatment as a percentage of vehicle control. CD138+ cells: triangles; bone marrow cells (BMC): squares.

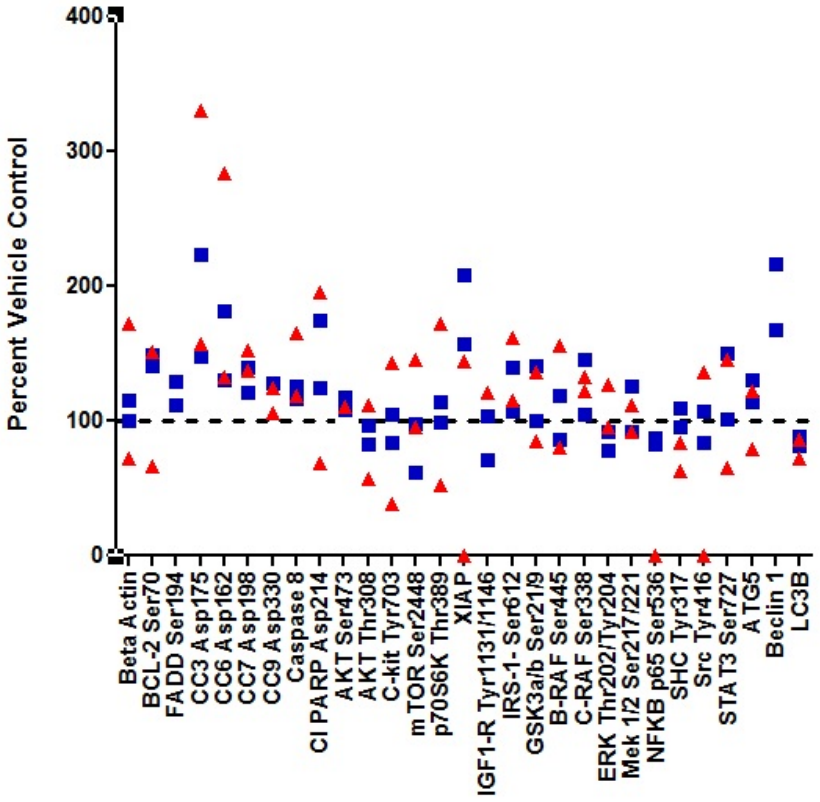


Fig. 3.22: Ex-vivo treatment with 100nM Bortezomib response profile for a male, treatment naıve, multiple myeloma patient: cleavage of caspase 3 and 9 was induced, as well suppression of phosphorylation of NFkBp65, the well defined targets of Bortezomib. IRS-1 activationis not abrogated, however Akt activation status is not induced. Values on the y-axis represent treatment as a percentage of vehicle control. CD138+ cells: triangles; bone marrow cells (BMC): squares.

overcome the compensatory activation of AkT signaling 3.24, without a real effect on activation of pro-apoptotic signaling in MM.

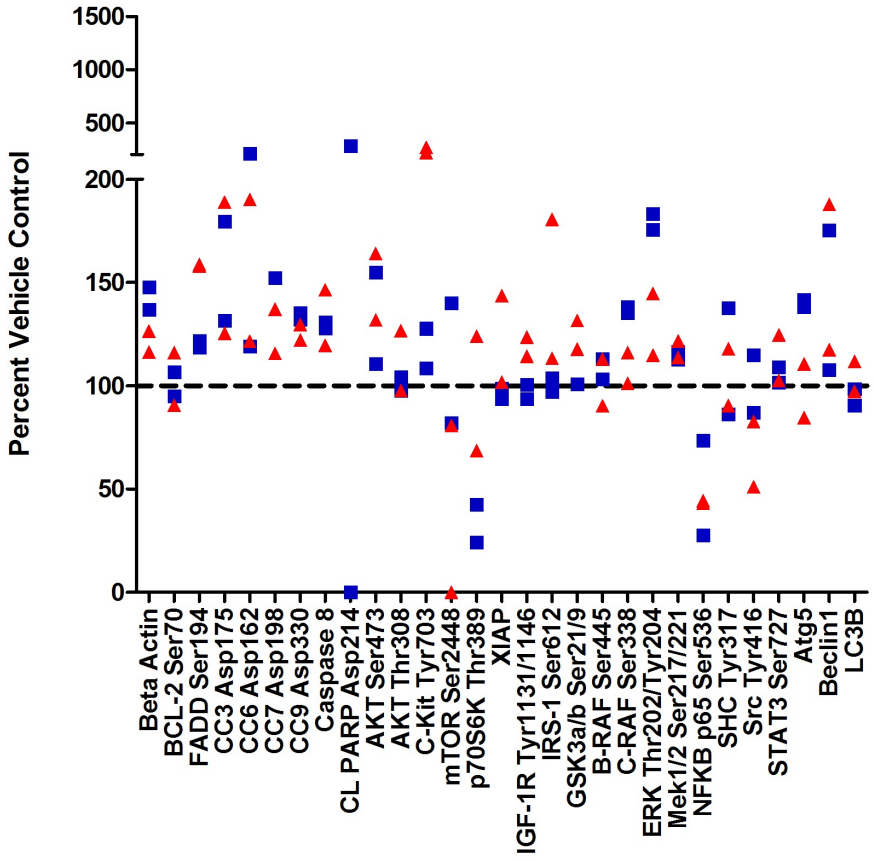


Fig. 3.23: Ex-vivo treatment with 500nM Rapamycin and 14uM IGF-1R Inhibitor II response profile for a male, treatment naıve, multiple myeloma patient: IRS1-Ser 312 is partially controlled and the increase in AkT phosphorylation is less pronounced. Values on the y-axis represent treatment as a percentage of vehicle control. CD138+ cells: triangles; bone marrow cells (BMC): squares.

Taken together, our findings suggest that by activating AKT, mTOR inhibitors could theoretically enhance an antiapoptotic mechanism in multiple myeloma cells, without clinical benefits for patients. In contrast, combination of rapamycin with dexamethasone or with lenalidomide [115] (as we showed

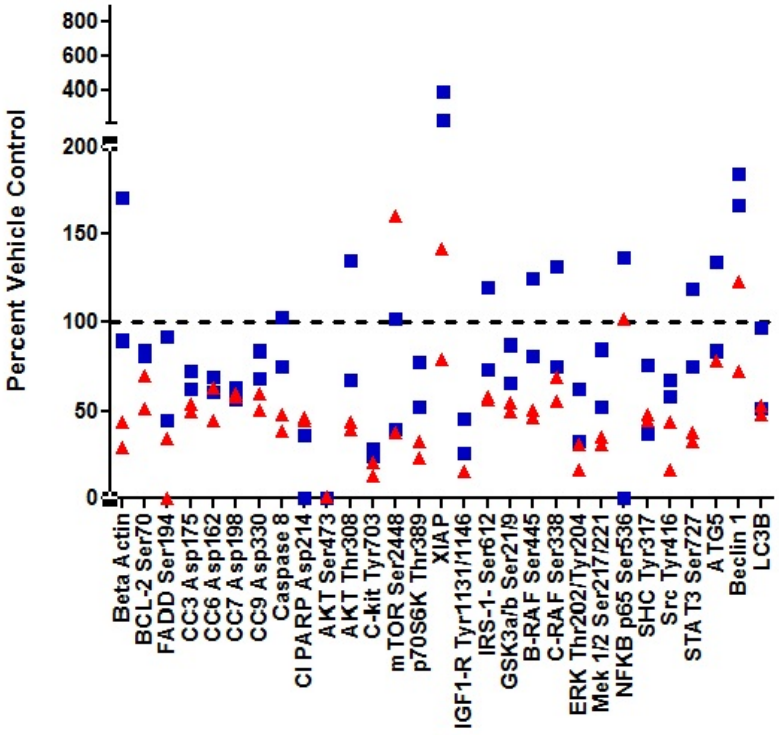


Fig. 3.24: Ex-vivo treatment with 20nM RAD001 response profile for a male, treatment naıve, multiple myeloma patient: despite of inhibition of Akt signaling and lack of compensatory pathway IRS-1/IGF-r mediated the pro-apoptotic signaling is depressed. Values on the y-axis represent treatment as a percentage of vehicle control. CD138+ cells: triangles; bone marrow cells (BMC): squares.

above its ability to reduce AkT activation) have been tested in vitro resulted in enhanced multiple myeloma cell death and overcoming drug resistance. Thus, some interactions between mTOR inhibitors and anti-myeloma agents may be antagonistic possibly due to activation of the antiapoptotic AKT, and other interactions may be synergistic, but preclinical additional studies are needed. Our assay is absolutely affordable in predicting outcome of combinatorial therapy, confirming observations in vitro known in literature and suggesting new key-points of compensatory pathways.

## 3.5 Role of serotonin in MM

We identified serotonin as a new therapeutic target for bone disease by measuring its content in blood, platelets, CD138$\hat{+}$ plasma cells, and bone marrow microenvironment cells:

1. there is a shift of the serotonin pool from peripheral blood to the bone marrow microenvironment associated with increased bone disease in multiple myeloma patients. The concentration of serotonin was increased in platelets (detected in ELISA), as showed in fig.3.25A and $CD138^+$ plasma cells in patients with bone disease (detected in RPMA), but surprisingly it was reduced in sera (mean 673.2 $\pm$ 190.9 ng/mL vs 1845 $\pm$ 175.2 ng/mL, p=0.02);

2. the increased levels of serotonin in the bone marrow microenvironment are associated with presence of osteolytic bone disease (detected in RPMA on CD138 $\hat{-}$ cells). In contrast, blood (serum) serotonin concentration is lower in patients with presence of osteolytic bone disease, as showed in fig.3.25B;

3. there is a trend in changes of serotonin with both well-defined bone modelling biomarkers and chemokines/cytokines present in bone marrow microenvironment, such as TNF-$\alpha$alpha, IL-6 or IL-10 (fig.3.26).

In core biopsies, serotonin was increased in MM subjects with active lesions (p=0.03) as shown in fig.3.26. However the intensity of serotonin signal was not correlated to the number of plasmacells detectable either on the bone marrow aspirates or cores. We interpretated this finding as the proof of a promoting contribute to the bone disease, uncoupled by the myeloma itself, exactly as the clinical behavior of MM bone disease. Normalising serotonin level in platelets for the total amount of circulating platelets for each patient the finding was confirmed, suggesting that serotonin in platelets is actually higher in MM patients with bone disease(data not shown). There was no difference in the total amount of serotonin among the 2 groups, thus in accord that MM patients do not generally refer symptoms due to hyper-serotoninergic tone.

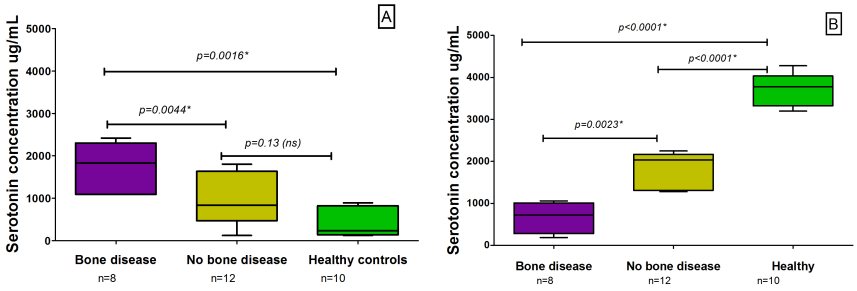


Fig. 3.25: Serotonin concentration, expressed in ug/mL, in platelets (right panel, A) and serum (left panel, B) isolated from peripheral blood of MM patients with or without bone disease compared to healthy controls.

Some clinical observations match with these experimental findings. First, the status of hypercoagulability typical of MM: even if universally present in both solid and haematological cancers, there is no evidence of appreciable defects in the coagulation cascade or in the platelets themselves. In our model, the initial excess of external serotonin in the bone marrow, as suggested by findings in the core biopsies, can be the consequence of the aberrant expression of TPH2 in neoplastic plasmacells, capable of inducing serotonylation of glutamine residues in cytoskeleton proteins (alpha-actin, beta-actin, gamma-actin, myosin heavy chain, filamin A) and GTPase (RhoA and RhoB), with consequent platelets‘ activation and degranulation of $\alpha$ granules [116]. Second, platelets can inter-

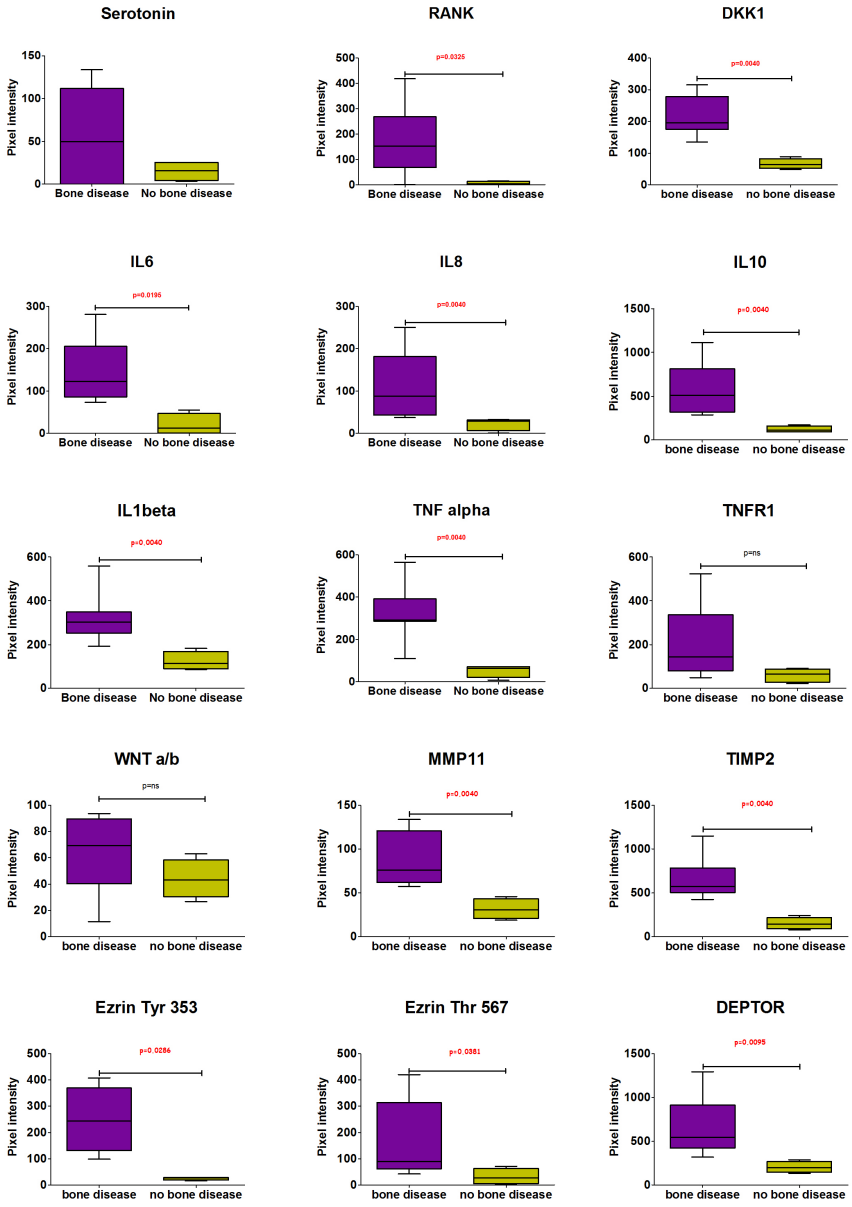


Fig. 3.26: Endpoints in MM patients with and without bone disease evaluating bone marrow core biopsies at RPMA

nalize serotonin as well during the megakaryocyte maturation [117, 118, 119]. MM patients treated with thalidomide and lenalidomide exhibit an increased risk of developing thrombotic events [120, 121, 122], and clinical trials to identify the best preventive strategy are ongoing as reviewed in [123]. Interestingly, in absence of additional risk factors aspirin was not inferior to warfarin and heparin,suggesting the need to act against the platelets‘ activation status [124]. Thalidomide and their analogs can selectively block the SERT [61], as we indirectly found in plasmacells treated ex-vivo with lenalidomide where we observed an increase in serotonin intensity value after treatment with 100nM lenalidomide for 18 hrs (fig. 3.27). After exposure to lenalidomide serotonin intensity

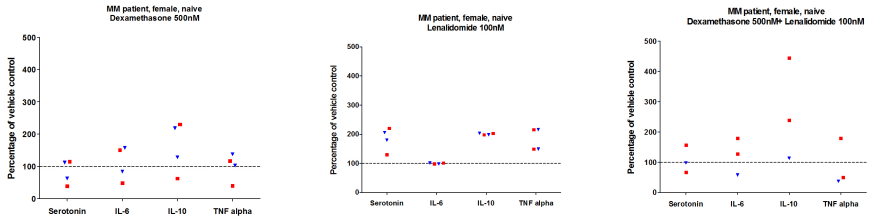


Fig. 3.27: Changes in relative intensity mean value of serotonin, IL-6, IL-10 and TNF$\alpha$ after exposure to dexamethasone, lenalidomide or their combination. Values on the y-axis represent treatment as a percentage of vehicle control. CD138$^+$ cells: triangles; bone marrow cells (BMC): squares.

value mean at RPMA was increased, likely for the partial block of SERT, while at the opposite after treatment with dexamethasone serotonin levels decreased, suggesting an improved ability to release or reduce the serotonin synthesis. The combo dexamethasone+lenalidomide is the neat result of these two opposite mechanisms.

The interactions between serotonin and blood cells and its modulatory effect on immune cells (monocytes/macrophages, T, B and NK cells) are well documented. Interestingly, serotonin can act as Th1/Th2 response relay: intracellular 5-HT is necessary for IFN$\gamma$ and IL-10 production by whole blood cells, while the external 5-HT decreases IFN$\gamma$ production, thus reflecting the cytokine imbalance present in Myeloma. We confirmed on both plasmacells (fig.3.28)

and bone marrow core biopsies (fig. 3.29) the positive correlation between serotonin and Th2 mediators, suggesting its pathogenetic role in Multiple Myeloma through the modulation of cellular signaling either directly through specific serotonin receptors and transporters or by modulating release of chemokines and cytokines.

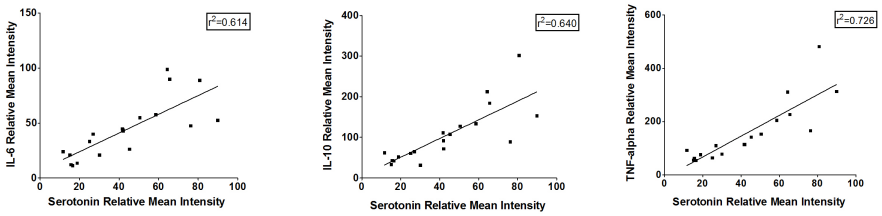


Fig. 3.28: In CD138$^+$ bone marrow aspirate cells, IL-6, Il-8 and TNF alpha intensity values detected by RPMA are positively correlated to Serotonin ones

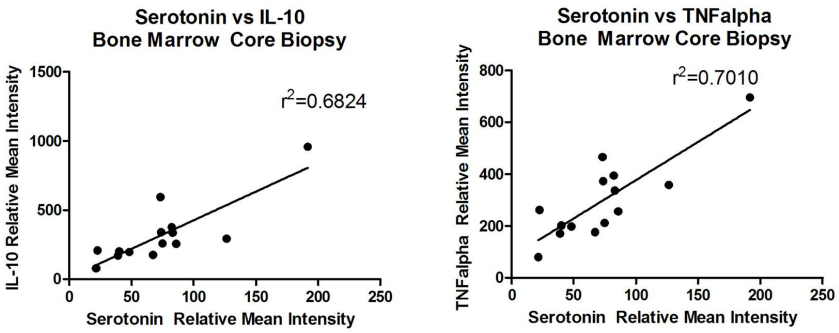


Fig. 3.29: The cellular concentration of Serotonin in bone marrow core biopsy samples from patients with multiple myeloma show a positive trend toward correlation with IL-10 and TNF$\alpha$ intensity values detected by RPMA.

## 3.6 Discussion of the results

Little is known about the cellular or molecular basis of MDS or about the progression of *early* MDS to *late* (or advanced) MDS or to AML. We provided for the first time a semiquantitative estimate of the fraction of leukemic cells carrying the 11q CN-LOH in a case of AML secondary to MDS and showed an

expansion of this clone during the AML progression. During the early phase of the relapse, we detected by MC few clones carrying only del20q, suggestsing that it might be one of the first abnormalities to appear. Other chromosomal aberrations, such as loss of chromosome 7 and t(8;17), can be acquired later on the background of the del20q-bearing clone. The predominant clones during the frank leukemic phases were derived from the same initiating clone as shown by the identical position of the breakpoints, both in the interstitial deletion of 20q and in the unbalanced translocation (8;17). We mapped the breakpoints of a novel rare unbalanced translocation involving 8q24 band and 17p13.3.

We worked with a mixture of neoplastic and non neoplastic cells to evaluate the proteomic and genomic profile in the bone marrow in toto, although with different and considerable amount of blasts in the samples at diagnosis. A potential criticism is that the mixture of neoplastic and normal cells that can generate false results. In the genomic profile we were able to distinguish the contribution of blasts, as showed with the bioinformatic implemented method [125]. In terms of proteomics, our data seem to confirm the recent and fascinating hypothesis of Autophagic Tumor Stroma Model [126]. Cancer cells induce oxidative stress in surrounding micoenvironment cells, leading to the induction of stromal autophagy. This has at least threee consequences: (a) it induces genomic instability in cancer cells; (b) it protects cancer cells against apoptosis and induces prosurvival pathways in the responsive microenvironment cells activating NFkB;(c) it provides cancer cells with recycled nutrients, fueling the anabolic growth of the tumor.

A strong rationale links autophagy to the survival of MDS progenitors. Physiologically, the stem cell niche provides signals that keep the HSC quiescent and largely protected from oxidative stress. The prolonged myelo-suppression seen in patients with MDS, and in patients with AML following MDS, suggests a limited hematopoietic reserve and implies that patients with MDS likely lose normal HSCs over time (perhaps due to defective self-renewal) and accumulate MDS HSCs (which may be better suited for competing for stem cell niches). Moreover, erythroblasts isolated from patients affected by low-risk MDS show

features of enhanced autophagy at an earlier stage of erythroid differentiation than in normal controls. The enhanced autophagy might be a cell protective mechanism to remove defective iron-laden mitochondria. Proliferating MDS precursors accumulating within the niche do not have access to the vasculature. Since autophagy is an established strategy for a cell to avoid apoptosis in the face of oxidative, hypoxic and nutrient deprivation stress, its activation seems reasonable in order to divert the hypoxic cells away from apoptosis and thereby support the survival and growth. Moreover the role of autophagy pathway in matrix degradation. Leukemia transformation is associated with interruptions, remodelling, and enzymatic breakdown of the extracellular matrix. Autophagy may facilitate cell movement through areas of degraded matrix by the phagocytic processing of matrix breakdown fragments. The malignant MDS precursor cells can use the compensatory answer to genetic remodelling induced by Azacitidine to up-regulate autophagy as a necessary means to generate anchorage independent elements. Few studies on AML are available, however it is clear that high-mobility group box 1 (HMGB1), the best characterized damage-associated molecular pattern, was released from leukemia cell lines after chemotherapy-induced cytotoxicity and activated autophagy to protect against injury. Treatment with HMGB1-neutralizing antibodies increased the sensitivity of leukemia cells to chemotherapy; exogenous HMGB1, on the contrary, rendered these cells more resistant to drug-induced cytotoxicity, again suggesting the role of a potential compensatory activation of autophagy after exposure to chemotherapy [127].

We found, analogously, the response to Dexamethasone in MM cells to be a double-edged sword. Clinical observations confirm its benefic therapeutic role, but also the quick development of resistance. Our data show clearly the compensatory induction of NFkB pathway, which is able to select the most aggressive clone, with a preferential activation in the plasma cell fraction.

In this regard, the assay developed for MM patients offers us the unique opportunity to test our theoretical approach to a living system that, even if unable to simulate entirely the patient, can take into account the complex of

interactions between neoplastic clone and the microenvironment.

The role of surrounding cells and the possibility to modulate them is a novel and intriguing field. Each patient can respond differently to a given chemotherapy not only for biological features of his tumor cells or his specific metabolism, but also for the compensatory pathways present as a consequence of cross-talking between cancer and stroma. We found this potential pathologic role in both MDS and MM, and our ability to modulate these escape-ways can lead to design with more awareness innovative combinations including old drugs .

The role of AKT in maintaining the MM neoplastic clone is known, but poorly investigated. It can be abrogated by Perifosine, a synthetic novel alkylphospholipid, which targets cell membranes and inhibits Akt activation. It has demonstrated significant antitumor activity in a human plasmacytoma mouse model and a synergic effect to induce MM cell cytotoxicity when combined to dexamethasone, doxorubicin, melphalan, and bortezomib [128], providing the rationale for clinical trials to improve patient outcome. However, it can not be used as single agent. The most promising study (Richardson, oral communication at ASH 2009, abstract #1869) included perifosine in combination with bortezomib (± dexamethasone) in both heavily pre-treated or bortezomib-refractory patients. It has been generally well tolerated, with an overall response rate (ORR) of 38% and overall survival (OS) of 16 months. We are waiting further results of a phase III randomized trial evaluating perifosine vs. placebo when combined with Vel and Dex in Vel-exposed patients with relapsed and refractory MM, started at the end of the last year, that will be presented at next ASH meeting.

New interactions have to be considered, as well. Starting from the observation that some drugs, like lenalidomide, were able to induce accumulation in the plasma cells, we started to investigate the neuro-immuno-endocrino system. Our data suggest that serotonin may modulate cell signalling in the bone marrow microenvironment via chemokines, cytokines, and invasion/inflammation pathways, as a component of the pathogenesis of osteolytic bone disease. Serotonin release is under neuro-endocrin control of leptin, and consequently it is

related to the energetic status of the body, linked to mTOR activation status. Further studies are ongoing in order to demonstrate the ability of malignant plasma cells to produce serotonin by itself to modify the microenvironment and take a survival advantage. Again, like for MDS precursors, the main advantage is the survival in an hypoxic niche rather than the proliferation, typical of more advanced stages.

Understanding mechanisms underlying the clonal selection and in particular the contribution of serotonin-driven pathway can promote treatment strategies for the whole spectrum of myeloma disease. Malignant B cells exhibit universally an aberrant SERT, and its modulation is controversial in lymphoproliferative disorders: serotonin drives apoptosis in biopsy-like Burkitt lymphoma cells after its entry through an active transport mechanism [57]. However, data available only on cell lines or primary cells, lacking the interaction with the microenvironment counterparts, are not enough detailed to elucidate these mechanisms. Conversely, two analogs of 5-HT-receptor antagonists (ICI-735 and ICI-685) induced cytotoxicity and a decrease in proliferation in several MM cell lines both sensitive and resistant to conventional therapies, as well as freshly isolated MM cells, even when co-cultured with IL-6, IGF-1 or long-term patient BM stromal cells [129]. Fluphenazine is a known antipsychtic and 5-HT(3) receptor antagonist, actually studied in a phase 1/2a (TX84040) for Relapsed or Relapsed-and-Refractory Multiple Myeloma for its ability to induce MM plasma cell death in vitro. Preliminary observations (S. Roth from ProImmune, oral communication) suggest a preferential accumulation in the bone marrow with minimal side effects (4/18 patients had a grade 1 extrapyramidal adverse event). Data on efficacy are available at the moment only for 5 patients that show stable disease after 4 cycles. We plan to test modulators of drugs active against serotonin transporter and receptors with our ex-vivo assay, alone and in combination with drugs used currently for MM, to verify how cytokine release can be affected and any potential synergistic effect.

# Chapter 4

# Conclusion and Future Perspectives

It is well established that the transition from normal to neoplastic growth involves deregulation at various cellular levels, including gene-specific mutational events, alterations in signal transduction and growth control pathways, dysfunctional DNA synthesis and repair mechanisms, resulting in the generation of chromosomal abnormalities. At the chromosomal level, it is now accepted that some degree of CNV and copy-neutral LOH exists in the normal karyotype. However, additional aberrancies can rapidly emerge during the course of in vitro culture, acting as the drivers of the dominant neoplastic phenotype, as is clearly shown in solid tumours (e.g. breast cancer). Transformed cells containing regions of excessive CNV can change the dosage of key regulatory genes and protein output, while *de novo* regions of LOH can potentially expose harmful recessive alleles [130]. In the context of genomic instability, looking at the differential *driver* and *passenger* mutations may seem to be only of academic interest. However, thanks to the application of SNP array, we showed that it is potentially possible to understand a role of *driver* for a specific aberration, but it is unlikely to find a unique alteration common to a class of patients to use to target the therapy.

It is clear that MDS has features that are quite distinct from those that characterize AML, with a more extensive genomic instability. While in AML one or two hits of focal genomic damage (e.g. represented by mutational status of FLT3, NPM, AML1 and so on) are enough to confer an advantageous phenotype, in MDS many, but smaller, changes are needed. Higher density microarrays, gene expression studies, and gene sequencing can be applied in candidate gene approaches using these data as a starting point. Even in the case in which different patients show different patterns of aberration, the same or similar regulatory pathways related to cell survival, oxidative stress, angiogenesis, or autophagy may be involved. The observation that hot regions identified increased gene dosage (e.g. c-myc in MDS, [99]) without a concomitant change in gene expression, confirms the importance to integrate analysis of network interferences at different levels (e.g. methylation, transcription, translation). In AML, targetting common and well-known puntiform mutations such as FLT3 has not yet produced significant responses, even if the clinical development of FLT3 inhibitors (SU11248 PKC412, CEP-701, MLN518) is still in early phases. More in general, we do not rely upon the selection of single agent based therapies good for all categories of patients, but on a personalised approach combining new and old agents, with either cytotoxic or other molecular targeted mechanism of action. As we better define the mechanisms underlying genomic instability we may be able to rationally choose therapies based on the genetic or gene expression profiles. Acquiring a better understanding of the nature of the interaction of MDS HSPCs with the bone marrow microenvironment will be critical as well.

In particular, the example of autophagy activation after exposure to Azacitidine in our MDS substudy is enlightening. In fact, it is well known that azacitidine is not able, for itself, to induce complete and persistant complete remissions in high risk MDS, but only to delay the transformation in AML or to stabilise the hematological values. Our observation, now, suggests the importance of a compensatory pathway, based on autophagy activation, able at the beginning to induce differentiation and apoptosis in those precursors resistant

and responsible of MDS phenotype. At later stages, under genomic instability and its selective pressure, the same clone able to respond increasing autophagy proteins to ungenerous ambiental conditions can become competely independent, starting over the progression to AML.

Similarly, the preliminary observation that Msi-2 can predict the stemness aggessiveness of MDS clone and the response to the treatment with Azacitidine led us to proceed in accord to a new paradigm: a proteic marker for a genomic drug in a well-defined genomic disease. A prospective evaluation of Msi-2 expression in fresh bone marrow aspirates from MDS patients in flow cytometry is ongoing to confirm our finding and enlarge the cohort of patients involved. Similarly, we will follow Msi-2 status month by month to correlate it with parameters of clinical response (increase of hemoglobin and platelets count, reduction of transfusional load). A bank of more than 400 core biopsies is available at Hematology Division and we plan to study Msi-2 also in immunohistochemistry, as potential biomarker at diagnosis. Meanwhile, we are setting up a method to reveal Msi-2 expression directly in cytochemistry, thus to work on bone marrow aspirates, in a cheaper and faster way, potentially available in all Hematology Centers, even if not possessing a Flow Cytometry facility.

A similar approach is ongoing also to test serotonin in the bone marrow aspirates, to extend its clinical application. Its evaluation could be included in the follow up of patients who did not achieve a complete/stringent remission, as additional marker of residual disease or aggressiveness at diagnosis. As regulator of cytokines type 2 serotonin will be evaluated in the context of immunological impairment in MM. An ongoing research at the Division of Hematology in Catania has established the role of a novel subpopulation secerning TNF$\alpha$ involved in the progression from MGUS to MM. Further studies will be addressed to understand the contribution of the different microenvironment subpopulations in serotonin release. On the other hand, preliminary experiments not discussed in this work have clearly shown that malignant plasma cells are able to produce serotonin.

Multiplexed phosphoprotein cell signalling analysis before or after treatment

with ex vivo inhibitors may predict patient-specific therapeutic response and/or off-target effects. Selected agents that show efficacy in ex vivo studies may be considered for further in vivo clinical studies in which signal profiling of the bone marrow cellular populations could be performed before and after molecular targeted therapy. The method identifies the therapy or combination of therapies most likely to yield the best results for a particular individual. In addition to improving clinical outcome, such theranostic evaluations could dramatically reduce health care costs, by avoiding ineffective therapies.

# Bibliography

[1] C. Aul, A. Giagounidis, and U. Germing. Epidemiological features of myelodysplastic syndromes: results from regional cancer surveys and hospital-based statistics. *International journal of hematology*, 73(4):405–410, 2001.

[2] J.E. Parker, G.J. Mufti, F. Rasool, A. Mijovic, S. Devereux, and A. Pagliuca. The role of apoptosis, proliferation, and the Bcl-2-related proteins in the myelodysplastic syndromes and acute myeloid leukemia secondary to MDS. *Blood*, 96(12):3932, 2000.

[3] M. Delforge. Understanding the pathogenesis of myelodysplastic syndromes. *The Hematology Journal*, 4(5):303–309, 2003.

[4] M. Parker. Ineffective haemopoiesis and apoptosis in myelodysplastic syndromes. *British journal of haematology*, 101(2):220–230, 1998.

[5] D.P. Steensma. The spectrum of molecular aberrations in myelodysplastic syndromes: in the shadow of acute myeloid leukemia. *Haematologica*, 92(6):723, 2007.

[6] J.W. Vardiman, J. Thiele, D.A. Arber, R.D. Brunning, M.J. Borowitz, A. Porwit, N.L. Harris, M.M. Le Beau, E. Hellstrom-Lindberg, A. Tefferi, et al. The 2008 revision of the World Health Organization (WHO) classification of myeloid neoplasms and acute leukemia: rationale and important changes. *Blood*, 114(5):937, 2009.

[7] L.P. Gondek, R. Tiu, C.L. O'Keefe, M.A. Sekeres, K.S. Theil, and J.P. Maciejewski. Chromosomal lesions and uniparental disomy detected by SNP arrays in MDS, MDS/MPD, and MDS-derived AML. *Blood*, 111(3):1534, 2008.

[8] P. Fenaux. Inhibitors of DNA methylation: beyond myelodysplastic syndromes. *Nature Clinical Practice Oncology*, 2:S36–S44, 2005.

[9] H. Kantarjian, S. O'Brien, J. Cortes, W. Wierda, S. Faderl, G. Garcia-Manero, J.P. Issa, E. Estey, M. Keating, and E.J. Freireich. Therapeutic advances in leukemia and myelodysplastic syndrome over the past 40 years. *Cancer*, 113(S7):1933–1952, 2008.

[10] R. Gurion, L. Vidal, A. Gafter-Gvili, Y. Belnik, M. Yeshurun, P. Raanani, and O. Shpilberg. 5-azacitidine prolongs overall survival in patients with myelodysplastic syndrome-a systematic review and meta-analysis. *Haematologica*, 95(2):303, 2010.

[11] P.A. Link, M.R. Baer, S.R. James, D.A. Jones, and A.R. Karpf. p53-Inducible Ribonucleotide Reductase (p53R2/RRM2B) Is a DNA Hypomethylation–Independent Decitabine Gene Target That Correlates with Clinical Response in Myelodysplastic Syndrome/Acute Myelogenous Leukemia. *Cancer research*, 68(22):9358, 2008.

[12] C. Cutler and J.H. Antin. Peripheral blood stem cells for allogeneic transplantation: a review. *Stem Cells*, 19(2):108–117, 2001.

[13] H.M. Kantarjian, S. O'Brien, X. Huang, G. Garcia-Manero, F. Ravandi, J. Cortes, J. Shan, J. Davisson, C.E. Bueso-Ramos, and J.P. Issa. Survival advantage with decitabine versus intensive chemotherapy in patients with higher risk myelodysplastic syndrome. *Cancer*, 109(6):1133–1137, 2007.

[14] L.R. Silverman, E.P. Demakos, B.L. Peterson, A.B. Kornblith, J.C. Holland, R. Odchimar-Reissig, R.M. Stone, D. Nelson, B.L. Powell, C.M. DeCastro, et al. Randomized controlled trial of azacitidine in patients

with the myelodysplastic syndrome: a study of the cancer and leukemia group B. *Journal of Clinical Oncology*, 20(10):2429, 2002.

[15] L.R. Silverman, D.R. McKenzie, B.L. Peterson, J.F. Holland, J.T. Backstrom, CL Beach, and R.A. Larson. Further analysis of trials with azacitidine in patients with myelodysplastic syndrome: studies 8421, 8921, and 9221 by the Cancer and Leukemia Group B. *Journal of Clinical oncology*, 24(24):3895, 2006.

[16] A. Kumar, A.F. List, I. Hozo, R. Komrokji, and B. Djulbegovic. Decitabine versus 5-azacitidine for the treatment of myelodysplastic syndrome: adjusted indirect meta-analysis. *Haematologica*, 95(2):340, 2010.

[17] C. Herbst, K. Bauer, and K.A. Kreuzer. Meta-analysis on hypomethylating agents in myelodysplastic syndromes. *Haematologica*, 95(2):342, 2010.

[18] D.P. Steensma and R.M. Stone. Practical recommendations for hypomethylating agent therapy of patients with myelodysplastic syndromes. *Hematology/oncology clinics of North America*, 24(2), 2010.

[19] A. Jemal, R. Siegel, E. Ward, T. Murray, J. Xu, and M.J. Thun. Cancer statistics, 2007. *CA: a cancer journal for clinicians*, 57(1):43–66, 2007.

[20] Y. Inamoto, S. Kurahashi, N. Imahashi, N. Fukushima, T. Adachi, T. Kinoshita, K. Tsushita, K. Miyamura, T. Naoe, and I. Sugiura. Combinations of cytogenetics and international scoring system can predict poor prognosis in multiple myeloma after high-dose chemotherapy and autologous stem cell transplantation. *American journal of hematology*, 84(5):283–286, 2009.

[21] M. Hallek, P. Leif Bergsagel, and K.C. Anderson. Multiple myeloma: increasing evidence for a multistep transformation process. *Blood*, 91(1):3, 1998.

[22] T. Hideshima, C. Mitsiades, G. Tonon, P.G. Richardson, and K.C. Anderson. Understanding multiple myeloma pathogenesis in the bone marrow

to identify new therapeutic targets. *Nature Reviews Cancer*, 7(8):585–598, 2007.

[23] F. Xu, S. Sharma, A. Gardner, Y. Tu, A. Raitano, C. Sawyers, and A. Lichtenstein. Interleukin-6-induced inhibition of multiple myeloma cell apoptosis: support for the hypothesis that protection is mediated via inhibition of the JNK/SAPK pathway. *Blood*, 92(1):241, 1998.

[24] A. Ogata, D. Chauhan, G. Teoh, S.P. Treon, M. Urashima, R.L. Schlossman, and K.C. Anderson. IL-6 triggers cell growth via the Ras-dependent mitogen-activated protein kinase cascade. *The Journal of Immunology*, 159(5):2212, 1997.

[25] S. Côté, R. Lemieux, and C. Simard. The survival of IL-6-dependent myeloma cells critically relies on their capability to transit the G1 to S phase interval of the cell cycle. *Cellular signalling*, 17(5):615–624, 2005.

[26] M. Adib-Conquy, A.F. Petit, C. Marie, C. Fitting, and J.M. Cavaillon. Paradoxical priming effects of IL-10 on cytokine production. *International immunology*, 11(5):689, 1999.

[27] H. Quach, D. Ritchie, AK Stewart, P. Neeson, S. Harrison, MJ Smyth, and HM Prince. Mechanism of action of immunomodulatory drugs (IMiDS) in multiple myeloma. *Leukemia*, 2009.

[28] T. Hideshima, P. Richardson, and K.C. Anderson. Novel therapeutic approaches for multiple myeloma. *Immunological reviews*, 194(1):164–176, 2003.

[29] PW Thavasu, RK Ganjoo, SA Maidment, SB Love, AH Williams, JS Malplas, and FR Balkwill. Multiple myeloma: an immunoclinical study of disease and response to treatment. *Hematological oncology*, 13(2):69–82, 1995.

[30] F. Wan and M.J. Lenardo. The nuclear signaling of NF-$\kappa$B: current knowledge, new insights, and future perspectives. *Cell Research*, 20(1):24–33, 2009.

[31] U. Senftleben, Y. Cao, G. Xiao, F.R. Greten, G. Krahn, G. Bonizzi, Y. Chen, Y. Hu, A. Fong, S.C. Sun, et al. Activation by IKKalpha of a second, evolutionary conserved, NF-kappa B signaling pathway. *Science*, 293(5534):1495, 2001.

[32] M.S. Hayden and S. Ghosh. Shared principles in NF-[kappa] B signaling. *Cell*, 132(3):344–362, 2008.

[33] C. Conticello, R. Giuffrida, L. Adamo, G. Anastasi, D. Martinetti, E. Salomone, C. Colarossi, G. Amato, A. Gorgone, A. Romano, et al. NF-$\kappa$B localization in multiple myeloma plasma cells and mesenchymal cells. *Leukemia research*, 2010.

[34] D.J. McConkey. Bortezomib paradigm shift in myeloma. *Blood*, 114(5):931, 2009.

[35] Teru Hideshima, Hiroshi Ikeda, Dharminder Chauhan, Yutaka Okawa, Noopur Raje, Klaus Podar, Constantine Mitsiades, Nikhil C. Munshi, Paul G. Richardson, Ruben D. Carrasco, and Kenneth C. Anderson. Bortezomib induces canonical nuclear factor-kappaB activation in multiple myeloma cells. *Blood*, 114(5):1046–1052, 2009.

[36] N.W.C.J. van de Donk, H.M. Lokhorst, M. Dimopoulos, M. Cavo, G. Morgan, H. Einsele, M. Kropff, S. Schey, H. Avet-Loiseau, H. Ludwig, et al. Treatment of relapsed and refractory multiple myeloma in the era of novel agents. *Cancer Treatment Reviews*, 2010.

[37] S.L. Planey and G. Litwack. Glucocorticoid-Induced Apoptosis in Lymphocytes. *Biochemical and Biophysical Research Communications*, 279(2):307–312, 2000.

[38] P.A. Moalli and S.T. Rosen. Glucocorticoid receptors and resistance to glucocorticoids in hematologic malignancies. *Leukemia & Lymphoma*, 15(5-6):363–374, 1994.

[39] N.L. Krett, S. Pillay, P.A. Moalli, P.R. Greipp, and S.T. Rosen. A variant glucocorticoid receptor messenger RNA is expressed in multiple myeloma patients. *Cancer research*, 55(13):2727, 1995.

[40] P.A. Moalli, S. Pillay, D. Weiner, R. Leikin, and S.T. Rosen. A mechanism of resistance to glucocorticoids in multiple myeloma: transient expression of a truncated glucocorticoid receptor mRNA. *Blood*, 79(1):213, 1992.

[41] E. Ayroldi and C. Riccardi. Glucocorticoid-induced leucine zipper (GILZ): a new important mediator of glucocorticoid action. *The FASEB Journal*, 23(11):3649, 2009.

[42] D. Chauhan, D. Auclair, E.K. Robinson, T. Hideshima, L. Guilan, K. Podar, D. Gupta, P. Richardson, R.L. Schlossman, N. Krett, et al. Identification of genes regulated by dexamethasone in multiple myeloma cells using oligonucleotide arrays. *Oncogene*, 21(9):1346–1358, 2002.

[43] J.D. Karkera, S.E. Taymans, G. Turner, T. Yoshikawa, S.D. Detera-Wadleigh, and R.G. Wadleigh. Deletion of a consensus oestrogen response element half-site in the glucocorticoid receptor of human multiple myeloma. *British journal of haematology*, 99(2):372–374, 1997.

[44] P. de Lange, C.M. Segeren, J.W. Koper, E. Wiemer, P. Sonneveld, A.O. Brinkmann, A. White, I.J. Brogan, F.H. de Jong, and S.W.J. Lamberts. Expression in hematological malignancies of a glucocorticoid receptor splice variant that augments glucocorticoid receptor-mediated effects in transfected cells. *Cancer research*, 61(10):3937, 2010.

[45] G.W. Muller, R. Chen, S.Y. Huang, L.G. Corral, L.M. Wong, R.T. Patterson, Y. Chen, G. Kaplan, and D.I. Stirling. Amino-substituted thalidomide analogs: Potent inhibitors of TNF-[alpha] production. *Bioorganic & medicinal chemistry letters*, 9(11):1625–1630, 1999.

[46] E.P. Sampaio, E.N. Sarno, R. Galilly, Z.A. Cohn, and G. Kaplan. Thalidomide selectively inhibits tumor necrosis factor alpha production

by stimulated human monocytes. *The Journal of experimental medicine*, 173(3):699, 1991.

[47] V. Kotla, S. Goel, S. Nischal, C. Heuck, K. Vivek, B. Das, and A. Verma. Mechanism of action of lenalidomide in hematological malignancies. *J Hematol Oncol*, 2:36, 2009.

[48] R. Lahtinen, M. Laakso, I. Palva, I. Elomaa, and P. Virkkunen. Randomised, placebo-controlled multicentre trial of clodronate in multiple myeloma. *The Lancet*, 340(8827):1049–1052, 1992.

[49] J.A. Kanis. Primer on the metabolic bone diseases and disorders of mineral metabolism. *British Medical Journal*, 53(3):157, 1994.

[50] C.M. Edwards, J. Zhuang, and G.R. Mundy. The pathogenesis of the bone disease of multiple myeloma. *Bone*, 42(6):1007–1013, 2008.

[51] M. Abe, K. Hiura, J. Wilde, A. Shioyasono, K. Moriyama, T. Hashimoto, S. Kido, T. Oshima, H. Shibata, S. Ozaki, et al. Osteoclasts enhance myeloma cell growth and survival via cell-cell contact: a vicious cycle between bone destruction and myeloma expansion. *Blood*, 104(8):2484, 2004.

[52] W.K. Kroeze, K. Kristiansen, and B.L. Roth. Molecular biology of serotonin receptors-structure and function at the molecular level. *Current Topics in Medicinal Chemistry*, 2(6):507–528, 2002.

[53] J. Hannon and D. Hoyer. Molecular biology of 5-HT receptors. *Behavioural brain research*, 195(1):198–213, 2008.

[54] M. Kubera, M. Maes, G. Kenis, Y.K. Kim, and W. Lason. Effects of serotonin and serotonergic agonists and antagonists on the production of tumor necrosis factor [alpha] and interleukin-6. *Psychiatry research*, 134(3):251–258, 2005.

[55] R. Zilkha-Falb, I. Ziv, N. Nardi, D. Offen, E. Melamed, and A. Barzilai. Monoamine-induced apoptotic neuronal cell death. *Cellular and molecular neurobiology*, 17(1):101–118, 1997.

[56] A. Serafeim, G. Grafton, A. Chamba, C.D. Gregory, R.D. Blakely, N.G. Bowery, N.M. Barnes, and J. Gordon. 5-Hydroxytryptamine drives apoptosis in biopsylike Burkitt lymphoma cells: reversal by selective serotonin reuptake inhibitors. *Blood*, 99(7):2545, 2002.

[57] A. Serafeim, M.J. Holder, G. Grafton, A. Chamba, M.T. Drayson, Q.T. Luong, C.M. Bunce, C.D. Gregory, N.M. Barnes, and J. Gordon. Selective serotonin reuptake inhibitors directly signal for apoptosis in biopsy-like Burkitt lymphoma cells. *Blood*, 101(8):3212, 2003.

[58] I.P. Kema, E.G.E. de Vries, and F.A.J. Muskiet. Clinical chemistry of serotonin and metabolites. *Journal of Chromatography B: Biomedical Sciences and Applications*, 747(1-2):33–48, 2000.

[59] X. Zhang, J.M. Beaulieu, T.D. Sotnikova, R.R. Gainetdinov, and M.G. Caron. Tryptophan hydroxylase-2 controls brain serotonin synthesis. *Science*, 305(5681):217, 2004.

[60] J. Gordon and N.M. Barnes. Lymphocytes transport serotonin and dopamine: agony or ecstasy? *TRENDS in immunology*, 24(8):438–443, 2003.

[61] E.J. Meredith, M.J. Holder, A. Chamba, A. Challa, A. Drake Lee, C.M. Bunce, M.T. Drayson, G. Pilkington, R.D. Blakely, M.J.S. Dyer, et al. The serotonin transporter (SLC6A4) is present in B-cell clones of diverse malignant origin: probing a potential antitumor target for psychotropics. *The FASEB Journal*, page 04, 2005.

[62] V.L. Serebruany, A.H. Glassman, A.I. Malinin, C.B. Nemeroff, D.L. Musselman, L.T. van Zyl, M.S. Finkel, K.R.R. Krishnan, M. Gaffney, W. Harrison, et al. Platelet/endothelial biomarkers in depressed patients treated

with the selective serotonin reuptake inhibitor sertraline after acute coronary events: the Sertraline AntiDepressant Heart Attack Randomized Trial (SADHART) Platelet Substudy. *Circulation*, 108(8):939, 2003.

[63] J.P. Ruddick, A.K. Evans, D.J. Nutt, S.L. Lightman, G.A.W. Rook, and C.A. Lowry. Tryptophan metabolism in the central nervous system: medical implications. *Expert reviews in molecular medicine*, 8(20):1–27, 2006.

[64] E.J. Siddiqui, C.S. Thompson, D.P. Mikhailidis, and F.H. Mumtaz. The role of serotonin in tumour growth (review). *Oncology reports*, 14(6):1593, 2005.

[65] V. Pai, A. Marshall, L. Hernandez, A. Buckley, and N. Horseman. Altered serotonin physiology in human breast cancers favors paradoxical growth and cell survival. *Breast Cancer Research*, 11(6):R81, 2009.

[66] A. Slominski, J. Wortsman, and D.J. Tobin. The cutaneous serotoninergic/melatoninergic system: securing a place under the sun. *The FASEB Journal*, 19(2):176, 2005.

[67] L.M. Vicentini, M.G. Cattaneo, and R. Fesce. Evidence for receptor subtype cross-talk in the mitogenic action of serotonin on human small-cell lung carcinoma cells. *European journal of pharmacology*, 318(2-3):497–504, 1996.

[68] E.J. Siddiqui, M. Shabbir, D.P. Mikhailidis, C.S. Thompson, and F.H. Mumtaz. The role of serotonin (5-hydroxytryptamine1A and 1B) receptors in prostate cancer cell proliferation. *The Journal of urology*, 176(4):1648–1653, 2006.

[69] G. Alpini, P. Invernizzi, E. Gaudio, J. Venter, S. Kopriva, F. Bernuzzi, P. Onori, A. Franchitto, M. Coufal, G. Frampton, et al. Serotonin metabolism is dysregulated in cholangiocarcinoma, which has implications for tumor growth. *Cancer research*, 68(22):9184, 2008.

[70] B.C. Fuchs and B.P. Bode. Amino acid transporters ASCT2 and LAT1 in cancer: partners in crime? In *Seminars in cancer biology*, volume 15, pages 254–266. Elsevier, 2005.

[71] RK Singh and GP Siegal. Amino acid transport systems modulate human tumor cell growth and invasion: A working hypothesis. *Medical hypotheses*, 44(3):195–201, 1995.

[72] X. Liu, S.V. Reyna, D. Ensenat, K.J. Peyton, H. Wang, A.I. Schafer, and W. Durante. Platelet-derived growth factor stimulates LAT1 gene expression in vascular smooth muscle: role in cell growth. *The FASEB Journal*, page 308861, 2004.

[73] A.L. Edinger and C.B. Thompson. Akt maintains cell size and survival by increasing mTOR-dependent nutrient uptake. *Science's STKE*, 13(7):2276, 2002.

[74] T. Peng, T.R. Golub, and D.M. Sabatini. The immunosuppressant rapamycin mimics a starvation-like signal distinct from amino acid and glucose deprivation. *Molecular and cellular biology*, 22(15):5575, 2002.

[75] G. Karsenty. Regulation of Bone Mass by Serotonin: Molecular Biology and Therapeutic Implications. *Medicine*, 62:2011, 2010.

[76] P. Ducy and G. Karsenty. The two faces of serotonin in bone biology. *The Journal of Cell Biology*, 191(1):7, 2010.

[77] L. Beil. Serotonin: What the gut feeds the bones: Chemical messenger plays a surprising role in determining the strength of the skeleton. *Science News*, 175(12):16–19, 2009.

[78] J. Hawiger, S. Steckley, D. Hammond, C. Cheng, S. Timmons, A.D. Glick, and R.M. Des Prez. Staphylococci-induced human platelet injury mediated by protein A and immunoglobulin G Fc fragment receptor. *Journal of Clinical Investigation*, 64(4):931, 1979.

[79] R. Kurup, R.A. Nair, and P.A. Kurup. Isoprenoid pathway related cascade in multiple myeloma. *Pathology & Oncology Research*, 9(2):107–114, 2003.

[80] J.P. Maciejewski, R.V. Tiu, and C. OKeefe. Application of array-based whole genome scanning technologies as a cytogenetic tool in haematological malignancies. *British journal of haematology*, 146(5):479–488, 2009.

[81] A.J. Iafrate, L. Feuk, M.N. Rivera, M.L. Listewnik, P.K. Donahoe, Y. Qi, S.W. Scherer, and C. Lee. Detection of large-scale variation in the human genome. *Nature genetics*, 36(9):949–951, 2004.

[82] K.K. Wong, R.J. DeLeeuw, N.S. Dosanjh, L.R. Kimm, Z. Cheng, D.E. Horsman, C. MacAulay, R.T. Ng, C.J. Brown, E.E. Eichler, et al. A comprehensive analysis of common copy-number variations in the human genome. *The American Journal of Human Genetics*, 80(1):91–104, 2007.

[83] M. Jakobsson, S.W. Scholz, P. Scheet, J.R. Gibbs, J.M. VanLiere, H.C. Fung, Z.A. Szpiech, J.H. Degnan, K. Wang, R. Guerreiro, et al. Genotype, haplotype and copy-number variation in worldwide human populations. *Nature*, 451(7181):998–1003, 2008.

[84] KW Choy, SR Setlur, C. Lee, and TK Lau. The impact of human copy number variation on a new era of genetic testing. *BJOG: An International Journal of Obstetrics & Gynaecology*, 117(4):391–398, 2010.

[85] RR Tubbs, JD Pettay, PC Roche, MH Stoler, RB Jenkins, and TM Grogan. Discrepancies in clinical laboratory testing of eligibility for trastuzumab therapy: apparent immunohistochemical false-positives do not get the message. *Journal of Clinical Oncology*, 19(10):2714, 2001.

[86] J.M. Korn, F.G. Kuruvilla, S.A. McCarroll, A. Wysoker, J. Nemesh, S. Cawley, E. Hubbell, J. Veitch, P.J. Collins, K. Darvishi, et al. Integrated genotype calling and association analysis of SNPs, common copy number polymorphisms and rare CNVs. *Nature genetics*, 40(10):1253–1260, 2008.

[87] S.A. McCarroll, F.G. Kuruvilla, J.M. Korn, S. Cawley, J. Nemesh, A. Wysoker, M.H. Shapero, P.I.W. de Bakker, J.B. Maller, A. Kirby, et al. Integrated detection and population-genetic analysis of SNPs and copy number variation. *Nature genetics*, 40(10):1166–1174, 2008.

[88] A.J. Dunbar, L.P. Gondek, C.L. O'Keefe, H. Makishima, M.S. Rataul, H. Szpurka, M.A. Sekeres, X.F. Wang, M.A. McDevitt, and J.P. Maciejewski. 250K single nucleotide polymorphism array karyotyping identifies acquired uniparental disomy and homozygous mutations, including novel missense substitutions of c-Cbl, in myeloid malignancies. *Cancer research*, 68(24):10349, 2008.

[89] V. ESPINA, L. LIOTTA, and E. PETRICOIN. Ex vivo therapeutic screening of living bone marrow cells for multiple myeloma, February 18 2010. WO Patent WO/2010/019,227.

[90] V. Espina, C. Mueller, K. Edmiston, M. Sciro, E.F. Petricoin, and L.A. Liotta. Tissue is alive: New technologies are needed to address the problems of protein biomarker pre-analytical variability. *PROTEOMICS–Clinical Applications*, 3(8):874–882, 2009.

[91] L.A. Liotta, E.F. Petricoin III, D. Geho, and V.A. Espina. TISSUE PRESERVATION AND FIXATION METHOD, October 26 2007. US Patent App. 20,100/068,690.

[92] B. Wilson, L.A. Liotta, and E. Petricoin III. Monitoring proteins and protein networks using reverse phase protein arrays. *Disease Markers*, 28(4):225–232, 2010.

[93] C. Mueller, L.A. Liotta, and V. Espina. Reverse phase protein microarrays advance to use in clinical trials. *Molecular Oncology*, 2010.

[94] A. VanMeter, M. Signore, M. Pierobon, V. Espina, L.A. Liotta, III Petricoin, and F. Emanuel. Reverse-phase protein microarrays: application to biomarker discovery and translational medicine. *Expert review of molecular diagnostics*, 7(5):625–633, 2007.

[95] G.S. Mundinger, V. Espina, L.A. Liotta, E.F. Petricoin, and K.R. Calvo. Clinical phosphoproteomic profiling for personalized targeted medicine using reverse phase protein microarray. *Targeted Oncology*, 1(3):151–167, 2006.

[96] F.G. Rücker, L. Bullinger, C. Schwaenen, D.B. Lipka, S. Wessendorf, S. Fröhling, M. Bentz, S. Miller, C. Scholl, R.F. Schlenk, et al. Disclosure of candidate genes in acute myeloid leukemia with complex karyotypes using microarray-based molecular characterization. *Journal of Clinical Oncology*, 24(24):3887, 2006.

[97] M.L. Slovak, J.P. Ho, M.J. Pettenati, A. Khan, D. Douer, S. Lal, and S. Thomas Traweek. Localization of amplified MYC gene sequences to double minute chromosomes in acute myelogenous leukemia. *Genes, Chromosomes and Cancer*, 9(1):62–67, 1994.

[98] K. Alitalo, R. Winqvist, J. Keski-Oja, M. Ilvonen, K. Saksela, R. Alitalo, M. Laiho, S. Knuutila, and A. De La Chapelle. Acute myelogenous leukaemia with c-myc amplification and double minute chromosomes. *The Lancet*, 326(8463):1035–1039, 1985.

[99] C.T. Storlazzi, T. Fioretos, C. Surace, A. Lonoce, A. Mastrorilli, B. Strömbeck, P. D'Addabbo, F. Iacovelli, C. Minervini, A. Aventin, et al. MYC-containing double minutes in hematologic malignancies: evidence in favor of the episome model and exclusion of MYC as the target gene. *Human molecular genetics*, 15(6):933, 2006.

[100] F.H. Grand, C.E. Hidalgo-Curtis, T. Ernst, K. Zoi, C. Zoi, C. McGuire, S. Kreil, A. Jones, J. Score, G. Metzgeroth, et al. Frequent CBL mutations associated with 11q acquired uniparental disomy in myeloproliferative neoplasms. *Blood*, 113(24):6182, 2009.

[101] M. Sanada, T. Suzuki, L.Y. Shih, M. Otsu, M. Kato, S. Yamazaki, A. Tamura, H. Honda, M. Sakata-Yanagimoto, K. Kumano, et al. Gain-

of-function of mutated C-CBL tumour suppressor in myeloid neoplasms. *Nature*, 460(7257):904–908, 2009.

[102] K.J. Hope, S. Cellot, S.B. Ting, T. MacRae, N. Mayotte, N.N. Iscove, and G. Sauvageau. An RNAi Screen Identifies Msi2 and Prox1 as Having Opposite Roles in the Regulation of Hematopoietic Stem Cell Activity. *Cell Stem Cell*, 7(1):101–113, 2010.

[103] Y. Nishimoto and H. Okano. New insight into cancer therapeutics: Induction of differentiation by regulating the Musashi/Numb/Notch pathway. *Cell Research*, 2010.

[104] A. Rascle and E. Lees. Chromatin acetylation and remodeling at the Cis promoter during STAT5-induced transcription. *Nucleic acids research*, 31(23):6882, 2003.

[105] S.G. Rane, R. PREMKUMAR, et al. JAKs, STATs and Src kinases in hematopoiesis. *Oncogene*, 21(21):3334–3358, 2002.

[106] J. Hsu, Y. Shi, S. Krajewski, S. Renner, M. Fisher, J.C. Reed, T.F. Franke, and A. Lichtenstein. The AKT kinase is activated in multiple myeloma tumor cells. *Blood*, 98(9):2853, 2001.

[107] Y. Tu, A. Gardner, and A. Lichtenstein. The phosphatidylinositol 3-kinase/AKT kinase pathway in multiple myeloma plasma cells: roles in cytokine-dependent survival and proliferative responses. *Cancer research*, 60(23):6763, 2000.

[108] T. Hideshima, N. Nakamura, D. Chauhan, and K.C. Anderson. Biologic sequelae of interleukin-6 induced PI3-K/Akt signaling in multiple myeloma. *Oncogene*, 20(42):5991, 2001.

[109] R.D. Harvey and S. Lonial. PI3 kinase/AKT pathway as a therapeutic target in multiple myeloma. *Future Oncology*, 3(6):639–647, 2007.

[110] Y.T. Tai, K. Podar, N. Mitsiades, B. Lin, C. Mitsiades, D. Gupta, M. Akiyama, L. Catley, T. Hideshima, N.C. Munshi, et al. CD40 in-

duces human multiple myeloma cell migration via phosphatidylinositol 3-kinase/AKT/NF-kappa B signaling. *Blood*, 101(7):2762, 2003.

[111] E. Menu, R. Kooijman, E. Van Valckenborgh, K. Asosingh, M. Bakkus, B. Van Camp, and K. Vanderkerken. Specific roles for the PI3K and the MEK–ERK pathway in IGF-1-stimulated chemotaxis, VEGF secretion and proliferation of multiple myeloma cells: study in the 5T33MM model. *British journal of cancer*, 90(5):1076–1083, 2004.

[112] T. Hideshima, N. Nakamura, D. Chauhan, and K.C. Anderson. Biologic sequelae of interleukin-6 induced PI3-K/Akt signaling in multiple myeloma. *Oncogene*, 20(42):5991, 2001.

[113] C.S. Mitsiades, N. Mitsiades, V. Poulaki, R. Schlossman, M. Akiyama, D. Chauhan, T. Hideshima, S.P. Treon, N.C. Munshi, P.G. Richardson, et al. Activation of NFkB and upregulation of intracellular anti-apoptotic proteins via the IGF-1/Akt signaling in human multiple myeloma cells: therapeutic implications. *Oncogene*, 21:5673–5683, 2002.

[114] Y. Shi, H. Yan, P. Frost, J. Gera, and A. Lichtenstein. Mammalian target of rapamycin inhibitors activate the AKT kinase in multiple myeloma cells by up-regulating the insulin-like growth factor receptor/insulin receptor substrate-1/phosphatidylinositol 3-kinase cascade. *Molecular cancer therapeutics*, 4(10):1533, 2005.

[115] N. Raje, S. Kumar, T. Hideshima, K. Ishitsuka, D. Chauhan, C. Mitsiades, K. Podar, S. Le Gouill, P. Richardson, N.C. Munshi, et al. Combination of the mTOR inhibitor rapamycin and CC-5013 has synergistic activity in multiple myeloma. *Blood*, 104(13):4188, 2004.

[116] D.J. Walther, J.U. Peter, S. Winter, M. Höltje, N. Paulmann, M. Grohmann, J. Vowinckel, V. Alamo-Bethencourt, C.S. Wilhelm, G. Ahnert-Hilger, et al. Serotonylation of small GTPases is a signal transduction pathway that triggers platelet [alpha]-granule release. *Cell*, 115(7):851–862, 2003.

[117] PK Schick and M. Weinstein. A marker for megakaryocytes: serotonin accumulation in guinea pig megakaryocytes. *The Journal of laboratory and clinical medicine*, 98(4):607, 1981.

[118] J.G. White. Serotonin storage organelles in human megakaryocytes. *The American Journal of Pathology*, 63(3):403, 1971.

[119] M. Yang, A. Srikiatkhachorn, M. Anthony, and BH Chong. Serotonin stimulates megakaryocytopoiesis via the 5-HT2 receptor. *Blood Coagulation & Fibrinolysis*, 7(2):127, 1996.

[120] S.V. Rajkumar, E. Blood, D. Vesole, R. Fonseca, and P.R. Greipp. Phase III clinical trial of thalidomide plus dexamethasone compared with dexamethasone alone in newly diagnosed multiple myeloma: a clinical trial coordinated by the Eastern Cooperative Oncology Group. *Journal of clinical oncology*, 24(3):431, 2006.

[121] S.V. Rajkumar. Thalidomide therapy and deep venous thrombosis in multiple myeloma. In *Mayo Clinic Proceedings*, volume 80, page 1549. Mayo Clinic, 2005.

[122] A. Palumbo, S. Bringhen, T. Caravita, E. Merla, V. Capparella, V. Callea, C. Cangialosi, M. Grasso, F. Rossini, M. Galli, et al. Oral melphalan and prednisone chemotherapy plus thalidomide compared with melphalan and prednisone alone in elderly patients with multiple myeloma: randomised controlled trial. *The Lancet*, 367(9513):825–831, 2006.

[123] J. Hirsh. Risk of Thrombosis With Lenalidomide and Its Prevention With Aspirin. *Chest*, 131(1):275, 2007.

[124] A. Palumbo, SV Rajkumar, MA Dimopoulos, PG Richardson, J. San Miguel, B. Barlogie, J. Harousseau, JA Zonder, M. Cavo, M. Zangari, et al. Prevention of thalidomide-and lenalidomide-associated thrombosis in myeloma. *Leukemia*, 22(2):414–423, 2007.

[125] V. Barresi, G.A. Palumbo, N. Musso, C. Consoli, C. Capizzi, C.R. Meli, A. Romano, F. Di Raimondo, and D.F. Condorelli. Clonal selection of

11q CN-LOH and CBL gene mutation in a serially studied patient during MDS progression to AML. *Leukemia research*, 34(11):1539–1542, 2010.

[126] U.E. Martinez-Outschoorn, D. Whitaker-Menezes, S. Pavlides, B. Chiavarina, G. Bonuccelli, T. Casey, A. Tsirigos, G. Migneco, A. Witkiewicz, R. Balliet, et al. The autophagic tumor stroma model of cancer or battery-operated tumor growth: A simple solution to the autophagy paradox. *Cell Cycle*, 9(21), 2010.

[127] L. Liu, M. Yang, R. Kang, Z. Wang, Y. Zhao, Y. Yu, M. Xie, X. Yin, KM Livesey, MT Lotze, et al. HMGB1-induced autophagy promotes chemotherapy resistance in leukemia cells. *Leukemia*, 2010.

[128] T. Hideshima, L. Catley, H. Yasui, K. Ishitsuka, N. Raje, C. Mitsiades, K. Podar, N.C. Munshi, D. Chauhan, P.G. Richardson, et al. Perifosine, an oral bioactive novel alkylphospholipid, inhibits Akt and induces in vitro and in vivo cytotoxicity in human multiple myeloma cells. *Blood*, 107(10):4053, 2006.

[129] Enrique M. Ocio, Teru Hideshima, Hiroshi Yasui, Kiziltepe Tanyel, Hirosi Ikeda, Yutaka Okawa, Sonia Vallet, Janice Jin, Kenji Ishitsuka, Noopur Raje, Laurence Catley, and Kenneth C. Anderson. Serotonin Receptor Antagonists Have an In Vitro and In Vivo Anti-Myeloma Effect That Is Mainly Mediated by Caspase Dependent Apoptosis. *ASH Annual Meeting Abstracts*, 108(11):2597–2598, 2006.

[130] V. Espina, B.D. Mariani, R.I. Gallagher, K. Tran, S. Banks, J. Wiedemann, H. Huryk, C. Mueller, L. Adamo, J. Deng, et al. Malignant Precursor Cells Pre-Exist in Human Breast DCIS and Require Autophagy for Survival. *PloS one*, 5(4):394–406, 2010.